Dissertation zur Erlangung des Doktorgrades
der Fakultät für Chemie und Pharmazie
der Ludwig-Maximilians-Universität München

Interrelation between AU-rich element mediated decay and the small RNA silencing system

Stephanie Helfer

aus Landshut

2012

Erklärung

Diese Dissertation wurde im Sinne von § 7 der Promotionsordnung vom 28. November 2011 von Herrn Professor Dr. Klaus Förstemann betreut

Eidesstattliche Versicherung

Diese Dissertation wurde eigenständig und ohne unerlaubte Hilfe erarbeitet.

München, den 06.11.2012

_____

Stephanie Helfer

Dissertation eingereicht am 06.11.2012

1. Gutachter: Prof. Dr. Klaus Förstemann
2. Gutachter: Dr. Dietmar Martin

Mündliche Prüfung am 13.12.2012

Table of Contents

1. Summary

Small RNAs like microRNAs (miRNAs) and short interfering RNAs (siRNAs) are 21 to 23 nucleotide long single-stranded molecules that are assembled together with proteins of the Argonaute family (Ago) into an effector complex called RISC (RNA induced silencing complex). Thus they are able to regulate cognate mRNAs through reduction of their stability or inhibition of their translation.

AU-rich elements (AREs), on the other hand, are a class of regulatory sequences in the 3'-UTR of many short-lived mRNAs. They are mainly destabilizing motifs that target the RNA for degradation by binding different cellular proteins (AU-rich binding proteins, AUBPs). This mechanism is described as AU-rich mediated decay. The AU-rich binding protein Tis-11 is the homologue of mammalian Tristetraprolin (TTP) in *Drosophila*. Tis-11 binds AREs of RNAs via its zinc-finger domain and accelerates deadenylation and the decay of the transcript. Previously a genomewide screen in *Drosophila* cell culture showed that *tis-11* is also involved in the RNAi pathway (Dorner, Lum et al., 2006).

A recent publication claimed that the function of AREs may be- at least in part- relayed through the miRNA pathway (Jing et al., 2005). We have revisited this hypothesis using *Drosophila* cell culture. In contrast to their results we found no evidence that the miRNA pathway is universally required for the function of AREs. In *Drosophila* S2 cells, both ARE-containing GFP reporter mRNAs and the endogenous cecA1-mRNA were resistant to depletion of the mi/siRNA factors *dcr-1*, *dcr-2*, *ago1* and *ago2*. Moreover, the *Drosophila* miRNA originally proposed to recognized AU-rich elements, miR-289, is not even detectably expressed in flies or cultured S2 cells. In addition our attempts to over-express this miRNA from its genomic hairpin sequence failed. Thus, this sequence cannot serve as link between the miRNA and the AU-rich element mediated silencing pathways. To sum up our study strongly argue that AREs can function independently of miRNAs.

Additionally we could demonstrate in cultured *Drosophila* cells that the correct functionality of Ago2-loaded RNA species depends on Tis-11, while it has no influence on Ago1-loaded RNAs. The effects of Tis-11 and Ago2 are not additive, thus the two factors act in the same pathway. Co-immunoprecipitation experiments displayed both isoforms of Tis-11 as associated with a small fraction of Ago2 and the RNaseIII enzyme Dcr-2, but not with the methyltransferase Hen1. The association of Tis-11 and Ago2 is RNA dependent. Furthermore neither miR-277 nor the hairpin-derived endo-siRNA (CG4068B) are stably bound to Tis-11. Generally miR-277 is predominantly loaded in RISC with Ago2 and only a minor fraction in RISC with Ago1. Our data showed that the

loading into the effector complexes and also the distribution of the Ago2-loaded RNAs is altered when *tis-11* is inhibited. And after depletion of *tis-11* we could observe that the processing of mature miR-277 is diminished compared to the control. Though Ago2 protein levels did not appear to be changed upon depletion of *tis-11*, the ago2-mRNA level was clearly reduced. As a result highly repetitive sequences in the mRNAs of *tis-11* and *ago2* implied an indirect effect on the RNAi system after knock-down of *tis-11*, which explains at least part of the effects we detected so far.

2. Introduction

2.1 Various mechanisms to control mRNA stability

Gene regulation depends on the interplay among elements that control gene expression at multiple steps including transcription, mRNA stability, post-transcriptional processing and translation.
All functional mRNAs are generally composed of a 7-methyl-guanylate-cap structure at the 5'-end, a 5'-UTR, a coding region, a 3'-UTR and the poly (A)-tail, a stretch of 100-250 adenine residues, at the 3'-end. Gene expression is often regulated by elements located in the 3'-UTR of a transcript. Next there are two major regulatory mechanisms described that can induce the destabilization of target mRNAs.

2.1.1 AU-rich elements

Due to the presence of regulatory sequences in some vertebrate transcripts their half-life can vary from 20 min to more than 24 h (Brennan and Steitz 2001; Sharova, Sharov et al. 2009). A well studied example of such *cis*-acting sequence elements are AU-rich elements (AREs) that are 50-150 nt long and rich in adenosine and uridine bases. Usually they are located in the 3'-UTR of many but not all short-lived mRNAs encoding cytokines, cell cycle regulators and inflammatory mediators and lead to their destabilization (Barreau, Paillard et al. 2005; Baou, Jewell et al. 2009). Shaw and Kamen *et al*. showed that ARE from the cytokine GM-CSF mRNA caused rapid decay when inserted into 3'-UTR of the otherwise stable β-globin-mRNA. They promote rapid deadenylation and subsequent degradation of the transcript, this mechanism is called AU-rich mediated decay (AMD). AREs are evolutionary conserved and regulate gene expression in all mammalian organisms, as well as in *Saccharomyces cerevisiae* and *Drosophila melanogaster* (Beisang and Bohjanen ; Caput, Beutler et al. 1986; Shaw and Kamen 1986). Discovered 1986 in the 3'-UTR of TNFα-mRNA, AREs were classified into three groups according to their distinct sequence features and deadenylation kinetics (Table 1).

Table 2-1: Classification of AREs in mammals**.**

Class of ARE	Motif	Examples
I	1-5 copies of scattered AUUUA motif in an U-rich context	c-myc Interferon-γ
II	At least 2 overlapping copies of UUAUUUA(U/A)(U/A)-nonamer in an U-rich region	GM-CSF TNF-α
III	No AUUUA motif, U-rich region	c-jun hsp70

Different sets of RNA-binding proteins, so called AU-rich binding proteins (AUBPs), can be recruited to AREs and execute differential regulation of the transcript. The majority are destabilizing AUBPs, which induce AMD when bound to the sequence elements, among them are AUF1 and Tristetraprolin (TTP). TTP, for example, can bind to AREs via its tandem zinc-finger motif and acts as a suppressor of inflammation in mice by regulating the stability of the cytokine TNFα-mRNA (Ciais, Cherradi et al. ; Carballo, Lai et al. 1998). However the destabilizing activity of TTP is not constitutive, its activity is inhibited by phosphorylation in a mitogen-dependent manner. Kinase MK2 modifies TTP during immune activation and as a result allows binding of 14-3-3 proteins that reduce the destabilizing activity of TTP by lowering its affinity to bind to AREs (Clement, Scheckel et al. ; Sandler and Stoecklin 2008).

In mammals three major pathways for AMD were proposed (Figure 2-1). In the first pathway decapping enzymes such as Dcp1 and Dcp2 are recruited by AUBPs to the transcript. After removal of the cap structure the cellular 5'-to-3' exoribonuclease Xrn1/pacman can degrade the mRNA. AUBPs recruit endoribonucleases in the second pathway that cleave the transcript internally and the emerging fragments can be degraded by cellular exoribonucleases. In the third, cellular deadenylases are targeted to the mRNA to remove the poly (A)-tail and then the exosome can carry out the 3'-to-5'-decay. In contrast a smaller group of AUBPs, for example HuR, functions by stabilizing the cognate mRNA (Beisang and Bohjanen ; von Roretz and Gallouzi 2008).

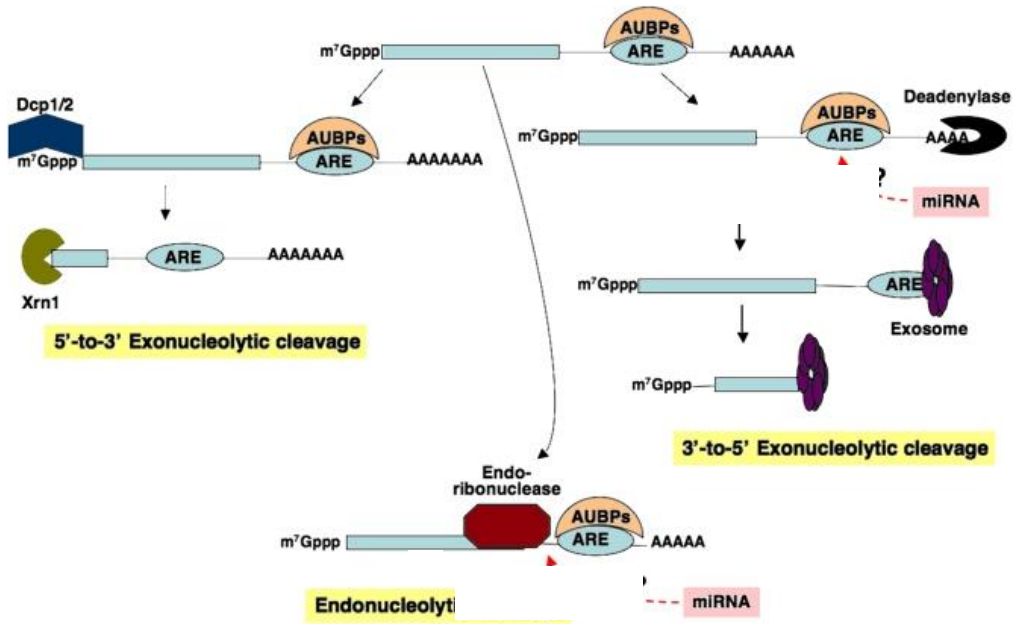

Figure 2-1: **Overview of the three pathways of AMD in eukaryotes.**
AUBPs bind to AREs in 3'-UTR of the transcript and promote decay by either recruiting decapping enzymes or deadenylases. After removal of the cap structure or the poly(A)-tail, exonucleases like Xrn1/pacman or the exosome can degrade the RNA from 5'-to-3' or from 3'-to-5' respectively. The mRNA can also be internally cleaved by endonucleases. Figure adapted from (von Roretz and Gallouzi 2008).

2.1.2 Small non-coding RNAs

Another form of mRNA degradation involves small non-coding RNAs, such as microRNAs (miRNAs) and short interfering (siRNAs). The latter can be divided into exogenous (exo) and endogenous (endo) siRNAs. Changes in levels of small RNAs are associated with many developmental and physiological defects. Small RNAs are precisely regulated *in vivo* by modulating the rates of their biogenesis and turnover (Ji and Chen).

miRNAs are encoded in the genome and transcribed by RNA Polymerase II as so called pri-miRNAs that are sequentially processed (Figure 2-2A). Pri-miRNAs form hairpins with imperfect complementarity that are cleaved by the nuclear RNase III enzyme Drosha and its dsRBP partner Pasha generating long precursor miRNAs (pre-miRNAs) about 70 nt in length (Lee, Jeon et al. 2002; Lee, Nakahara et al. 2004; Kim, Han et al. 2009). Pre-miRNAs have a single-stranded loop structure

with a partially base-paired stem. They are exported into the cytoplasm by Exportin 5 and further processed by the cytoplasmic RNase III enzyme Dicer. In Drosophila, Dicer-1 gets assistance from its partner Loquacious (Loqs, isoform Loqs-B) to liberate a 20-24 nt mature miR/miR*-duplex from the pre-miRNA (Grishok, Pasquinelli et al. 2001; Hutvagner, McLachlan et al. 2001; Ketting, Fischer et al. 2001).

The miRNA duplex is loaded into an effector complex with Argonaute proteins called RNA-induced-silencing-complex (RISC). In flies biogenesis of small RNAs is uncoupled from the subsequent loading step into RISC (Forstemann, Horwich et al. 2007). They are sorted into RISC with Ago1 or Ago2 according to their intrinsic structure of the duplex. miRNA duplexes typically containing bulges and mismatches bind to Ago1, while siRNAs with higher complementarity bind to Ago2. Depending on thermodynamic characteristics of the duplex, the miR*-strand is degraded to form mature RISC. After that the Ago1-loaded miRNA can bind to targets in the 3'-UTR of mRNAs with only partial complementarity and silence gene expression by inhibition of translation or induction of degradation (Ghildiyal and Zamore 2009).

In *Drosophila* two Dicer (Dcr) proteins exist. As described above Dicer-1 generates mature miRNAs whereas Dicer-2 converts long dsRNA into 21 nt siRNA duplexes. siRNAs and miRNAs have a common structure with 5'-phosphate groups and 3'-2nt-overhangs (Figure 2-2B). The long double-stranded precursor of exo-siRNAs is either introduced into the cell with the purpose of inducing RNA interference (RNAi) experimentally or appears during replication of certain RNA viruses (Liu, Rand et al. 2003; Lee, Nakahara et al. 2004; Ghildiyal and Zamore 2009). In addition, endo-siRNAs that are from endogenous origin can be produced from long hairpin structures with extensively paired stretches, convergent transcription or cryptic antisense transcription throughout the genome. The endo-siRNA pathway depends on Dcr-2 and the dsRBP Loqs (isoform Loqs-PD) in contrast to Dcr-2 and R2D2 in the exo-siRNA pathway. Due to their origin from a long dsRNA siRNA precursors are perfectly complementary (Czech, Malone et al. 2008; Okamura, Chung et al. 2008; Okamura and Lai 2008).

Despite their distinct biogenesis miRNAs and siRNAs participate in a common sorting step that loads them into Ago1- or Ago2-effector complexes. The RISC-loading-complex (RLC), consisting of Dcr-2 and R2D2, senses the thermodynamic stability of the 5'-ends of the siRNA duplex and binds it in a directional manner. Then the RNA is delivered to RISC with Ago2, because of their high degree of basepairing. Ago2 cleaves the passenger strand and the endonuclease C3PO converts pre-RISC

into mature RISC by degrading the nicked passenger fragments (Liu, Tan et al. ; Liu, Rand et al. 2003; Pham and Sontheimer 2004; Forstemann, Horwich et al. 2007). Mature RISC can then bind to

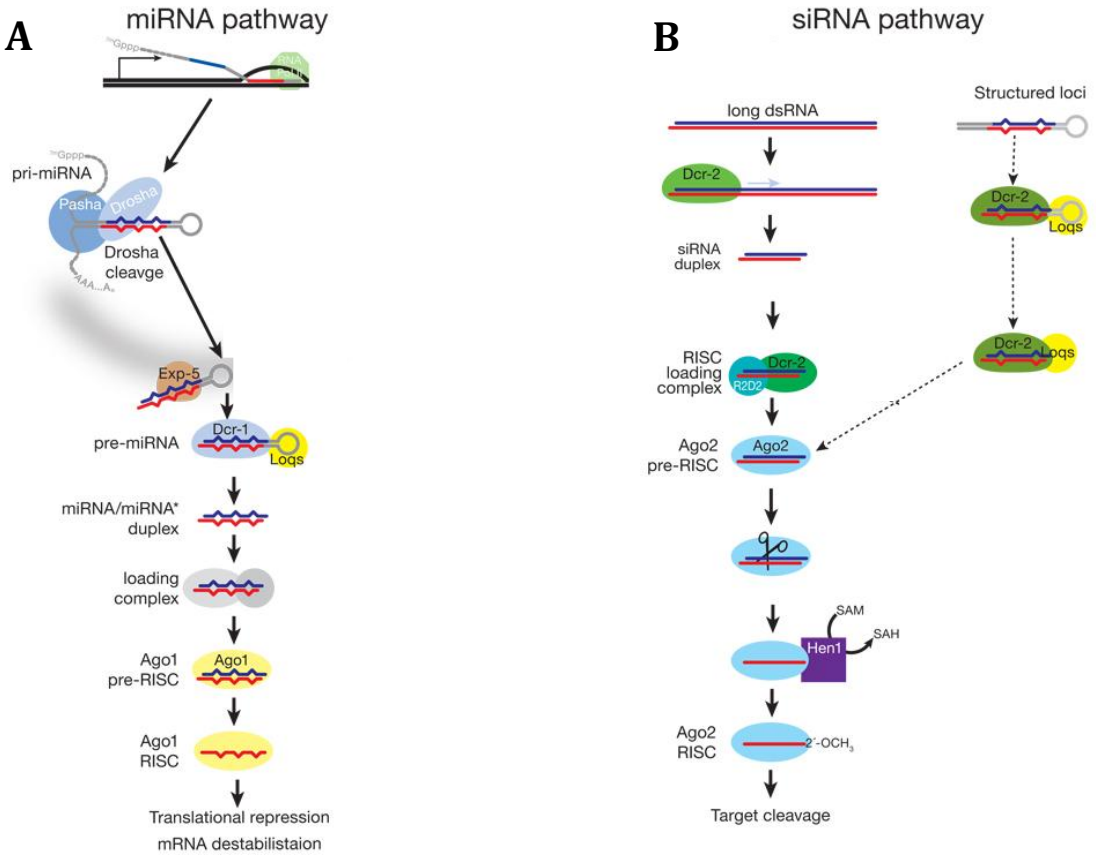

Figure 2-2: **Small silencing pathways in *Drosophila*.**
A) *miRNA pathway*. miRNAs are encoded in the genome and the RNA polymerase II primary transcript is cleaved by the RNaseIII enzyme Drosha. The resulting pre-miR is exported into the cytoplasm and further processed by the second RNaseIII enzyme Dcr-1 with the help of its dsRBP Loqs-PB. This cleavage liberates the miR/miR* duplex with partial complementarity that is loaded into an effector complex usually comprising Ago1. In order to generate mature RISC the duplex is unwound and miR* degraded. RISC can bind to its target sequences and repress translation or trigger destabilization.
B) *siRNA pathway*. Dcr-2 generates siRNAs from both endogenous and exogenous dsRNAs. Exo-siRNAs are either derived from long dsRNAs generated during viral replication or long dsRNAs introduced experimentally. Endo-siRNAs on the other hand can derive from long self-complementary hairpin structures, convergent transcription or antisense transcription throughout the genome. The dsRBP R2D2 participates in the production of exo-siRNAs, in contrast for endo-siRNA production Loqs-PD is required. The perfect complementary duplex is loaded by the RLC (Dcr-2 and R2D2) into RISC with Ago2. Cleavage of the passenger strand converts pre-RISC into mature RISC. DmHen1 methylates the siRNA at its 3'-end and enhances its stability. Mature RISC can cleave targets with perfect complementarity. Figure adapted from (Ghildiyal and Zamore 2009)

target sequences with perfect complementarity and trigger cleavage of the mRNA by its own endonucleolytic (slicer) activity. In *Drosophila*, Ago2-bound RNAs are also 2'-*O*-methylated at their 3'-end by the *S*-adenosyl-methionine (SAM)-dependent methyltransferase DmHen1 to increase their stability (Horwich, Li et al. 2007; Saito, Sakaguchi et al. 2007)see also chapter 4.9).

The minimal RISC complex is composed of Ago2 loaded with siRNA. In contrast holo RISC is a complex composed of many proteins in addition to Ago2. For example Tudor staphylococcal-nuclease-domain-containing protein (Tudor-SN), fragile-X-related protein (dFXR), Vasa intronic gene product (Vig) and a homolog of p68 RNA helicase (Dmp68) have been identified as RISC components in *Drosophila*. However, their function is yet unknown (Martinez, Patkaniowska et al. 2002; Tomari, Matranga et al. 2004; Dorner, Lum et al. 2006).

2.2 Crosstalk between the small RNA- and ARE-pathway

Experimental data suggest numerous similarities and connections between the small RNA pathway and the ARE mediated control of gene expression (reviewed in (Ciais, Cherradi et al. ; von Roretz and Gallouzi 2008).

Jing *et al*. (Jing, Huang et al. 2005) postulated in their publication that the components of the small RNA silencing system Dicer-1, Ago1 and Ago2 are required for AMD of TNF-α mRNA in *Drosophila* and human cell culture. They further demonstrated that first the human miR-16 has to bind to the AREs and afterwards recruit RISC and TTP to the transcript. The cooperation of small RNAs and AUBPs, like TTP, is essential in AMD. They further claimed that miR-289 supposedly mediates ARE recognition in *Drosophila* Schneider 2 cells (S2), because inhibition of miR-289 leads to stabilization of TNFα–mRNA.

In another report the sequence features of mRNAs are analyzed after depletion of Ago1 in S2 cells. They found that ARE-genes are significantly overrepresented in the fraction up-regulated after RNAi of Ago1. Therefore they speculate that these transcripts might be influenced by both the miRNA machinery and AUBPs (Hong, Hammell et al. 2009).

In liver cells CAT1-mRNA is targeted by miR-122 and located into P-bodies where its translation is repressed. However upon cellular stress the AUBP HuR binds to the ARE in the 3'-UTR of CAT1-mRNA and forces miR-122 to dissociate. The transcript is re-located into cytoplasm and translation resumes (Bhattacharyya, Habermacher et al. 2006).

In mammals miRNAs may also negatively regulate TTP-mediated decay through their competitive binding. Ma Cao *et al*. analyzed the binding behavior of TTP and miR-3661 to the 3'-UTR of IL-10 mRNA in mammals. Both TTP and miR-3661 compete for binding to AREs of the transcript and both trigger its degradation. But the decay induced by miR-3661 is much slower than that of TTP, so it finally results in a functional stabilization of IL-10 (Ma, Liu et al.).

Vasudevan and Steitz (Vasudevan and Steitz 2007; Vasudevan, Tong et al. 2007) found in their report the surprising fact that human Ago2 activates translation of mRNAs upon cell cycle arrest caused by serum starvation or contact inhibition. Mammalian cells exit under these conditions the cell cycle and accumulate in G0-phase, called quiescence. There the RISC associated proteins Fragile-X mental retardation-related protein 1 (FXR-1) and Ago2, usually negative regulators of the target, are transformed into effector molecules that bind ARE to activate translation. Moreover, miR369-3p directs the association of Ago2 and FXR-1 with the ARE.

Finally a genomewide screen in *Drosophila* cell culture showed that *tis-11* is involved in the RNAi pathway. Depletion of the AUBP Tis-11 leads to a stabilization of the luciferase-reporter that was shown to be regulated by the small RNA machinery (Dorner, Lum et al. 2006).

2.3 AMD in *Drosophila melanogaster*

Most research on AMD is done in mammals and very little is known about the mechanism in insects. A computational prediction identified conserved AREs in the 3'-UTR of transcripts in *Drosophila*. These ARE genes are enriched in various cellular and developmental processes (Stark, Lin et al. 2007; Cairrao, Halees et al. 2009).

Furthermore the components of the mammalian AMD pathway are conserved in *Drosophila*, because human AREs from TNFα and IL-6 3'-UTRs could induce the decay of a stable β-globin-mRNA in S2 cells. In addition expression of mammalian TTP in Schneider cells could compensate the effects after depletion of Tis-11, the homologue of TTP in *Drosophila*. Moreover silencing of *Drosophila* specific mRNA decay factors, like Tis-11 and Not1 stabilize a Luciferase-reporter with AREs of mouse IL-3 3'-UTR (Temme, Zhang et al. ; Temme, Zaessinger et al. 2004; Jing, Huang et al. 2005; Wei, Xiao et al. 2009). However flies are not only capable to induce AMD but also use this pathway to regulate the stability of endogenous transcripts. Eya-mRNA and Vir1-mRNA are among them and regulated by Tis-11. So far, Cecropin A1 (CecA1) and branchless (bnl) are the best studied

examples with functional AREs in their 3'-UTR in *Drosophila* (Spasic, Friedel et al. ; Yeh, Yang et al. ; Cairrao, Halees et al. 2009).

The immune response in *Drosophila* comprises the secretion of different antimicrobial peptides (AMPeps) in the hemolymph to eliminate pathogens. CecA1 is an AMPep transiently induced upon stimulation of S2 cells with *E.coli* peptidoglycan. The transcripts accumulate rapidly after infection and from then on AMPep levels decrease. CecA1 mRNA is short-lived due to AREs in the 3'-UTR. Tis-11 is recruited to ARE of CecA1 and promotes rapid degradation. It enhances the complete deadenylation by CCR4/CAF1/NOT1-complex and therefore triggers decapping and decay of the CecA1 transcript in both directions. Finally this raises the question if Tis-11 is a specific or general posttranscriptional regulator of immune genes in *Drosophila* (Vindry, Lauwers et al. ; Cairrao, Halees et al. 2009; Lauwers, Twyffels et al. 2009; Wei, Xiao et al. 2009).

2.4 Goals of the thesis

As already known is miR-277 predominantly loaded into RISC with Ago2 (Forstemann, Horwich et al. 2007) and can cleave targets with perfect complementarity. But it cannot repress a transcript with imperfect matches to the miR-277 sequence. However, there are no perfect matches to miR-277 in the whole *Drosophila* genome. So why is the majority of miR-277 is loaded into an effector complex that cannot exert the necessary function in the fly?

Two recent publications showed distinct aspects of the connection between miRNAs and AREs. On the one hand, factors of the miRNA pathway are required for AMD in *Drosophila* cultured cells and on the other hand miRNAs are involved in translational activation of mRNAs under certain stress conditions in human cells (Jing, Huang et al. 2005; Vasudevan and Steitz 2007; Vasudevan, Tong et al. 2007). According to the sequence, miR-277 has the potential to basepair with ARE of TNF-α 3'-UTR and maybe exerts a function in the context of the ARE pathway. We wanted to further examine this hypothesis and in general the connection between small RNAs and ARE-mediated post-transcriptional control in *Drosophila*.

In another report the AUBP Tis-11 was identified in S2 cells as involved in the small RNA silencing system (Dorner, Lum et al. 2006). Therefore, we wanted to elucidate the mechanism of Tis-11 action in the biogenesis and/or the function of small RNAs.

3. Materials and Methods

3.1 Materials

3.1.1 Laboratory equipment

90 µm (45-165 µm) GSH-Beads	GE Healthcare
Agarose gel running chamber	Carl Roth GmbH; Karlsruhe, Germany
BioLogic LP System	BioRad; Hercules, USA
BioPhotometer	Eppendorf AG; Hamburg, Germany
Branson Sonifier 250	Heinemann Ultraschall Labortechnik
Centrifuge 5417 R	Eppendorf AG; Hamburg, Germany
Centrifuge, Rotanta 460 R	Hettich
Desk Centrifuge, 220/230 VAC	Stuart
FACSCalibur flow cytometer	Becton, Dickinson; Franklin Lakes, USA
Filter, GF 1-2 µm	Rotilabo®
Flow buddy CO_2-distributer	Genesee Scientific; San Diego, USA
Fly anesthetic pad and pistol	Genesee Scientific; San Diego, USA
Fraction Collector Model 2110	BioRad; Hercules, USA
Gel Photometer	Intas
GSTrap™ High Performance	GE Healthcare
Heater	HLC
Incubator	WTC binder
Incubator Shaker Series	New Brunswick Scientific
INTAS UV Imaging System	INTAS; Göttingen, Germany
LAS 3000 mini Western Imager	Fujifilm; Tokyo, Japan
Leica MZ7 stereomicroscope	Leica Microsystems; Wetzlar, Germany
Magnetic Stirrer, MR 3001	Heidolph
Microplate Reader Infinite® F500	Tecan
Nanodrop	Thermo Scientific
Overhead Shaker, REAX 2	Heidolph

PAGE-electrophoresis	BioRad; Hercules, USA
Power supply	BioRad; Hercules, USA
PVDF Membrane (0.45 micron pore size)	Thermo Scientific
Q Sepharose™ High Performance	GE Healthcare
Roller Mixer, SRT9	Stuart
Semi-dry blotter BioRad	BioRad; Hercules, USA
Shaker, Polymax 1040	Heidolph Instruments
SLC-6000 Centrifuge	Eppendorf AG; Hamburg, Germany
Spectra/Por® Dialysis Membrane, MWCO: 6-8,000	Spectrum Laboratories, Inc.
SpectroLinker XL1500 UV Crosslinker	Spectronics Corporation; Westbury, USA
SterilGARD cell culture workbench	The Baker Company; Sanford, USA
Table top centrifuge (5417R and 5415R)	Eppendorf AG; Hamburg, Germany
Tank-blotting chamber	BioRad; Hercules, USA
Thermocycler Sensoquest	Sensoquest; Göttingen, Germany
TOptical Thermocycler	Biometra; Göttingen, Germany
Typhoon 9400 Variable Mode Imager	GE Healthcare; Freiburg, Germany
Vortex Genie 2	Scientific Industries
Water Bath	GFL
Western Blot Imager LAS 3000 mini	Fujifilm

3.1.2 Laboratory chemicals

[γ ^{32}P] ATP (SRP 501) 10 mCi/ml; 6000 Ci/mmol; 250 µCi	Hartmann Analytic; Braunschweig, Germany
2% Triton	Sigma-Aldrich
Acrylamide 40%	Carl Roth GmbH; Karlsruhe, Germany
Agarose Biozym	Biozym Scientific GmbH; Oldendorf, Germany
Ammonium peroxodisulfate (Kapsimali, Kloosterman et al.)	Roth GmbH; Karlsruhe, Germany
Ampicillin	Carl Roth GmbH; Karlsruhe, Germany
APS	Carl Roth GmbH; Karlsruhe, Germany

Bacto Agar	Becton, Dickinson; Franklin Lakes, USA
Bis-Tris Propane	Carl Roth GmbH; Karlsruhe, Germany
Bovine serum albumin (BSA)	New England Biolabs; Ipswich, USA
Bradford Assay	BioRad; Hercules, USA
Chloramphenicol	Carl Roth GmbH; Karlsruhe, Germany
Chloroform	Merck Biosciences GmbH; Schwalbach, Germany
Complete® without EDTA (Protease-inhibitor)	Roche Diagnostics; Mannheim, Germany
Coomassie G250	Carl Roth GmbH; Karlsruhe, Germany
Desoxyribonucleotides (dA/C/G/TTP)	Sigma Aldrich; Taufkirchen, Germany
Dimethyl sulfoxide (DMSO)	Carl Roth GmbH; Karlsruhe, Germany
Dithiothreitol (DTT)	Carl Roth GmbH; Karlsruhe, Germany
ECL-Solution	Thermo Scientific
Ethanol (p.a.)	Merck Biosciences GmbH; Schwalbach, Germany
FACS Flow/Clean/Rinse	Becton, Dickinson; Franklin Lakes, USA
Fetal bovine serum (FBS)	Thermo Fisher Scientific; Waltham, USA
Formaldehyde	Sigma Aldrich; Taufkirchen, Germany
Formamide	Sigma Aldrich; Taufkirchen, Germany
Fugene® HD transfection reagent	Roche Diagnostics GmbH; Mannheim, Germany
Glutathion	Sigma-Aldrich
Glycerin	Carl Roth GmbH; Karlsruhe, Germany
HEPES	Carl Roth GmbH; Karlsruhe, Germany
Isopropanol (p.a.)	Merck Biosciences GmbH; Schwalbach, Germany
Kanamycin	Carl Roth GmbH; Karlsruhe, Germany
Methanol (p.a.)	Merck Biosciences GmbH; Schwalbach, Germany
Polyacrylamide	National diagnostics
Powdered milk	Rapilait Migros; Zürich, Switzerland
Sodium dodecyl sulphate (SDS)	Merck Biosciences GmbH; Schwalbach, Germany
Syber Safe/Gold Invitrogen	Karlsruhe, Germany
TEMED	Carl Roth GmbH; Karlsruhe, Germany
Triton X-100	Sigma Aldrich; Taufkirchen, Germany

Trizol	Invitrogen; Karlsruhe, Germany
Tween 20	Carl Roth GmbH; Karlsruhe, Germany

All other standard laboratory chemicals were purchased from the Gene Center in house supply.

3.1.3 Enzymes

Polynucleotidekinase (PNK) with Buffer	Fermentas; St. Leon-Rot, Germany
Proteinase K	Fermentas; St. Leon-Rot, Germany
T4-DNA Ligase	New England Biolabs; Ipswich, USA
Pfu DNA Polymerase	Fermentas; St. Leon-Rot, Germany
Phusion Hot Start DNA Polymerase	Finnzymes
Superscript II, Reverse Transcriptase	Invitrogen; Karlsruhe, Germany
T7-polymerase	laboratory stock
Taq DNA Polymerase	laboratory stock
Restriction enzymes	New England Biolabs; Ipswich, USA
*BamH*I , *Not*I, *Xba*I, *Kpn*I	

3.1.4 Other materials

DyNAmo Flash SYBR Green qPCR Kit	Finnzymes
QIAGEN Gel extraction Kit	Qiagen; Hilden, Germany
QIAGEN PCR Purification Kit	Qiagen; Hilden, Germany
QIAGEN Plasmid Midi Kit	Qiagen; Hilden, Germany
QIAGEN Plasmid Mini Kit	Qiagen; Hilden, Germany
Sephadex spin column (G25)	Roche Diagnostics GmbH; Mannheim, Germany
Spin column (empty, for IP)	MoBiTec; Göttingen, Germany
SuperSignal West Dura Extended Duration	Thermo Fisher Scientific; Waltham, USA
Whatman 595 ½ Folded Filters	Whatman GmbH; Dassel, Germany
Blotting paper	Machery-Nagel; Düren, Germany
α-Flag affinity agarose A2220	Sigma Aldrich; Taufkirchen, Germany
α-myc affinity sepharose	Sigma Aldrich; Taufkirchen, Germany

3.1.5 Bacterial cells

E. coli BL21(DE3)pLysS	Laboratory stock
E. coli XL2-blue CaCl2-competent cells	Laboratory stock

All *E. coli* strains were cultivated in LB-medium or in SOC-medium following transformation. Antibiotic containing agar plates were purchased from in-house supply.

SOB-medium

0.5% (w/v) yeast extract

2% (w/v) Tryptone

10 mM NaCl

2.5 mM KCl

10 mM $MgCl_2$

10 mM $MgSO_4$

pH 7.0

SOC-medium

SOB-medium +

20 mM Glucose

LB-medium

1% (w/v) Tryptone

0.5% (w/v) yeast extract

1% (w/v) NaCl

pH 7.2

Antibiotics added to medium after autoclaving

100 µg/ml ampicillin (100 mg/ml stock)

10 µg/ml kanamycin (10 mg/ml stock)

25 µg/ml chloramphenicol (34 mg/ml stock)

3.1.6 *Drosophila melanogaster* cells

63-N1	endo-siRNA reporter	(Hartig, Esslinger et al. 2009)
67-1D	siRNA reporter; two perfect binding sites for miR-277 in GFP 3´-UTR	(Forstemann, Horwich et al. 2007)
S2 B2	parental cell line	laboratory stock

Cell culture medium and additives for Drosophila Schneider cells was purchased from Bio & Sell (Nürnberg, Germany) and supplemented with 10% heat-inactivated Fetal Bovine Serum (FBS; Thermo Fisher; Waltham, USA).

3.1.7 Fly stocks

Actin-Gal4	Actin5C-Gal4 driver line	BL3954	Bloomington Stock center
Elav-Gal4	Gal4 driver line in nervous system	BL8765	Bloomington Stock center
Mef2-Gal4	Muscle specific Gal4 driver line	BL27390	Bloomington Stock center
Mhc-Gal4	Muscle specific-Gal4 driver line		received from Stefan Sigrist
Tubulin-Gal4	Tubulin Gal4 driver line	BL5138	Bloomington Stock center
VDRC101765	Tis-11 RNAi	VDRC101765	VDRC stock center, Vienna
VDRC12259	Tis-11 RNAi	VDRC12259	VDRC stock center, Vienna
w1118	recessive white mutation	BL6326	Bloomington Stock center

3.1.8 Flyfood

Standard fly food was obtained from in-house supply.

5.8% corn meal

5.5% molasses

2.4% yeast extract

3.1.9 Plasmids

pKF63	constitutive myc-GFP expression under ubiquitin-promotor control	(Forstemann, Tomari et al. 2005)
pUASTattB	conditional expression under GAL4-control	(Bischof, Maeda et al. 2007)

pUC18	transfection control vector	(Yanisch-Perron, Vieira et al. 1985)
pGEX-6P-1	for recombinant expression of GST-tagged proteins	Amersham/GE Healthcare
pUC18	transfection control vector	(Yanisch-Perron, Vieira et al. 1985)
pHSneo	neomycin resistance selection of stable cell culture lines	
pC5T	pCasper-5 with 2kb tubulin promotor	
pSK2	pGEX-6P-1 for expression of GST-tagged Tis-11PA	
pSH2	pKF63-1xARE (artificial ARE element)	
pSH3	pKF63-2xARE (artificial ARE element)	
pSH4	pKF63-3xARE (artificial ARE element)	
pSH5	pKF63-TNF-α 3'-UTR inverse	
pSH6	pKF63-TNF-α 3'-UTR ΔARE	
pSH7	pKF63-IL-6 3'-UTR	
pSH8	pKF63-IL-8 3'-UTR	
pSH9	pKF63-TNF-α 3'-UTR	
pKF84	constitutive expression of pre-miR-277	
pSH12	constitutive expression of pre-miR-289	
Ban-si	pKF63 2x perfect match target sites for bantam in 3'-UTR	(Shah and Forstemann 2008)
Ban-mi	pKF63 4x bulged target sites for bantam in 3'-UTR	(Shah and Forstemann 2008)
pSH13	pC5T-myc$_2$Tis-11PA	
pSH15	pC5T-myc$_2$Tis-11PB	
pSH23	Flag-DmHen1	
pSH19	pUAST-attB Tis-11PA	
pSH21	pUAST-attB Tis-11PB	

3.1.10 Oligonucleotides

3.1.10.1 RNA-Interference

ds dcr-1	T7 dcr-1_as	TAATACGACTCACTATAGGTTT GGC CGC CGT GCA CTT GGC AAT
	T7 dcr-1_s	TAATACGACTCACTATAGGTTG GGC GAC GTT TTC GAG TCG ATC
ds dcr-2	T7 dcr-2_as	TAATACGACTCACTATAGG TTA CAG AGG TCA AAT CCA AGC TTG
	T7 dcr-2_s	TAATACGACTCACTATAGG CTG CCC ATT TGC TCG ACA TCC CTC C
ds DsRed	T7 DsRed_as	CGTAATACGACTCACTATAGGTGGTGTAGTCCTCGTTGTGG
	T7 DsRed_s	CGTAATACGACTCACTATAGGAGGACGGCTGCTTCATCTAC
ds elav_2	T7 elav_2as	TAATACGACTCACTATAGGGAGATTTTGGGGAGGAGATTTGTG
	T7 elav_2s	TAATACGACTCACTATAGGGAGACGCGTATCCCATTTTCATCT
ds elav_3	T7 elav_3as	TAATACGACTCACTATAGGGAGAAGTTGGGGATTGAGGAAAGC
	T7 elav_3s	TAATACGACTCACTATAGGGAGACGACAAGTCGCAGGTCTACA
ds elav	T7 elav_as	TAATACGACTCACTATAGGGAGATCATTGTTTGCGGCAAGTAG
	T7 elav_s	TAATACGACTCACTATAGGGAGACCCGATCCTCTCACCTATCA
ds fne	T7 fne_as	TAATACGACTCACTATAGGGAGATCGTTTAGCGTACAAATCAAATG
	T7 fne_s	TAATACGACTCACTATAGGGAGACTGGCTGGCGATCTATTGG
ds msi	T7 msi_as	TAATACGACTCACTATAGGGAGATACTGCCCTTGCAGGAGTTT
	T7 msi_s	TAATACGACTCACTATAGGGAGACGATACACGGAAGGCAAATTA
ds rbp6_2	T7 rbp6_2as	TAATACGACTCACTATAGGGAGAGCCGCCTGATAGTTGTTCAT
	T7 rbp6_2s	TAATACGACTCACTATAGGGAGATGGTGACGAGAACGAAGAAA
ds rbp6	T7 rbp6_as	TAATACGACTCACTATAGGGAGAGCTGCGTTACACCCCCTA
	T7 rbp6_s	TAATACGACTCACTATAGGGAGAAGTTCGCTGAGCGGATAGTG
ds rbp9	T7 rbp9_as	TAATACGACTCACTATAGGGAGATGAAAGTGGCTAGGCGAAGT
	T7 rbp9_s	TAATACGACTCACTATAGGGAGATCGACTCTCCCGAAGAAAAA
ds Renilla Luciferase	T7 RLuci_as	TAATACGACTCACTATAGGGAGAGGAATGATTTGATTGCCAAAAAT AGG
	T7 RLuci_s	TAATACGACTCACTATAGGGAGAATGAAACGATATGGGCTGAATAC
ds sqd	T7 sqd_as	TAATACGACTCACTATAGGGAGATAACCACCTCGTCCTCCGTA
	T7 sqd_s	TAATACGACTCACTATAGGGAGAGATTCGCCTTCATCGTGTTT
ds tis-11_2	T7 tis-11_2as	TAATACGACTCACTATAGGGAGACCGTAATTCGGTCCTTCTCA
	T7 tis-11_2s	TAATACGACTCACTATAGGGAGAACAATAGCGTTGGCAGCAAG

ds tis-11_3	T7 tis-11_3as	TAATACGACTCACTATAGGGAGACGCATTGTGAACAAAGTGACA
	T7 tis-11_3s	TAATACGACTCACTATAGGGAGAACTTGGGTGATTTCGATTGC
ds tis-11_4	T7 tis-11_4as	TAATACGACTCACTATAGGGAGACTACTGTTGCTACTTTGATTG
	T7 tis-11_4s	TAATACGACTCACTATAGGGAGACGATGAACACATCCAGATACAA
ds tis-11_5	T7 tis-11_5as	TAATACGACTCACTATAGGGAGACCTCCTGCTGCATCGGTGTGC
	T7 tis-11_5s	TAATACGACTCACTATAGGGAGACTGCCGCTAAGCCCACCGCT
ds tis-11	T7 tis-11_as	TAATACGACTCACTATAGGGAGACCATTCGATGCCAAATATCC
	T7 tis-11_s	TAATACGACTCACTATAGGGAGAATGCAAGTACGGCGAGAAGT

3.1.10.2 Molecular Cloning

1xARE	NotI_1ARE_s	GGCCATTTTATTTATATTATTTA
	Xba_1ARE_as	CTAGTAAATAATATAAATAAAAT
2xARE	NotI_2ARE_s	GGCCATTTTATTTATATTATTTAATTTTATTTATATTATTTA
	Xba_2ARE_as	CTAGTAAATAATATAAATAAAATTAAATAATATAAATAAAAT
3xARE	NotI_3ARE_s	GGCCATTTTATTTATATTATTTAATTTTATTTATATTATTTAATTTTATTTATATTATTTA
	Xba_3ARE_as	CTAGTAAATAATATAAATAAAATTAAATAATATAAATAAAATTAAATAATATAAATAAAAT
authentic 3'-UTRs (Jing *et al*.)	bglobin 3'UTR_XbaI_as	TCTAGATAATTTTTGGCAGAGGGAAAAAGATC
	bglobin end_NotI_s	GCGGCCGCCCTGGCTCACAAATACCACTGA
flag-DmHen1	Kpn_flagHen1_s	CAGGTACCTAATCCAAAATGGATTATAAAGATGATGATGATTTTTCGCACAAGTTTATTTGCGGG
	NotI_Hen1_as	GATGCGGCCGCTTATGATTCGGGGCCTTGATCC
myc_2-Tis11PA	KpnI_myc_2_tis11PA_s	ACGGTACCTAATAATCCAAAATGGAACAAAAACTTATTTCTGAAGAAGACTTGGAACAAAAACTTATTTCTGAAGAAGACTTGTCTGCTGATATTCTGCAGA
myc_2-Tis11PB	KpnI_myc_2_tis11PB_s	ACGGTACCTAATAATCCAAAATGGAACAAAAACTTATTTCTGAAGAAGACTTGGAACAAAAACTTATTTCTGAAGAAGACTTGAACGATCACTTGGGTGATT
myc_2-Tis11PA &	Xba_tis11PA_PB_as	TCTAGATTAGAGTCCCAAATTGGACTGC

-PB		
OE miR-289	BamHI_pre289_s	GATGGATCCTAAGCAGGCAGCATGTCATC
	Not_pre289_as	GCGGCCGCACCACTTCCAGCACGTTTTT
recombinant Tis-11PA	BamHI_tis11PA_s	CCAGGATCCTCTGCTGATATTCTGCAGAAA
	EcoRI_tis11PA_as	CCAGAATTCTTAGAGTCCCAAATTGGACTG

3.1.10.3 Quantitative PCR

	ago2 qPCR as	GACGCAATGGTGACCTTCTT
ago2	ago2 qPCR s	TCAATGCCGATGATCGAATA
CecA1	CecA1_fw	GGATCCAAGCTTCCACGATGATTATTTATAA
	CecA1_rev	GGATCCTTCTTCTTTAAATTTTTAAAATT
gapdh	gapdh_as	TGGACTCCACGATGTATTCG
	gapdh_s	AATTTTTCGCCCGAGTTTTC
GFP	GFP_1as	ACGTAAACGGCCACAAGTTC
	GFP_1s	TCGTGACCACCCTGACCTAC
rp49	rp49 A2	ATCGGTTACGGATCGAACA
	rp49 B2	ACAATCTCCTTGCGCTTCTT
tis-11 qPCR_1	tis-11 qPCR_1 as	GCTCCAGATCCACTGACCAC
	tis-11 qPCR_1 s	CAACAGTTCCGCCTCGTC
tis-11 qPCR_2	tis-11 qPCR_2 as	CCAGGTTCTCGGTGATGGT
	tis-11 qPCR_2 s	GAGGTGCGCAAGGAAATAAG
tis-11 qPCR_3 (Cairrao *et al.*)	tis-11 qPCR_3 as	CGCTCGAGTTAGGCGCGGGCCTCGTCCGCATTG
	tis-11 qPCR_3 s	CGTTCGAGGAGGCCGGAGAATGC

3.1.10.4 Northern Blotting

2S-rRNA	TACAACCCTCAACCATATGTAGTCCAAGCA
bantam	AATCAGCTTTCAAAATGATCTCA
CG4068B	GGAGCGAACTTGTTGGAGTCA
miR-277	TGTCGTACCAGATAGTGCATTTA
miR-277*	TGCAAATGCACTCCTGACACG
miR-289	AGTCGCAGGCTCCACTTAAATATTTA

3.1.10.5 Antisense Oligonucleotides

as-Luciferase	CAUCACGUACGCGGAAUACUUCGAAAUGUCC
as-miR-277	UCUUGUCGUCCAGAUAGUGCAUUUACU
as-miR-289	UCUAGUCGCAGGCUCCACUUAAAUAUUUACC

The constructs are 5'-cholesteryl-modified and all bases are 2'-O-methyl modified.

3.1.11 Antibodies

3.1.11.1 Primary antibodies

α- β-tubulin	mouse β-tub E7	1:1000 Western Blotting	DSHB
α-Ago1	mouse 1B8	1:1000 Western Blotting	(Okamura, Ishizuka et al. 2004)
α-Ago2	rb α-Ago2	1:500 Western Blotting	lab generated peptide antibody, Davids
α-Dcr-2	rb α-Dcr-2	1:1000 Western Blotting	abcam
α-flag	mouse α-flag M2	1:1000 Western Blotting	Sigma, F1804
α-myc	mouse α-myc	1:1000 Western Blotting	
α-Tis-11	α-Tis-11 HHY9	1:1000 Western Blotting	(Lauwers, Twyffels et al. 2009)

3.1.11.2 Secondary antibodies

Goat anti-mouse IgG (H+L) HRP-coupled	1:20 000	Pierce (Thermo Scientific)
Goat anti-rabbit IgG (H+L) HRP-coupled	1:50 000	Pierce (Thermo Scientific)

3.1.12 Commonly used buffers and stock solutions

Church buffer	1% (w/v)	bovine serum albumine (BSA)
	1 mM	EDTA
	0.5 M	phosphate buffer
	7% (w/v)	SDS
	pH 7.2	
Colloidal Coomassie staining solution	50 g/l	aluminum sulfate
	2% (v/v)	H_3PO_4 (conc.)
	10% (v/v)	ethanol
	0.5% (v/v)	Coomassie G250 stock
DNA loading buffer (6x)	0.25% (w/v)	bromophenol blue
	0.25% (w/v)	xylene cyanol
	30% (w/v)	glycerol
Dialysis buffer	100 mM	KAc
	10 mM	HEPES pH 7.4
	2 mM	MgAc
	5 mM	DTT
Formamide loading dye (2x)	80% (w/v)	formamide
	10 mM	EDTA, pH 8
	1 mg/ml	xylene cyanol
	1 mg/ml	bromophenol blue
GST-elution buffer	50 mM	Tris
	20 mM	glutathione
	1 mM	DTT

GST-high salt buffer	1 x	PBS
	800 mM	NaCl
	1 mM	DTT
GST-low salt buffer	1 x	PBS
	20 mM	NaCl
	1 mM	DTT
Laemmli SDS loading buffer (2x)	100 mM	Tris/HCl, pH 6.8
	4% (w/v)	SDS
	20% (v/v)	glycerol
	0.2% (w/v)	bromophenol blue
	200 mM	DTT (freshly added)
Lysis buffer for protein extraction	100 mM	KAc
	30 mM	HEPES
	2 mM	MgCl2
	1 mM	DTT
	1% (v/v)	Triton X-100
	2x	Complete® without EDTA (=protease inhibitor cocktail)
Lysis Buffer (GST-purification)	1 x	PBS
	2 % (v/v)	Triton
	500 mM	NaCl
	2x	Complete® without EDTA (=protease inhibitor cocktail)
	1 mM DTT	
PBS-T/TBS-T	PBS/TBS supplemented with 0.05% Tween-20	
SDS-running buffer (5x)	125 mM	Tris/HCl, pH 7.5
	1.25 M	glycine
	5%	SDS

SSC (20x)	3 M	NaCl
	0.3 M	sodium citrate
TAE (50x)	2 M	Tris-base
	5.71%	acetic acid (0,9 M)
	100 mM	EDTA
TBE (10x)	0.9 M	Tris base
	0.9 M	boric acid
	0.5 M	EDTA (pH 8)
TBS (10x)	50 mM	Tris
	150 mM	NaCl
	pH 7.4	
Western blotting stock (10x)	250 mM	Tris/HCl, pH 7.5
	1.92 M	glycine
Western blotting buffer (1x)	10%	Western blotting stock (10x)
	20%	methanol

3.2 Methods

3.2.1 Methods for molecular cloning

3.2.1.1 Amplification of DNA sequences by Polymerase Chain Reaction (PCR)

For molecular cloning purposes the standard reaction mix was as follows:

Standard reaction mixture:

1 µl	Template DNA
0.5 µl	forward primer (10µM)
0.5 µl	reverse primer (10µM)
5 µl	10x Taq-buffer with $(NH_4)_2SO_4$
4 µl	25 mM $MgCl_2$
0.3 µl	Taq-polymerase
0.2 µl	Pfu-Polymerase
add 50 µl	H_2O

Standard thermocycler protocol:

5 minutes 95°C initial denaturation	
35 cycles:	1 minute 95°C denaturation
	30 seconds 55°C annealing
	1 minute per kb product size 72°C extension
5 minutes 72°C final extension	
storage at 4°C	

According to the length of nucleotides to be separated 1 - 1.5% agarose gels (according to the expected product size) were prepared with 1x TAE buffer and stained with 1x SyberSafe

(Invitrogen; Karlsruhe, Germany). Gels were run at 55 V for 30 min and photographed in an Intas UV Imaging System. If higher sensitivity was required gels were re-stained in 1x SyberGold (Invitrogen; Karlsruhe, Germany) for 15 min. PCR products were excised and purified with Qiagen Gel Extraction Kit.

3.2.1.2 Specific digestion of DNA by restriction endonucleases

Endonucleolytic digestion of DNA was carried out with restriction endonucleases acquired from Fermentas (St. Leon-Rot, Germany) and New England Biolabs (Ipswich, USA) ac- cording to manufacturer's recommendations. Usually, reactions were incubated for 1 hour up to over night incubation at 37°C. To prevent recircularization the cloning vector DNA was dephosphorylated with FastAP Thermosensitive Alkaline Phosphatase (Fermentas; St. Leon-Rot, Germany) according to manufacturer's protocol.

3.2.1.3 Ligation of vector with insert DNA

Digested and purified insert and vector were combined in a approximately 1:3 molar ration:

50- 200ng	vector
x µl	insert
2 µl	T4 buffer (10x)
1 µl	T4 DNA Ligase
add 20 µl	H_2O

Optimally samples were ligated over night at 18◦C and used for bacterial transformation.

3.2.1.4 Bacterial transformation

Transformation of competent bacteria was carried out by standard heat shock procedures. Briefly, 50 µl XL2-blue $CaCl_2$-competent cells were thawed on ice. 1-5 µl of ligation sample were added and the mixture was incubated on ice for 30 min, subjected to a 1 min heat shock at 42°C and returned to ice for 1 min. 500 µl SOC-medium was added and cells were allowed to grow for 1 h in a 37°C shaking incubator. Cells were then centrifuged for 30 sec at full speed in a table top centrifuge, the supernatant was poured off and the resuspended cell pellet was streaked out on agarose plates with appropriate antibiotics for selection of transformants.

3.2.1.5 Test for correct transformants by colony-PCR

Individual colonies were tested for correct integration of the insert by colony-PCR with suitable primer pairs. A standard PCR reaction mix was inoculated with a single colony, which was subsequently streaked onto a fresh plate and labeled for later recognition. Standard amplification was carried out with 10 min initial denaturing for cell lysis of bacteria.

3.2.1.6 Preparation of plasmid DNA

Plasmid DNA was prepared from over-night cultures of 2 ml or 100 ml LB-medium, respectively, supplemented with appropriate antibiotics (usually 100 µg/ml ampicillin). QIAGEN Mini or Midi Kits (Qiagen; Hilden, Germany) were used according to the manufacturer's protocols.

3.2.1.7 DNA sequencing

The correctness of the sequences of the gained plasmids was verified by sequencing (Eurofins MWG, Ebersberg, Germany) and further analysis of the sequences using ApE (A plasmid Editor; http://biologylabs.utah.edu/jorgensen/wayned/ape/).

3.2.2 Methods with *Drosophila* Schneider 2 cells

3.2.2.1 Maintenance

Cells were cultured in Schneider´s Medium (Bio&Sell, Nürnberg, Germany) containing 10% heat inactivated fetal bovine serum (Thermo Fisher Scientific, Waltham, USA) in appropriate cell culture dishes (Sarstedt, Nümbrecht, Germany). Cells were split once to twice a week into fresh medium for up to 25 passages.

3.2.2.2 RNA interference (RNAi)

DsRNA for RNAi was generated using *in vitro* transcription (IVT) with T7-polymerase. Therefore templates of the genes of interest were used in which T7-promotor sites were introduced by PCR and afterwards further amplified by PCR using T7-promotor primer. The resulting PCR products were applied for over-night *in-vitro* transcription at 37°C.

IVT-Mix:

10 µl	T7-template DNA
10 µl	10x T7-buffer
0.5 µl	1 M DTT
5 µl	100 mM ATP
5 µl	100 mM CTP
5 µl	100 mM UTP
8 µl	100 mM GTP
2 µl	T7-polymerase
ad 100 µl	H_2O (54,5 µl)

The precipitate of magnesium pyrophosphate, which formed during the reaction, was pelleted and the dsRNA was precipitated from the supernatant with 1x volume of isopropanol and washed twice with 70% ethanol. The pellet was air-dried and re-dissolved in 100 µl of RNase-free H_2O. The sample was heated to 95°C for 5 minutes and slowly cooled down to room temperature. Concentration of dsRNA was estimated from an agarose gel in comparison to a DNA Ladder Mix (Fermentas; St. Leon-Rot, Germany).

To induce a knock down of a gene of interest cells were seeded at $0{,}5*10^6$ cells/ml and 12 µg of the corresponding dsRNA was added to the medium. After two days incubation with the dsRNA was repeated and on day 7 the resulting GFP fluorescence of the reporter cell lines was determined in a Becton Dickinson FACSCalibur flow cytometer. For this analysis 100 µl of cells were added to 200 µl of FACS flow. For each sample 10 000 cells were measured. Analysis of fluorescence intensity was carried out with CellQuest software (Becton Dickinson; Franklin Lakes, USA). GFP-negative reporter cells were excluded from the analysis and the mean fluorescence value for each sample was determined.

3.2.2.3 Transfection of plasmid DNA

, 2008).

For each well of a 24-well cell culture dish 100-500 ng of the vector of interest or 0.1 µl of 2'-*O*-methyl-antisense-oligo (100 nM) in 50 µl medium (without serum) and 4 µl of Fugene Transfection

Reagent (Roche Diagnostics; Mannheim, Germany) in 46 µl of medium (without serum) were mixed and incubated at RT for 1 hour. Cells were added to the transfection mix at 0.5 - 1x 10^6 cells/ml medium (+10% FBS). For transfections in 6-wells all amounts of reagents were scaled up.

3.2.2.4 Selection of clonal cell lines

To create cell lines that stably express a transgene the expression plasmid of interest was co-transfected with an antibiotic resistance plasmid into cells at 5-10 x 10^5 cells/ml. For native S2 cells 10 ng pHSneo (for neomycin resistance) were used together with 200 ng of the vector of interest. After 3 days, cells were split 1:5 into G418 containing medium, respectively. The concentration was 1.2 mg/ml of G418 for neomycin resistance. Cells were split 1:5 once a week for 4 weeks to obtain polyclonal stable cell lines.

3.2.2.5 Storage of cells in liquid nitrogen

Cell stocks were frozen by adding 500 µl cells to 100 µl Dimethylsulfoxide (DMSO) diluted in 400 µl cell culture medium (+10% FBS) in a Cryovial (Biozym; Oldendorf, Germany). Cryovials were slowly (1°C per hour) cooled to -80°C in an isopropanol freezing container (Nalgene/Thermo Fisher) and transferred into liquid nitrogen for long-term storage.

3.2.3 Protein analysis

3.2.3.1 Protein extraction

S2 cells were harvested (2,500 x g, 10 min) and washed with PBS. The pellet was resuspended in lysis buffer (30 mM HEPES, 100 mM KOAc pH 7.4, 2 mM $MgCl_2$, 1 mM fresh DTT, 1% (v/v) Triton X-100, 2x protease inhibitor cocktail (Roche Diagnostics GmbH; Mannheim, Germany) and frozen in liquid nitrogen. Samples were thawed on ice and cell debris were pelleted in a refrigerated microcentrifuge (Eppendorf; Hamburg, Germany) at 16 000 rpm. Protein concentrations were determined by Bradford assay (BioRad; Hercules, USA).

Fly protein was extracted by grinding flies in lysis buffer using a pistil (Sigma Aldrich; Taufkirchen, Germany) suitable for 1.5 ml reaction tubes and subsequent freeze-thaw lysis analogous to S2 cells.

3.2.3.2 Dual Luciferase assay

Cells were harvested and washed with 1x PBS. Then the cell pellet was resuspended in 100 µl 1x Passive Lysis Buffer (Promega). After centrifugation (15 min, 1000 rpm) the protein extracts were transferred into a 96-well plate and luminescence was measured in a plate-reading luminometer (Berthold).

3.2.3.3 Co-immunoprecipitation

30 µl of anti-flag or anti-myc affinity agarsoe beads per IP were washed three times in 1 ml lysis buffer respectively and incubated with 1- 2 mg total protein in lysis buffer at 4°C for 30-60 min on an overhead-rotator. If desired RNaseA (50 µg/ml) could be added to the suspension. -

, Germany) and washed three times with 500 µl lysis buffer. The bound proteins were eluted by heating the samples to 95°C with 30 µl 1x Laemmli buffer.

Alternatively, RNA was extracted by applying 200 µl Trizol (Invitrogen; Karlsruhe, Germany) and following the manufacturer's instructions. Before precipitation with isopropanol 1.5 µl of glycogen were added. RNA was dissolved in 10 µl H_2O.

3.2.3.4 Western-Blotting

Western-Blotting was performed as previously described in (Forstemann, Horwich et al. 2007). Briefly, proteins were separated using 10% or 12 % polyacrylamide gels for 90 minutes at 150 V in a BioRad electrophoresis tank. Proteins were transferred to a polyvinylidenfluoride (PVDF; Milipore; Billerica, USA) membrane by tank blotting (300 mA for 60 minutes). Afterwards the membrane was blocked in 5% milk for at least 30 minutes at room temperature. Incubation with primary antibodies was carried out over night at 4°C in a 50 ml Falcon tube using 2,5 ml antibody dilution in 1x PBS/TBS-solution with 0,05% Tween. For rabbit antibodies PBS-T (0.05% Tween) was used during all following washing steps, for mouse antibodies TBS-T (0.05% Tween) was employed. After primary antibody binding the membrane was washed three times 10 minutes in buffer and incubated with appropriate secondary antibody for at least 2 h at room temperature. After three times washing, Enhanced Chemiluminescence (ECL) substrate (Thermo Fisher Scientific; Waltham, USA) was applied and the resulting signal was measured in an LAS3000 mini Western Imager System (Fujifilm; Tokyo, Japan). If necessary, Western blots were stripped with 10 ml of Restore Stripping Solution (Thermo Fisher Scientific; Waltham, USA) for 15 minutes at 37°C

and 30 minutes at room temperature, washed with buffer and blocked for new primary antibody incubation.

3.2.4 RNA analysis

3.2.4.1 RNA isolation

RNA was extracted using TRizol (Invitrogen; Carlsbad / CA, USA) from cells according to the manufacturer's instructions and quantified using spectrophotometry.

3.2.4.2 β-elimination of RNA

40 µg total RNA resolved in 40.5 µl H_2O was incubated with 12 µl 5x borate buffer (148 mM borax, 148 mM boric acid pH 8.6) and 7.5 µl $NaIO_4$ (200mM dissolved in H_2O) for 10 min at RT. The oxidation was quenched by addition of 6 µl 100% glycerol (10 min, RT). 2M NaOH (5-7 µl) elavated the pH value (ensure that pH=12). After 90 min, 45°C the sample was transferred to a Mini quick spin oligo column (Chen, Larochelle et al.) and centrifuged (12 000 g, 2 min). 20- 40 µg glycogen were added and RNA was precipitated with 3x volume 100% EtOH (12 000 g, 15 min). RNA pellet was washed three times with 70% EtOH (last step 4°C, o/n) and dissolved in 20 µl 2x denaturating gel loading buffer. The samples were analyzed by Northern blotting.

3.2.4.3 Northern blotting

1-5 µg of RNA were separated on a 20 % Sequagel Acrylamid-Urea Gel (National Diagnostics; Atlanta/USA) at 200 V for 1-2 hours. RNA transfer was performed on a Nylon membrane (Roche Diagnostics; Mannheim, Germany) by semi dry blotting for 30 minutes at 20 V. Crosslinking of the RNA to the membrane was achieved by radiation with UV-light.

Membranes were pre-hybridized in Church buffer (1% (w/v) bovine serum albumine, 1 mM EDTA, 0.5 M phosphate buffer, 7% (w/v) SDS, pH 7.2) for at least 2 hours at 37°C in an oven under constant rotation. The probes were labeled by incubating 9 µl H_2O, 2 µl 10x PNK buffer, 2 µl 5 mM probe oligonucleotide (=10 pmol), 1 µl PNK (Fermentas) and 6 µl [γ-^{32}P] ATP for 1h at 37°C. Unbound radioactive nucleotides were removed using a Sephadex G-25 spin column (Roche Diagnostics; Mannheim, Germany).

Hybridization with labeled as-DNA-probes was performed overnight at 37°C in 5 ml Church buffer. Membranes were washed three times for 15 minutes with 2xSSC 0,1 % SDS and exposed on Phosphoimager Screens (FujiFilm; Tokio, Japan). Screens were scanned using a Typhoon scanner (Amersham Biosciences) and band intensities were quantified using Multi Gauge software (Fujifilm; Tokyo, Japan).
Stripping of the membrane was achieved by dipping it into boiling 1% SDS solution and incubating it for 5 minutes in the solution. After a second pre-hybridization the membrane was reused for hybridization with further probes.

3.2.4.4 Quantitative RT-PCR (qRT-PCR)

100 ng – 1 µg of total RNA extract was reverse transcribed according to the Superscript II Reverse Transcriptase protocol (Invitrogen; Karlsruhe, Germany):

1 µg	oligo(dT) (500 µg/ml)
x µl	100ng RNA
1 µl	dNTP Mix (10 mM each)
add 12 µl	H_2O

The mixture was heated to 65◦C for 5 min and quick chilled on ice. The contents of the tube were briefly centrifuged. Then following components were added:

4 µl	5x First-Strand Buffer
2 µl	0.1 M DTT
1 µl	RiboLock RNase inhibitor
1 µl	SuperScript II RT

The contents of the tube were mixed gently and incubated at 42°C for 50 min. The reaction was inactivated by heating at 70°C for 15 min. 100 µl of water were added to get a final volume of 120 µl. The qPCR reaction mix was as follows, according to the DyNAmo Flash SYBR Green qPCR Kit (Finnzymes; Finland).

Reaction mix for one well of a 96-well plate:

5 µl	Dynamo Flash Master Mix
0.5 µl	Oligo_as (10µM)
0.5 µl	Oligo_s (10µM)
2.9 µl	H_2O
0.1 µl	0.03% Zylencyanolblau

9µl of the mastermix solution was aliquoted in each well of a 96 well plate using an 8-canal pipette. 1 µl of the template was added and the samples cycled on an TOptical Thermocycler using the following PCR-program:

3 min 95°C	initial denaturation	
40 cycles:	1 min, 95°C	denaturation
	30 sec, 55°C	annealing
	30 sec, 72°C	extension

Expression was quantified with the 2-(ΔΔCt) method (Livak and Schmittgen 2001).

3.2.5 Methods with flies

3.2.5.1 Maintenance and handling

The fly stocks were maintained on standard agar food at 25°C and transferred to new food once a week. For phenotype selection flies were anesthetized with CO_2 and sorted on a CO_2-emitting pad (Genesee Scientific; San Diego, USA) using a Leica MZ7 stereomicroscope (Leica Microsystems; Wetzlar, Germany). To slow proliferation by reducing metabolic rates flies were kept at 18°C if they were not used for a current experiment and were transferred to new food every 4 weeks.

3.2.5.2 Generation of transgenic flies

The myc_2-Tis-11PA and myc_2-Tis-11PB constructs were sub-cloned into pUASTattB vector and sent for injection into "zh-86Fb" (BL24749) fly embryos (Rainbow Transgenic Flies; Newbury Park, USA). This fly stock carries the attP-landing site on the 3rd chromosome (3R 86F genomic location). Transgenic offspring, marked by red eye color, were twice crossed with w1118 flies to reduce the risk of secondary mutations. Siblings were then mated to produce homozygous stable lines.

3.2.6 Recombinant expression and purification of GST-tagged Tis-11PA

3.2.6.1 Recombinant expression of GST-Tis-11PA

The 100 ml pre-culture (LB medium, 100 µl ampicillin, 100 µl chloramphenicol, 0.5 % glucose) inoculated with *E. coli* cells transformed with pSK2 and incubated at 250 rpm and 37° C over night. The 6 l expression culture, that contained appropriate antibiotics, was inoculated with 40 ml of pre-cultured transformed bacteria (dilution 1:80). After cell growth to OD_{600} = 0.6 at 37° C and 130 rpm in baffled flasks, protein expression was induced by adding 1 mM IPTG. After incubating for 4 hours at 37° C, the bacteria were harvested by centrifugation for 30 min at 4500 rpm at 4° C. The obtained bacterial pellets were suspended in 300 ml lysis buffer (1 x PBS, 2 % Triton, 500 mM NaCl, 2 x PI, 1 mM DTT) and stored at 80 ° C.

The pellet was three times for 1 min on ice resuspended with a sonicator (output 5-6, amplitude 20-30). Afterwards, the solution was centrifuged for 30 min at 4500 rpm at 4° C. Before loading on the GSH-beads, the supernatant was filtered through a filter (glass fiber, 1-2 µm pore size).

3.2.6.2 Affinity purification of recombinant Tis-11PA

Purification of heterologous Tis-11PA fused to GST was achieved by binding to glutathione, immobilized to a sepharose matix (Glutathione Sepharose 4-Fast-Flow GSH-beads). 3 ml GSH-beads were previously equilibrated with GST-low salt (1x PBS, 20 mM NaCl, 1 mM DTT pH 7.0), GST-high salt (1x PBS, 800 mM NaCl, 1 mM DTT pH 7.0) and again low salt buffer. Then 40 ml protein solution were loaded on 500 µL GSH-Beads at 4° C over night. The fractions of GSH-beads were collected into a column. The column was washed with 15 ml low salt, 15 ml high salt and 10 ml low

salt buffer. Afterwards, the column was incubated with 15 ml GST elution buffer (50 mM Tris, 20 mM glutathione, 1 mM DTT pH 8.0) over 30 min.

150 µg of the PreScission protease were added to the elution fraction to remove the GST-tag from Tis-11PA. The 15 ml protein solution was dialyzed against 3 l dialysis buffer (dilution 1:200) in a dialysis membrane with molecular weight cut off of 6-8 kDa, while stirring at 4° C over night.

The GSTrap™ HP column was previously equilibrated as above. Then the protein solution after dialysis was loaded to the column. The GST-tag and uncut fusion protein bind to the column and the desired protein Tis-11PA is set out in the flow through. Afterwards, the uncut protein and the GST-tag were eluted with 10 ml GST-elution buffer.

4. Results

4.1 Artificial and authentic mammalian AREs repress GFP reporters in *Drosophila* cells

Jing *et al*. (Jing, Huang et al. 2005) draw the conclusion that miRNAs were required for AU-rich mediated decay (AMD) in mammals and *Drosophila*. In order to characterize this finding more in detail, the 3'-UTR sequences of mammalian TNF-α, IL-6 and IL-8 mRNAs - identical to those used in the proposal of Jing *et al*.- were inserted downstream of the GFP coding sequence in a *Drosophila* expression vector (pKF63). The 3'-UTRs of TNF-α with deleted AREs or AREs inserted in opposite orientation were used as controls. In addition we generated constructs with one, two or three repeats of an artificial ARE-sequence, which resembles that of the interferon-γ mRNA (Worthington, Pelo et al. 2002). This sequence belongs to group I AREs that was not tested for its functionality in *Drosophila* yet (Figure 4-1). Stable cells were selected for each reporter construct to avoid variations due to differences in transfection efficiency.

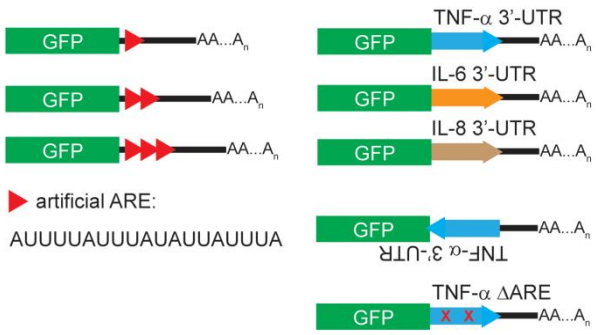

Figure 4-1: **Schematic representation of the ARE-reporter constructs.** The sequence of one artificial ARE is indicated 5' to 3' (modelled after the interferon-γ element). One repeat of artifical ARE is depicted as a triangle and the authentic mammalian 3'-UTRs are shown as arrows.

Transcription was inhibited with α-amanitin and RNA was isolated at different time points. Thereby it was possible to examine if the TNF-α mRNA with AREs in its 3'-UTR was destabilized and degraded in S2 cells. The TNF-α mRNA showed indeed a decreased half-life compared to the control

without any AREs (Figure 4-2A). Also the steady-state level of GFP-TNF-α mRNA was around four times lower than control GFP-mRNA before the transcriptional block (Figure 4-2B). Mammalian AREs destabilize transcripts in S2 cells.

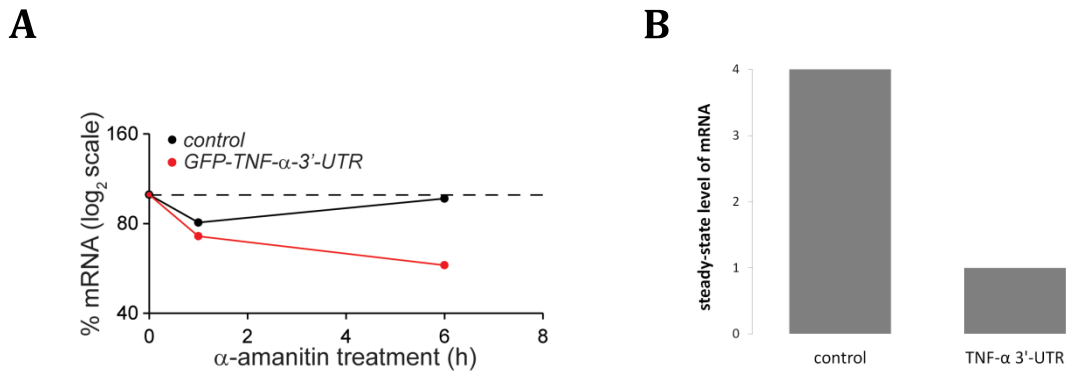

Figure 4-2: **Analysis of reporter mRNA decay.**
A) Transiently transfected S2 cells were treated with α-amanitin (5 µg/ml) for 0, 1 and 6 hours. Introduction of the TNF-α 3'-UTR sequence destabilizes the reporter mRNA.
B) Steady-state level of GFP-TNF-α mRNA and GFP-mRNA without any AREs before treatment with α-amanitin.

Tis-11 was depleted in different stable cell lines using RNAi. GFP fluorescence was measured by flow cytometry and normalized to the knock-down of a non-specific control (DsRed, Figure 4-3). Reporters with two or three artificial ARE-repeats as well as IL-6 and TNF-α were de-repressed after silencing of *tis-11*. This indicated that ARE pathway represses the mRNAs in S2 cells. In contrast to the data of Jing *et al.*, the IL-8 reporter failed to respond. In this particular case a possible explanation may be that the ARE-motif from this sequence is less accessible in our construct. Or the constitutive, high-level expression of this 3'-UTR from our construct sequestered important cellular binding factors and the selection of stable expression counter-selected against the more responsive cells. Taken together we generated GFP-cell culture reporters that responded to depletion of *tis-11*.

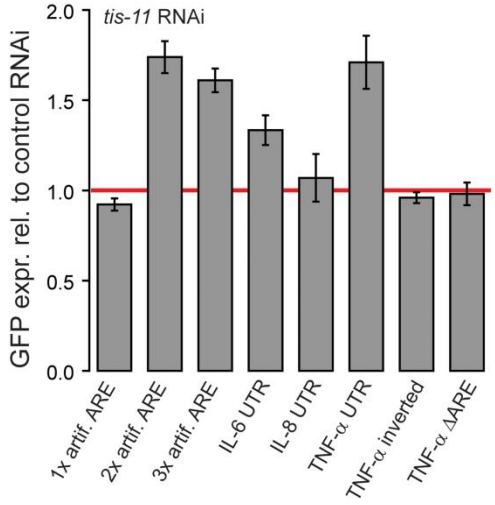

Figure 4-3: **GFP-reporter cells respond to depletion of the AUBP Tis-11.** GFP fluorescence of stable polyclonal cell lines was measured by flow cytometry and normalized to control knock-down targeting DsRed. Values are mean ± SD (n=3). The changes were significant for 2xARE, 3xARE, IL-6 3'-UTR and TNF- α 3'-UTR when compared to the TNF-αΔARE control ($p<0.05$, student's t-test, n=4). The horizontal line marks no change compared to the control.

4.2 Depletion of mi/siRNA factors does not lead to de-repression of ARE reporters

If miRNAs indeed participate in the recognition of AREs, then GFP fluorescence should be de-repressed upon depletion of miRNA biogenesis factors. Factors of the small RNA biogenesis system, *dcr-1*, *dcr-2*, *ago1* and *ago2*, were depleted with RNAi in stable reporter cells and the GFP signal was measured. GFP levels did not change after impairment of the mi/siRNA biogenesis factors compared to the control knock-down directed against DsRed (Figure 4-4A and Figure 4-4B). In some cases there was a slight de-repression after *ago2* and *dcr-2* silencing detectable. But these changes did not correlate with the extent of de-repression observed after depletion of *tis-11* and in addition they were not comparable with the reported effects of Jing *et al*.

Furthermore there was no change of steady-state mRNA levels of the GFP-3xARE reporter or CecropinA1 (CecA1), an endogenous mRNA that contains AREs, after depletion of *dcr-2* or *ago2* (Figure 4-5). In contrast, silencing of *tis-11* significantly increased the steady state mRNA level of both, GFP-3xARE and CecA1. There is also no indication for translational repression of reporter

mRNAs recognizable since de-repression upon *tis-11* knock-down was 1.57 x for mRNA and 1.61 x for GFP fluorescence (Figure 4-5 and Figure 4-3).

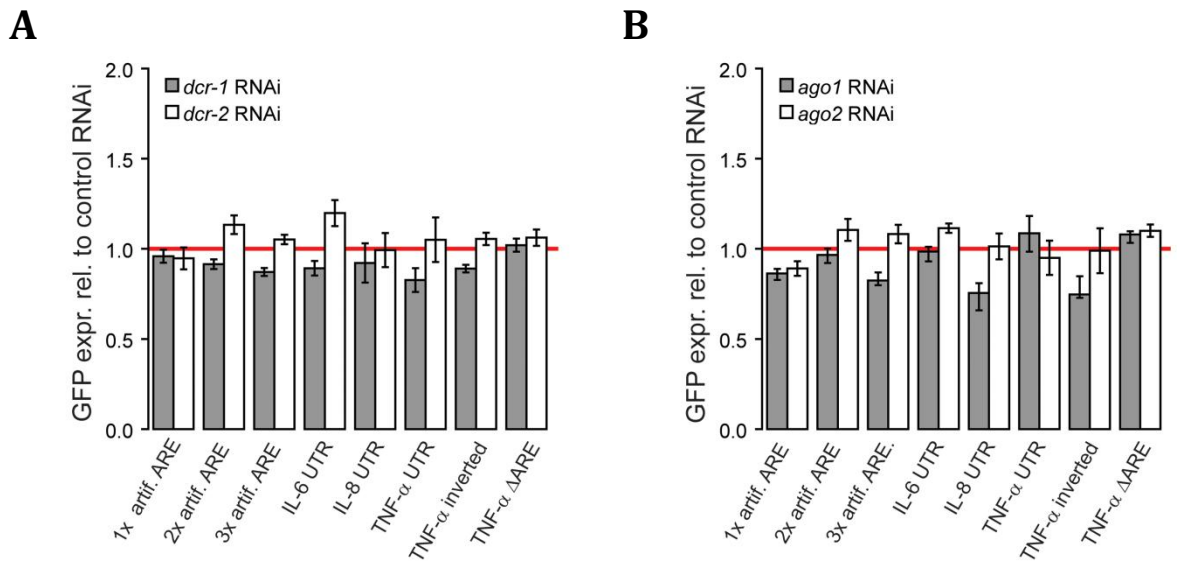

Figure 4-4: **Response of stable ARE-reporter cells to depletion of components of the small RNA silencing pathway.**
A) Silencing of *dcr-1* or *dcr-2*. Stable polyclonal reporter cells were treated with dsRNAs targeting *dcr-1* or *dcr-2*. The resulting GFP signal was measured by flow cytometry and normalized to DsRed control. Values are mean ± SD (n=3). The horizontal line marks no change compared to the control.
B) analogous to **A)** depletion of *ago1* or *ago2*.

In theory it is possible that during selection of stable cell lines, reporter cells somehow gain the ability to bypass the requirement for miRNAs in AMD because only a small fraction of the original population is retained. To exclude this we measured the GFP fluorescence after depletion of *ago1*, *ago2*, *dcr-1* and *dcr-2* in cells transiently transfected with the reporter constructs. In this experiment it was also necessary to normalize the values to those of a control construct without AREs in the 3'-UTR (pKF63). Depletion of certain cellular factors prior to transfection can cause toxic side effects and influence the efficiency, because in most of the cases proliferation rates were changed. But this additional normalization introduces more measurement noise (Figure 4-6). TNF-α- and IL-8-reporter, the latter did not respond in the stable cell line, were de-repressed after silencing of *tis-11* in transiently transfected cells. A similar trend could be observed for IL-6 as well as for all three artificial ARE reporter. Again silencing of the small RNA biogenesis factors did not result in a consistent de-repression of the transiently transfected reporter constructs. Only the

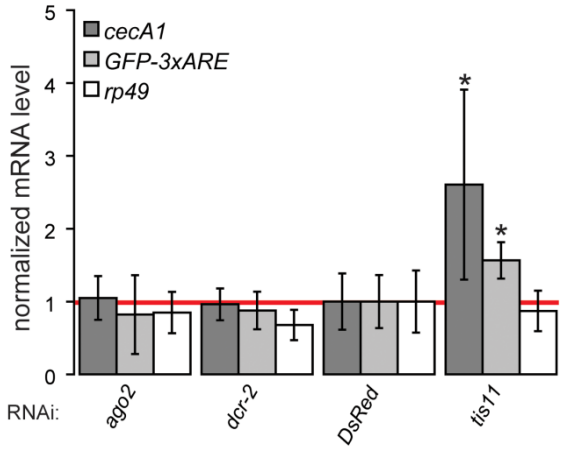

Figure 4-5: **Analysis of mRNA steady-state level changes upon depletion of *tis-11*, *ago2* and *dcr-2*.**
Quantitative RT-PCR analysis was performed for the indicated transcripts (*cecA1* = endogenous ARE target, GFP-3xARE = stable ARE reporter, *rp49* = ribosomal protein mRNA), normalized to the mRNA levels of *gapdh*. Changes were calculated relative to control RNAi directed against DsRed. The horizontal line marks no change compared to the control. The asterisk (*) indicates a significant change relative to control ($p<0.03$, Wilcoxon's rank sum test, n=6).

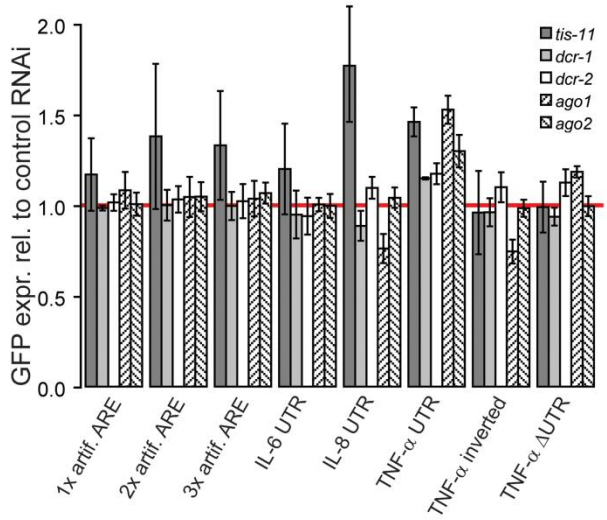

Figure 4-6: **Response of transiently transfected ARE-reporter cells to silencing of *dcr-1* or *dcr-2* and *ago1* or *ago2*.**
Depletion of *dcr-1*, *dcr-2, ago1* or *ago2* in transiently transfected reporter cells. The GFP fluorescence was measured by flow cytometry and normalized to the control targeting DsRed. Values are mean ± SD (n=3). The horizontal line marks no change compared to the control.

TNF-α reporter was repressed by Ago1, Ago2, Dcr-1 and Dcr-2. But all other constructs remained unaffected. Hence it is possible that under certain circumstances miRNAs can function synergistically with ARE-sequences, but there could be no general requirement of miRNAs for AMD detected. Taken together we showed that the small RNA silencing system is not universally required for ARE-mediated mRNA degradation.

4.3 Direct inhibition or over-expression of miR-289 and miR-277 does not influence ARE-reporters

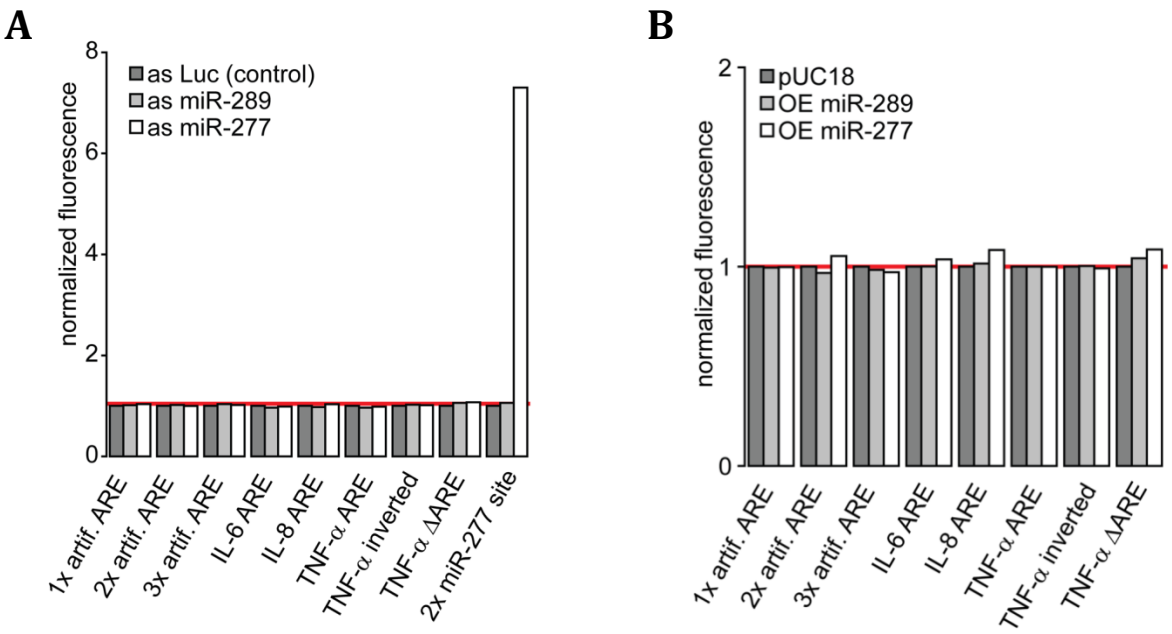

Figure 4-7: **Repression of ARE-reporter cells is independent of miR-289 activity.**
A) miR-289 and miR-277 were inhibited by transfection of antisense oligonucleotides in GFP-reporter cells (stable, polyclonal) and miR-277 reporter cell line (stable, monoclonal). GFP fluorescence was measured by flow cytometry and normalized to control directed against part of the firefly luciferase coding sequence. Values are the mean of two experiments. The horizontal line marks no change compared to the control.
B) Response of ARE-reporters to over-expression of miR-289 and miR-277 (transiently transfected). An unrelated plasmid (pUC18) served as control for normalization. Values are the mean of two experiments. The horizontal line marks no change compared to the control.

MiR-289 was identified in the publication of Jing *et al.* to recognize AREs in S2 cells. To revisit this hypothesis the reporter cells were treated with 2'-*O*-methyl-modified RNA oligonucleotides

directed against miR-289 as well as miR-277, a second *Drosophila* miRNA that can potentially basepair with ARE-sequences. Inhibition of both miRNAs did not lead to a de-repression of GFP fluorescence in any of the reporter constructs (Figure 4-7A). As expected the miR-277 reporter construct with two perfectly complementary target sites for miR-277 in the 3'-UTR of GFP (pKF67) showed a strongly enhanced GFP-signal when treated with the miR-277 inhibitor (Forstemann, Horwich et al. 2007). The construct is specifically silenced by miR-277 because GFP is not stabilized after treatment with the miR-289 inhibitor. Furthermore, over-expression of the miRNAs from plasmids generating the putative hairpin precursors of miR-277 and miR-289 did not enhance the repression of the reporter cells (Figure 4-7B).

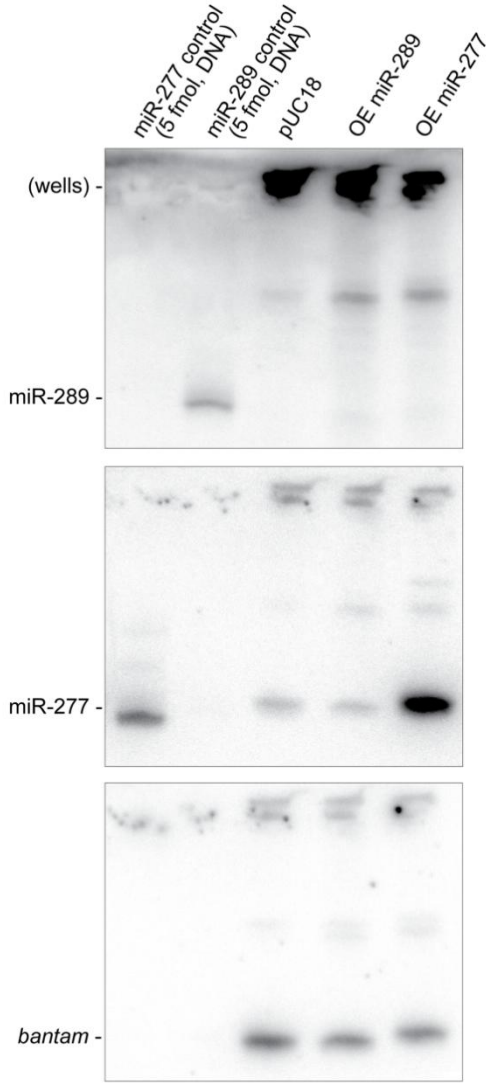

Figure 4-8: **Expression of mature miR-289** (figure legend continued on p.46).

(figure legend continued p.45)
S2 cells were transfected with plasmids over-expressing the putative hairpin of miR-289 and miR-277. pUC18 served as a control. RNA was analyzed by Northern blotting. 5 fmol of the miR-277 and miR-289 DNA oligo were also loaded. DNA probes against miR-289 (upper panel) and miR-277 (second panel) served as positive controls for the hybridization. bantam (bottom panel) served as a control for loading.

In addition the analysis of several deep sequencing libraries from S2 cells and also flies (published by the modEncode consortium (mod, Roy et al.)) did not provide any sequence that corresponds to mature miR-289 (in contrast to $1.5x10^6$ reads matching to other miRNAs in *Drosophila*, data not shown). To make sure that this finding is not only an artefact due to a strong unfavourable cloning bias for the deep sequencing libraries, it was tested by Northern blotting if miR-289 is expressed in S2 cells at all (Figure 4-8). The Northern blot was probed for miR-289, miR-277 and as loading control bantam. Mature miR-289 could not be detected in the control cells transfected with the unrelated control pUC18. As a positive control, 5 fmol of the miR-289 control-DNA-oligonucleotide was visible. In addition miR-289 was not detectable in cells transfected with the vector expressing the putative miR-289 hairpin precursor under the control of the strong ubiquitin promotor. For comparison miR-277 is already visible in the control cells and the transfection of a plasmid driving the expression of the miR-277 hairpin precursor resulted in a strong over-expression of mature miR-277. To sum up there is no proof for the existence of mature miR-289 in *Drosophila*. Hence it is unclear how this sequence could be identified as the miRNA necessary for ARE recognition in S2 cells by Jing *et al*.

4.4 ARE-binding proteins have an impact on miR-277-reporter cells, primarily targeted by Ago2-RISC

In mammals different classes of proteins that can bind to AREs exist and lead either to destabilization or stabilization of the corresponding transcript (Beisang and Bohjanen). We depleted several *Drosophila* homologues of HuR, AUF and TTP in stable reporter cell lines expressing GFP under the control of small RNAs to analyze their potential relevance in the siRNA pathway.

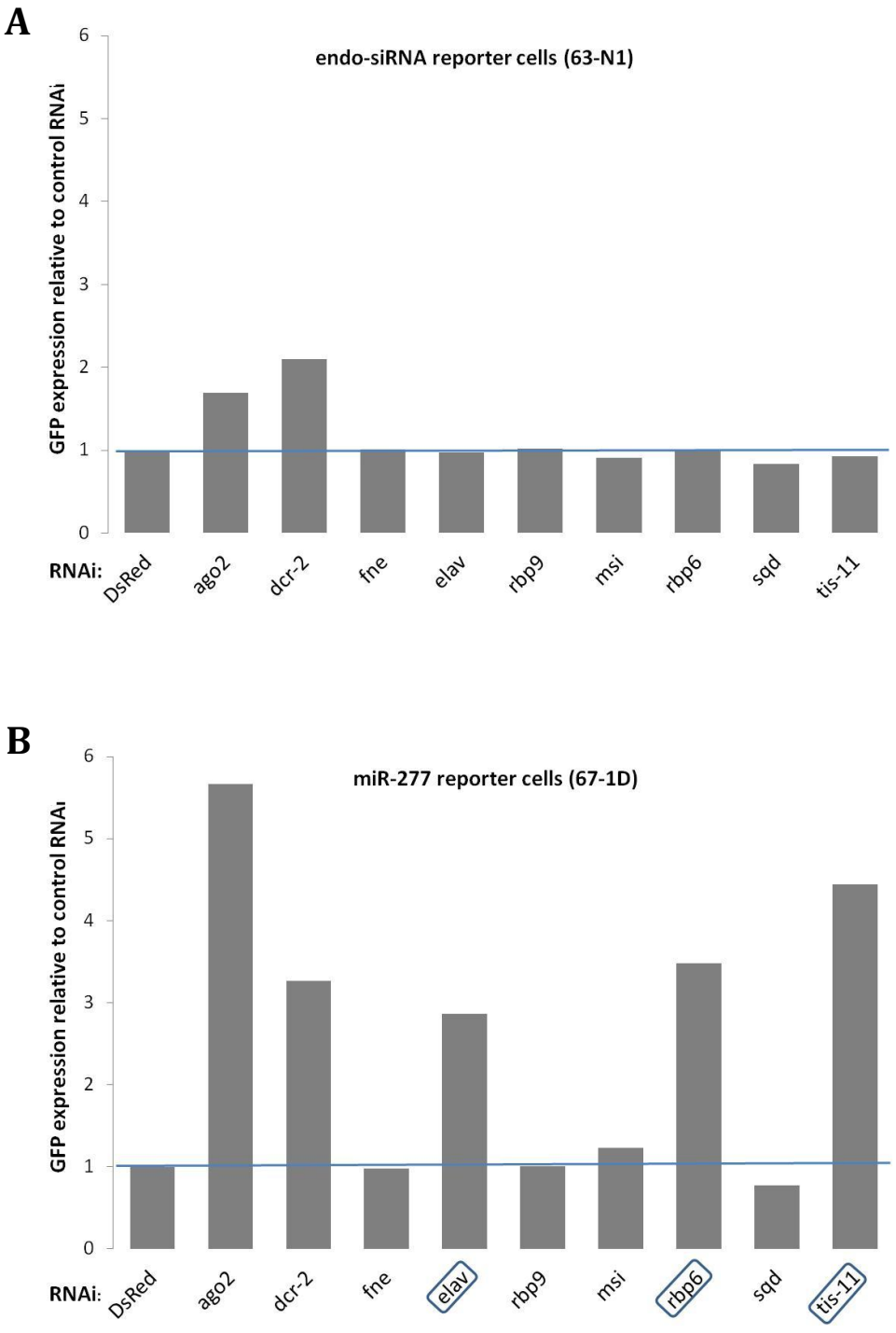

Figure 4-9: **Depletion of some *Drosophila* AUBP homologues have an impact on miR-277-reporter cells.**
(figure legend continued on p.48)

(figure legend continued from p.47)
A) Endo-siRNA reporter cells (63-N1) were treated twice with dsRNA constructs indicated below the bars. Fne, Elav, Rbp9 are homologues of the mammalian HuR; Msi, Rbp6, Sqd of AUF and Tis-11 is the homologue of TTP. Ago2 and Dcr-2 served as positive controls. GFP-fluorescence was measured by flow cytometry and normalized to control knock-down DsRed. Values are the mean of two experiments. The horizontal blue line marks no change compared to the control.
B) analogous to **A)** using miR-277 reporter cells (67-1D), with two perfectly matching sites for miR-277 in the 3'UTR of GFP.

Figure 4-9 illustrates the mean GFP fluorescence of cells after seven days treatment with the corresponding dsRNA, measured by flow cytometry and normalized to a control knock-down targeting DsRed. In Figure 4-9A the response of the cell line 63-N1 is depicted, which serves as a suitable reporter for the endo-siRNA pathway. Depletion of Ago2 and Dcr-2 leads to an expected increase in fluorescence. Both are major components of the siRNA pathway and therefore necessary for the functionality of the siRNA response. There was no significant stabilization of GFP observable for the seven AUBPs. So they all seem not to participate in endo-siRNA mediated gene silencing.
However, silencing of three out of seven AUBPs resulted in a de-repression of the GFP fluorescence using exo-siRNA reporter cells (67-1D, Figure 4-9B). They contain two perfectly matching sites for miR-277 in the 3'-UTR of the GFP coding sequence, which are targeted primarily by miR-277 loaded into RISC with Ago2. Thus the candidates *rbp6, elav,* and *tis-11* may have a role in small RNA silencing.
To confirm this hypothesis, additional dsRNAs targeting different parts of the three genes were designed. Then both reporter cell lines were treated with these triggers and the ones used in Figure 4-9. Afterwards the fluorescence was measured. Again the silencing of Ago2 and Dcr-2 as key factors of the siRNA machinery resulted in an increased GFP expression due to the impaired exo-siRNA pathway (Figure 4-10). Elav and Rbp6, the homologues of mammalian HuR and AUF, respectively, could not be validated to participate in siRNA-mediated gene silencing. In each case, a de-repression of the fluorescence signal of the 67-1D cells was only observed with the treatment of one out of two or three dsRNA respectively (Figure 4-10A).
None of the three different dsRNAs directed against *tis-11* showed an effect on the endo-siRNA reporter cells (63-N1, Figure 4-10B). But the treatment of 67-1D cells with two out of the three tested triggers against *tis-11* resulted in a significant loss of exo-siRNA mediated repression. This effect was comparable to depletion of *dcr-2* (2.7-fold and 2.4-fold de-repression of GFP in the case of *dstis-11* and *dstis-11_3* vs. 2.1-fold for *dsdcr-2*). Taken together Tis-11 may contribute to exo-siRNA mediated gene regulation.

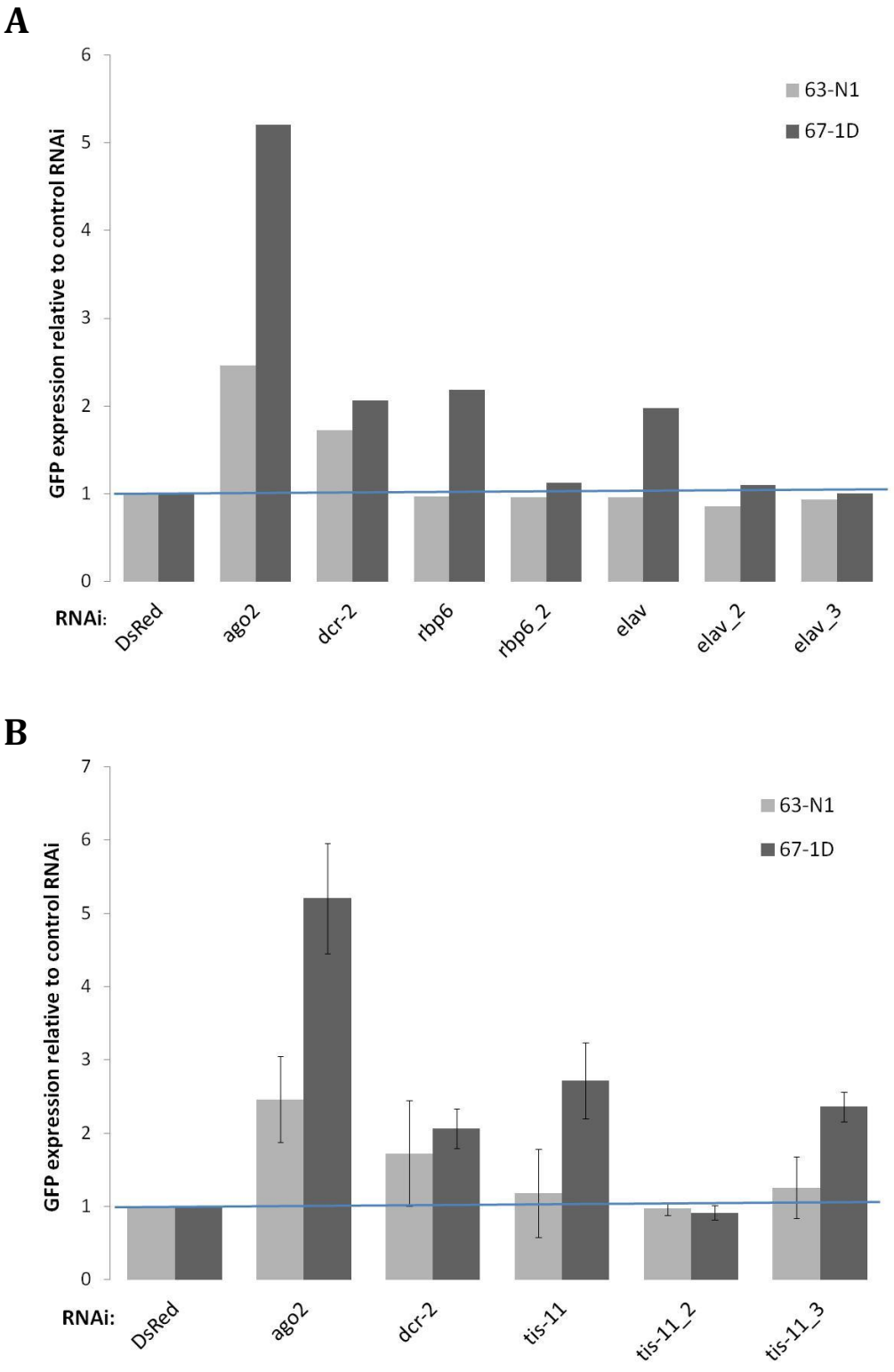

Figure 4-10: **Silencing of the AUBP genes *rbp6, elav* and *tis-11* with dsRNA constructs targeting different regions of the transcripts.** (figure legend continued on p.50)

(figure legend continued from p.49)
A) Endo-siRNA reporter cells (63-N1) and miR-277 reporter cells (67-1D) were treated twice with dsRNA constructs indicated below the bars targeting *rbp6* and *elav*. Ago2 and Dcr-2 served as positive controls. GFP-fluorescence was measured by flow cytometry and normalized to control knock-down directed against DsRed. Values are the mean of two experiments. The horizontal blue line marks no change compared to the control.
B) analogous to **A)** using three different dsRNA constructs directed against *tis-11*. Values are mean ± SD (n=4 for 63-N1; n=6 for 67-1D). These changes in 67-1D cells were significant when compared to the DsRed control ($p<0.08$, student's t-test, n=6).

In order to ensure that the dsRNA constructs against *tis-11* are reliable, S2 cells were incubated with the triggers. After five days RNA and proteins were isolated. The *tis-11* mRNA level was measured by qRT-PCR using two different sets of oligonucleotides. The obtained values were normalized to *rp49*-mRNA and a control knock-down (DsRed, Figure 4-11A). In all three cases the *tis-11* mRNA level was lowered to about 40% or less compared to the control. Next the protein level of endogenous Tis-11 after incubation with the dsRNA constructs was analyzed. Especially in the extracts treated with *dstis-11* the signal of Tis-11 was nearly completely diminished or significantly lowered for *dstis-11_3* (Figure 4-11B). However in the case of *dstis-11_2* the protein level is only slightly lowered. Therefore, the incomplete depletion of Tis-11 protein could explain the missing effect of *dstis-11_2* on 67-1D cells (see Figure 4-10B).

4.5 *tis-11* has a general effect on Ago2-loaded RNA species

In the last chapter it was demonstrated that silencing of *tis-11* resulted in de-repression of the reporter in miR-277-responsive cells (67-1D, Figure 4-10B). This raised the question if this effect is restricted to miR-277 or also other small RNAs that are loaded into an effector complex with Ago2 are affected.

Therefore S2 cells were transiently transfected with GFP-expression constructs targeted by the miRNA bantam and incubated with certain dsRNAs (Figure 4-12). Ban-si harbours two perfect matching sites for bantam in the 3'-UTR of the GFP coding sequence. It was previously shown (Shah and Forstemann 2008) and after silencing of *ago2* easily visible that this reporter is repressed by Ago2-loaded bantam. The measured fluorescence was not only normalized to a control RNAi (DsRed) but also to pKF63, a control construct without any bantam-binding sites in the 3'-UTR of

GFP. This approach correct for variations in transfection efficiency. GFP expression was enhanced for both dsRNA constructs directed against *tis-11*. This means that not only miR-277, but also Ago2-loaded bantam is influenced by Tis-11.

A

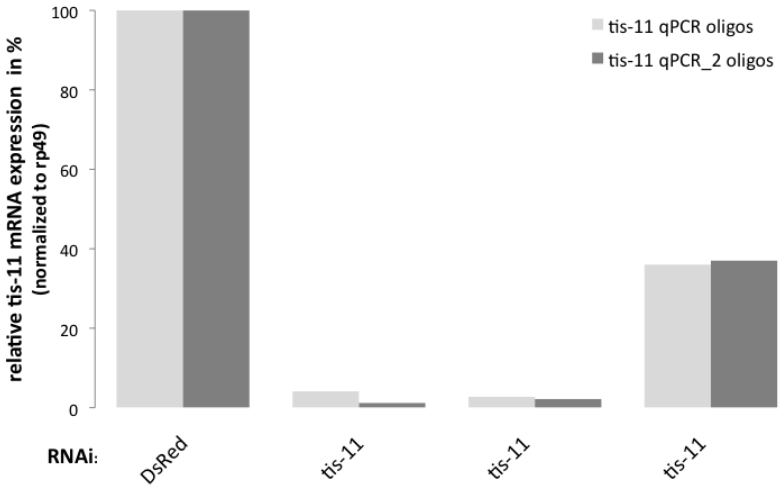

B

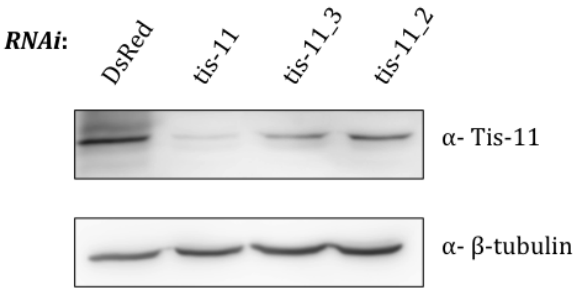

Figure 4-11: **Verification of the Tis-11 knock-down efficiency using RNAi triggers directed against *tis-11*.**

A) S2 cells were treated twice with the three dsRNA constructs targeting *tis-11*. RNA was isolated, reverse transcribed and the *tis-11* mRNA level was measured by qRT-PCR. Two different pairs of oligonucleotides were used to quantify *tis-11* transcripts. The values represent the fold change of each RNA (normalized to rp49) and control cells (DsRed). Values represent the mean of two experiments. The horizontal blue line indicates a value of 1 (=no change relative to control).

B) S2 cells were treated as above to determine the protein amount of endogenous Tis-11 after triggering RNAi. Proteins were isolated and analyzed by Western blotting. Tis-11 HHY9 (Lauwers, Twyffels et al. 2009) antibody could detect endogenous Tis-11 (upper panel). Anti-β-tubulin served as loading control (lower panel).

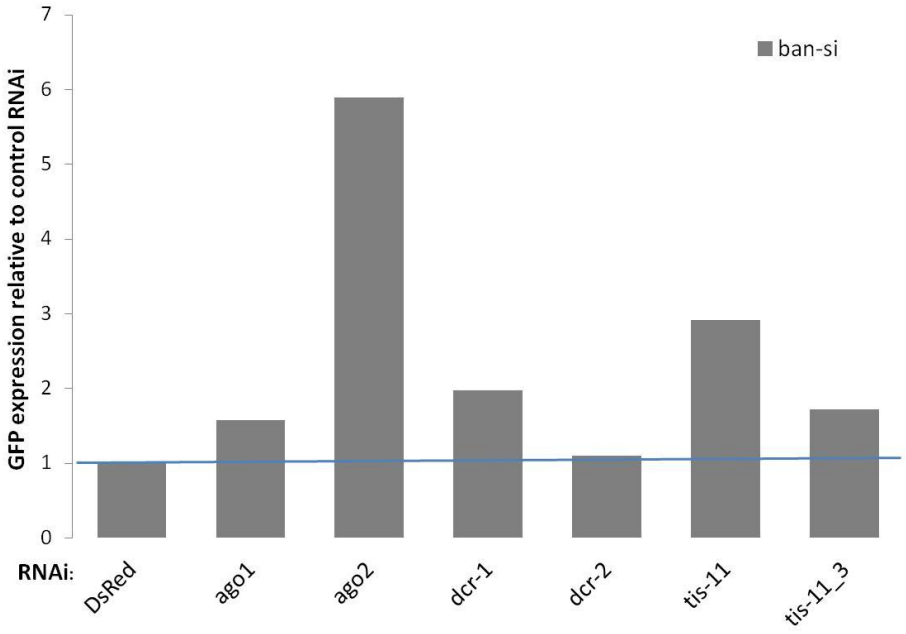

Figure 4-12: **Silencing of *tis-11* also affects reporter constructs targeted by Ago-2 loaded bantam.**
S2 cells were treated twice with dsRNA constructs indicated below the bars targeting *tis-11, ago1, ago2, dcr-1* and *dcr-2*. Afterwards they were transiently transfected with the ban-si reporter construct. Ban-si is analogous to the construct integrated into 67-1D cells (see Figure 4-10B) and carries two perfectly matching sites for bantam, instead of miR-277, in the 3'-UTR of GFP. GFP-fluorescence was measured by flow cytometry and normalized to control knock-down DsRed and to the transfection control pKF63 (GFP without binding sites in its 3'-UTR). Values are the mean of two experiments. The horizontal blue line marks no change compared to the control.

In order to analyze if *tis-11* is universally involved in exo-siRNA silencing, S2 cells were treated with dsRNAs directed against components of the small RNA pathway and *tis-11*. The cells were then incubated with dsRNA against GFP or DsRed as a control and transfected with the GFP-expression vector pKF63 to illustrate the exo-siRNA silencing efficiency (Figure 4-13A). Priming of Ago2-RISC with dsRNA directed against GFP will decrease in efficiency if the first dsRNA depletes an essential factor of the exo-siRNA silencing pathway. If so, the GFP fluorescence after pKF63 transfection will increase (Figure 4-13B). This is the case after silencing of *ago2* and *dcr-2* in the first step compared to the non-essential control DsRed (55% and 15% of relative GFP level, respectively compared to 1.5%). Knock-down of *tis-11* also reduced the efficiency of exo-siRNA silencing, resulting in 11% fluorescence relative to the control. All together *tis-11* is an essential factor in the exo-siRNA pathway.

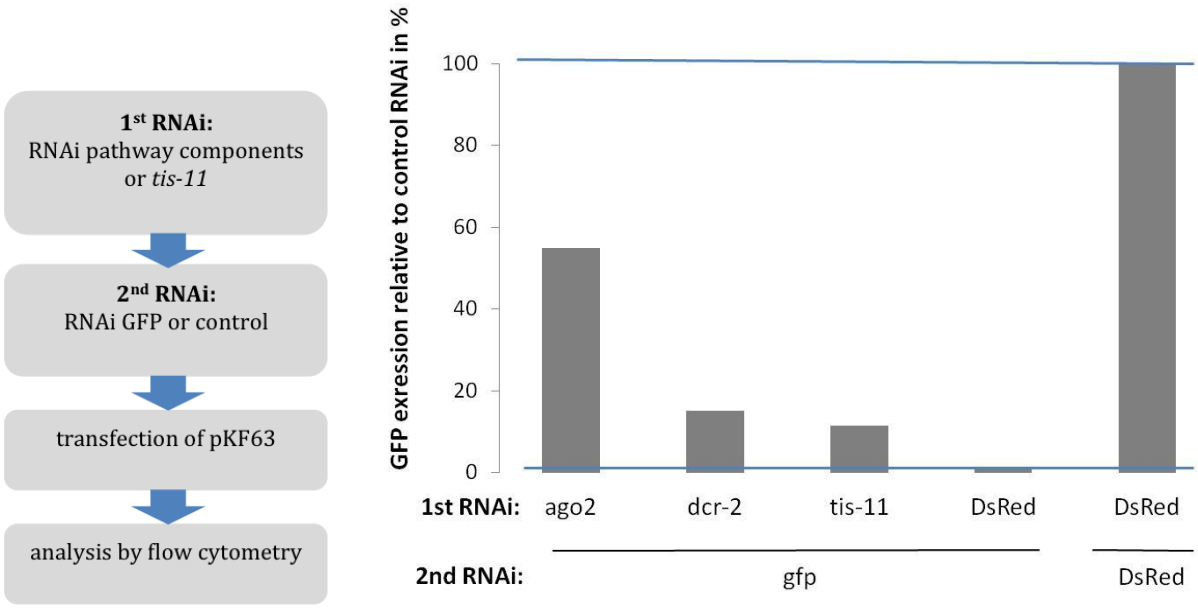

Figure 4-13: **Tis-11 is necessary for exo-siRNA dependent silencing.**
A) Flow diagram for exo-siRNA silencing assay. S2 cells were treated twice with RNAi against components of the small RNA silencing pathway and *dstis-11*. Ago2-RISCs were then primed with RNAi triggers against *gfp* or DsRed as a control and transfected with an expression plasmid for GFP (pKF63). GFP fluorescence was measured by flow cytometry.
B) GFP fluorescence relative to treatment with DsRed control in both RNAi steps (upper horizontal line was set as 100%) and DsRed control only used in the first RNAi step (lower horizontal line). RNAi triggers are indicated below the bars. The lower horizontal line marks GFP levels when the exo-siRNA silencing is unaltered. Values are the mean of two experiments.

The observed effect of *tis-11* on the GFP-reporters seemed to be specific for the exo-siRNA pathway because the endo-siRNA reporter 63-N1 was not affected (see Figure 4-10B). To test this S2 cells with stably integrated sequences of Renilla-luciferase and Firefly-luciferase were used. These cells are a reliable reporter system to measure endo-siRNA response. They were treated with dsRNA against *tis-11*, *ago2*, *dcr-2* and further controls and the Renilla-luciferase signal was measured and normalized to Firefly-luciferase, the internal control. A de-repression of the normalized luciferase ratio was shown after silencing of *ago2* and *dcr-2*, as known factor of the endo-siRNA machinery but also for *tis-11* (Figure 4-14). So silencing of *tis-11* has a general effect on all Ago2-loaded species and is not restricted to the exo-siRNA pathway.
In order to investigate whether Ago2 and Tis-11 act nevertheless in two independent pathways, the exo-siRNA reporter cells 67-1D were treated with RNAi triggers against *ago2* and *tis-11* at the same time. Ago2 and Tis-11 operate in parallel pathways, if this fluorescence value is significantly higher

than the de-repression of GFP when only one factor is depleted. Figure 4-15 depicts the GFP expression relative to a control RNAi against DsRed. Simultaneous silencing of *ago2* and *tis-11* does not enhance the de-repressive effect. Thus Ago2 and Tis-11 function in the same pathway.

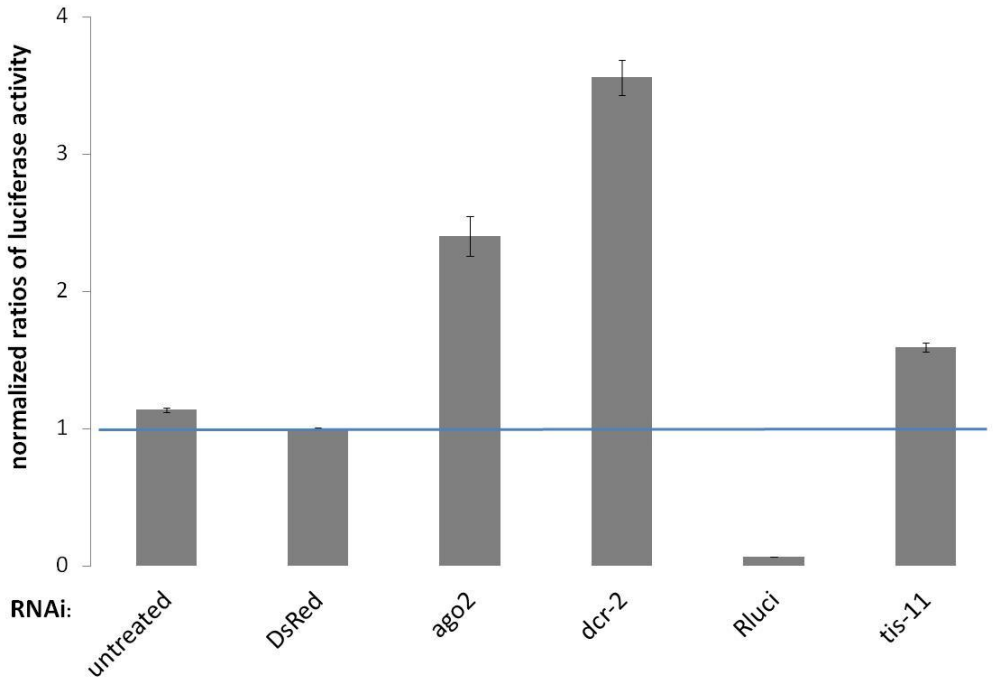

Figure 4-14: **Tis-11 has an effect on all Ago2-loaded RNA species.**
The stable cell line used in this experiment expressing Renilla-luciferase is known to be a suitable reporter to detect endo-siRNA response. RNAi triggers were depicted below the bars. *ago2* and *dcr-2* as known endo-siRNA factors served as positive controls. Luciferase-activity was measured and normalized to both the internal control Firefly-Luciferase and to the unrelated RNAi construct DsRed. Values are mean ± SD (n=3). The horizontal blue line marks no change compared to the control.

4.6 Tis-11 does not affect Ago1-mediated silencing

The depletion of *tis-11* results in de-repression of GFP in Ago2-RISC reporter cells (Figure 4-10B and 4-12). This led to the question if also Ago1-loaded RNAs are regulated by Tis-11.

S2 cells were transiently transfected with reporter constructs harbouring four partially complementary binding sites for bantam (ban-mi, Figure 4-16) in the 3'-UTR of GFP. *Drosophila*

Ago1 and Ago2 have distinct preferences for the architecture of their target sites. Ago1 will primarily silence a bulged match reporter while Ago2 targets a perfect match reporter (Shah and Forstemann 2008). After two days si/miRNA factors and *tis-11* were depleted and fluorescence measured by flow cytometry on day 7. The values were then normalized to control RNAi and a transfection control (pKF63) to avoid differences due to transfection efficiency.

Silencing of Ago1 and Dcr-1, required for miRNA biogenesis showed an increased GFP fluorescence compared to the control RNAi directed against DsRed (Figure 4-16). However depletion of *tis-11* could not de-repress the reporter. So Tis-11 has exclusively an effect on Ago2-loaded RNAs and not on Ago1-loaded RNAs.

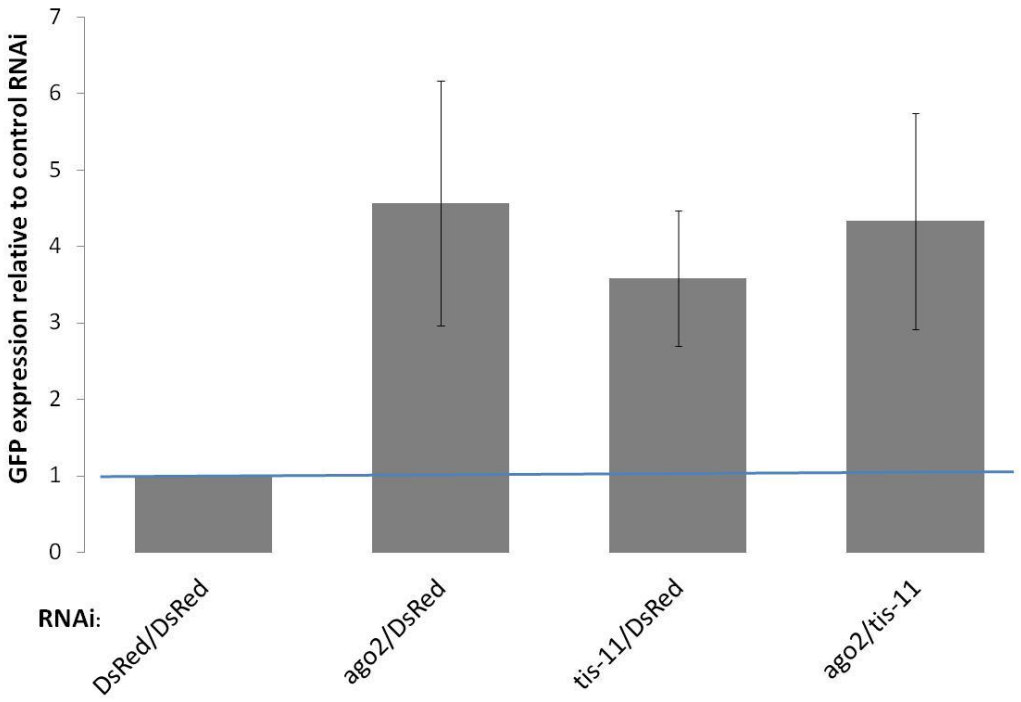

Figure 4-15: **Ago2 and Tis-11 act in the same pathway.**
miR-277 reporter cells (67-1D) were treated with RNAi triggers against *tis-11* and *ago2* at the same time. RNAi constructs were indicated below the bars. GFP fluorescence was measured with flow cytometry and normalized to control RNAi targeting DsRed. Values are mean ± SD (n=3). The horizontal blue line marks no change compared to the control.

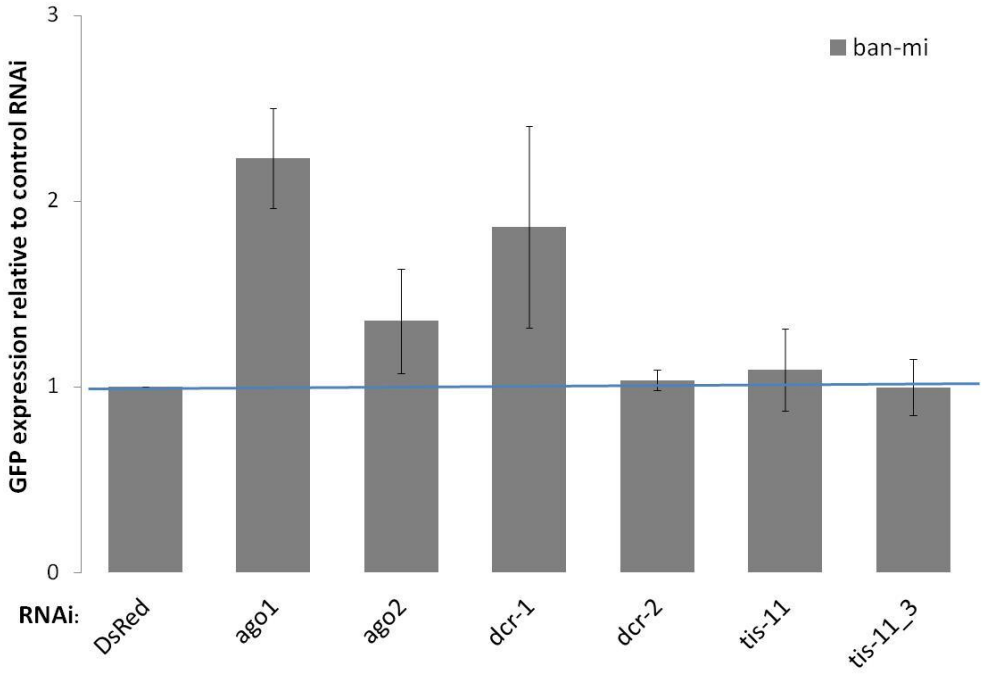

Figure 4-16: **Tis-11 does not influence Ago1-mediated silencing.**
S2 cells were treated twice with dsRNA constructs indicated below the bars targeting *tis-11* with two different constructs, *ago1, ago2, dcr-1* and *dcr-2*. Then they were transiently transfected with the ban-mi reporter construct. Ban-mi harbours four bulged binding sites for bantam in the 3'-UTR of GFP and is targeted by Ago1-loaded bantam. GFP-fluorescence was measured by flow cytometry and normalized to control knock-down DsRed and to the transfection control pKF63 (GFP without binding sites in its 3'-UTR). Values are mean ± SD (n=3). The horizontal blue line indicates a value of 1 (=no change relative to control).

4.7 Silencing of Tis-11 does not alter protein levels of Ago2 and Dcr-2

To exclude the possibility that indirect effects on the overall expression of Ago2 and/or Dcr-2 could simply explain the effects of depleted Tis-11, S2 cells were incubated with dsRNAs against si/miRNA factors and *tis-11*. Subsequently the protein levels were visualized via Western blotting. Ago2 levels were presented in Figure 4-17A and quantified relative to the loading control β-tubulin (Figure 4-17B). Knock-down of *tis-11* with both constructs does not lead to reduced Ago2 protein amounts compared to the control RNAi against DsRed. Solely the treatment with *dsago2* diminishes the Ago2 protein. Dcr-2 protein levels were investigated with the same procedure as used before (Figure 4-18A). One of the RNAi trigger *tis11_3* seems to lower Dcr-2 amount about 15% (Figure 4-

18B). But there was a technical problem with the transfer to the membrane in this lane, because not only the signal of Dcr-2 but also the one of R2D2 looks irregular. Summing up the depletion of *tis-11* does not appear to alter the protein levels of Ago2 and Dcr-2.

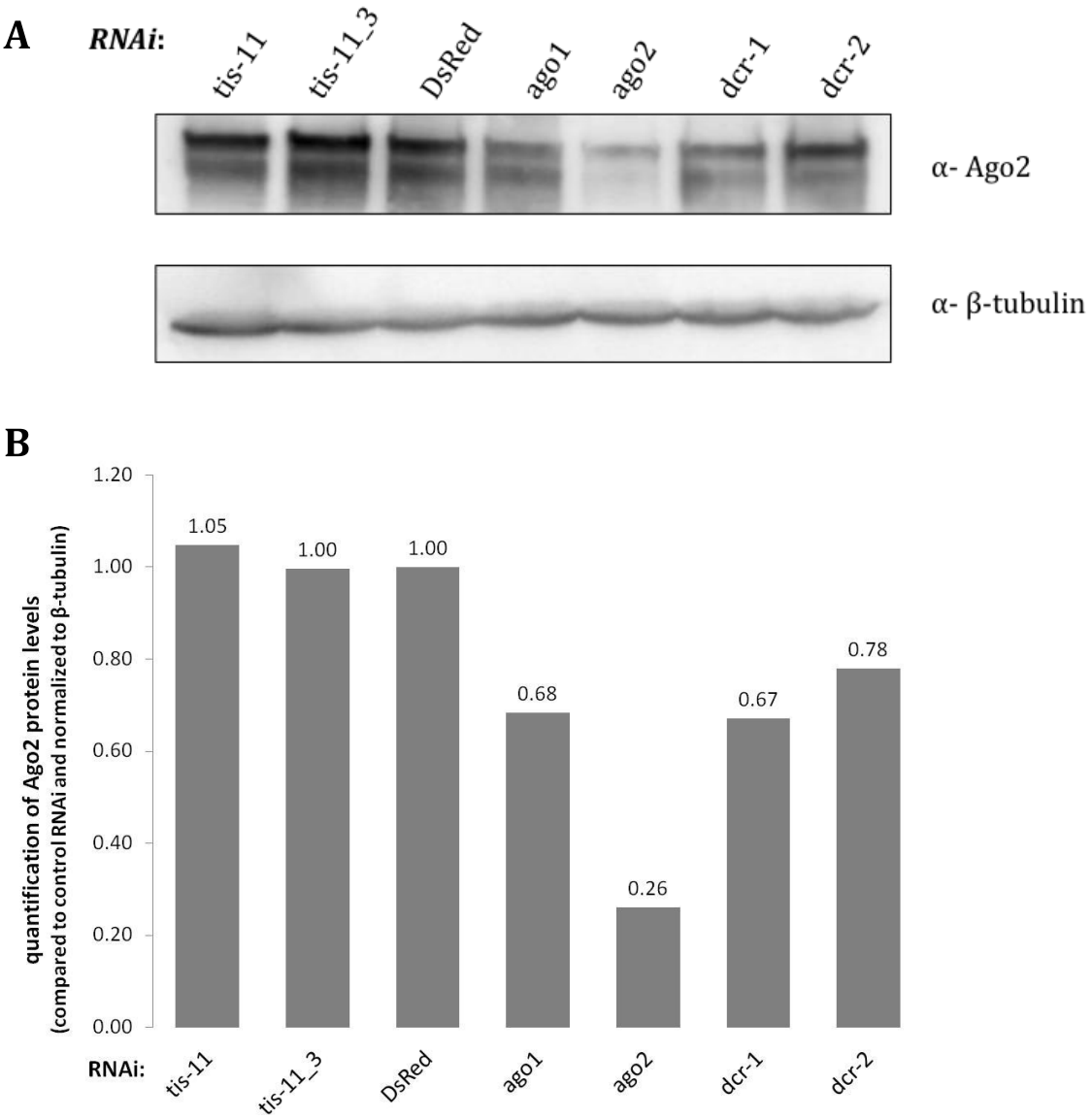

Figure 4-17: **Proteinlevel of Ago2 remained unchanged after knock-down of *tis-11*.**
A) S2 cells were treated twice with dsRNA constructs targeting *tis-11*, *ago1*, *ago2*, *dcr-1*, *dcr-2* and DsRed as control.). Proteins were isolated and analyzed by Western blotting. α-Ago2-QGQ visualizes endogenous Ago2 (upper panel). Anti-β-tubulin served as loading control (lower panel).
B) Quantification of Ago2 protein levels compared to control RNAi and loading control β-tubulin. The obtained values were indicated above the bars.

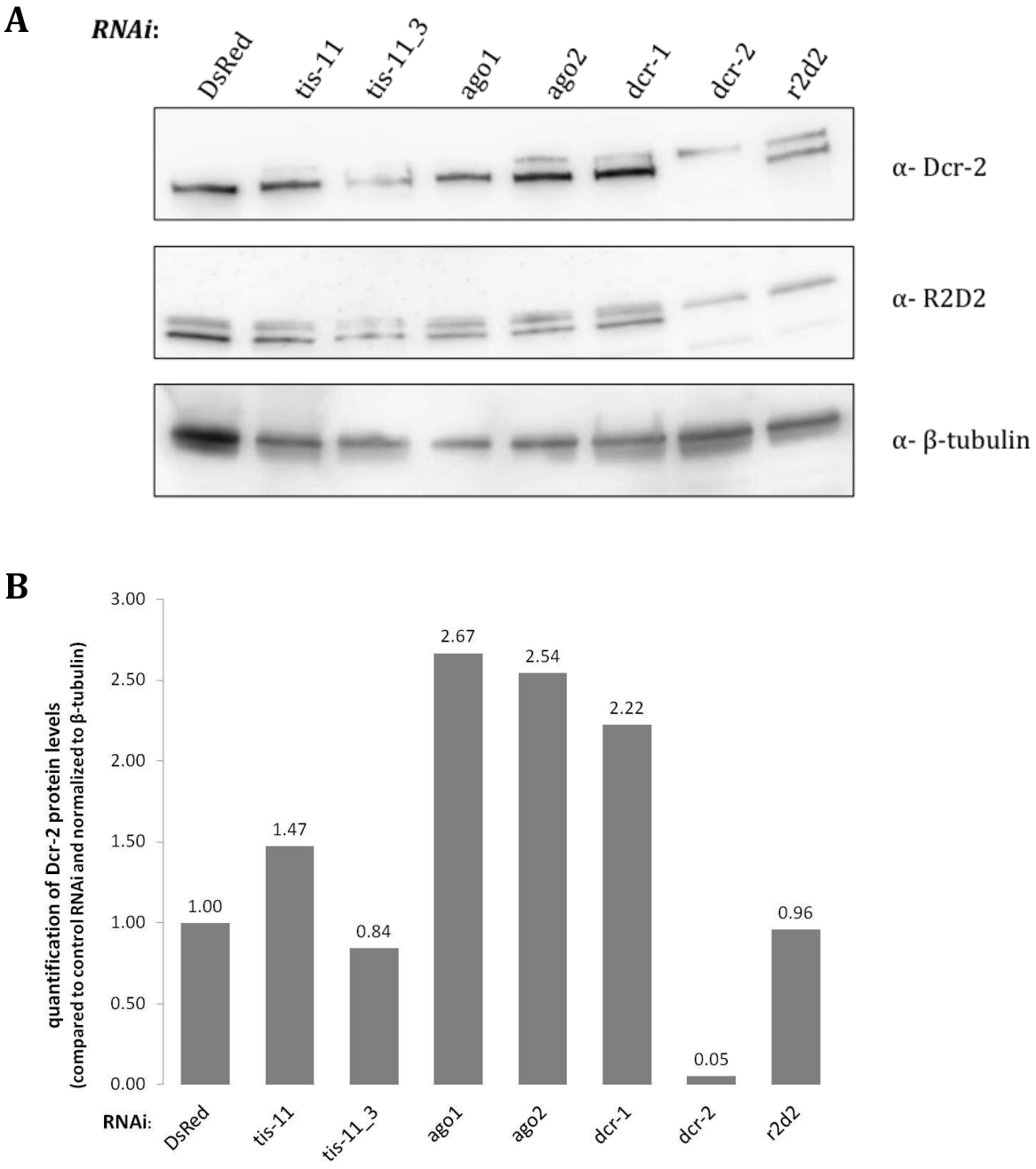

Figure 4-18: **Dcr-2 protein levels did not change after depletion of *tis-11*.**

A) S2 cells were treated twice with dsRNA constructs targeting *tis-11*, *ago1*, *ago2*, *dcr-1*, *dcr-2, r2d2* and DsRed as control.). Proteins were isolated and analyzed by Western blotting. α-Dcr-2 could detect endogenous Dcr-2 (upper panel). α-R2D2 visualized endogenous R2D2, which is unstable in the absence of Dcr-2. Anti-β-tubulin served as loading control (lower panel).

B) Quantification of Dcr-2 protein levels compared to control RNAi and loading control β-tubulin. The obtained values were indicated above the bars.

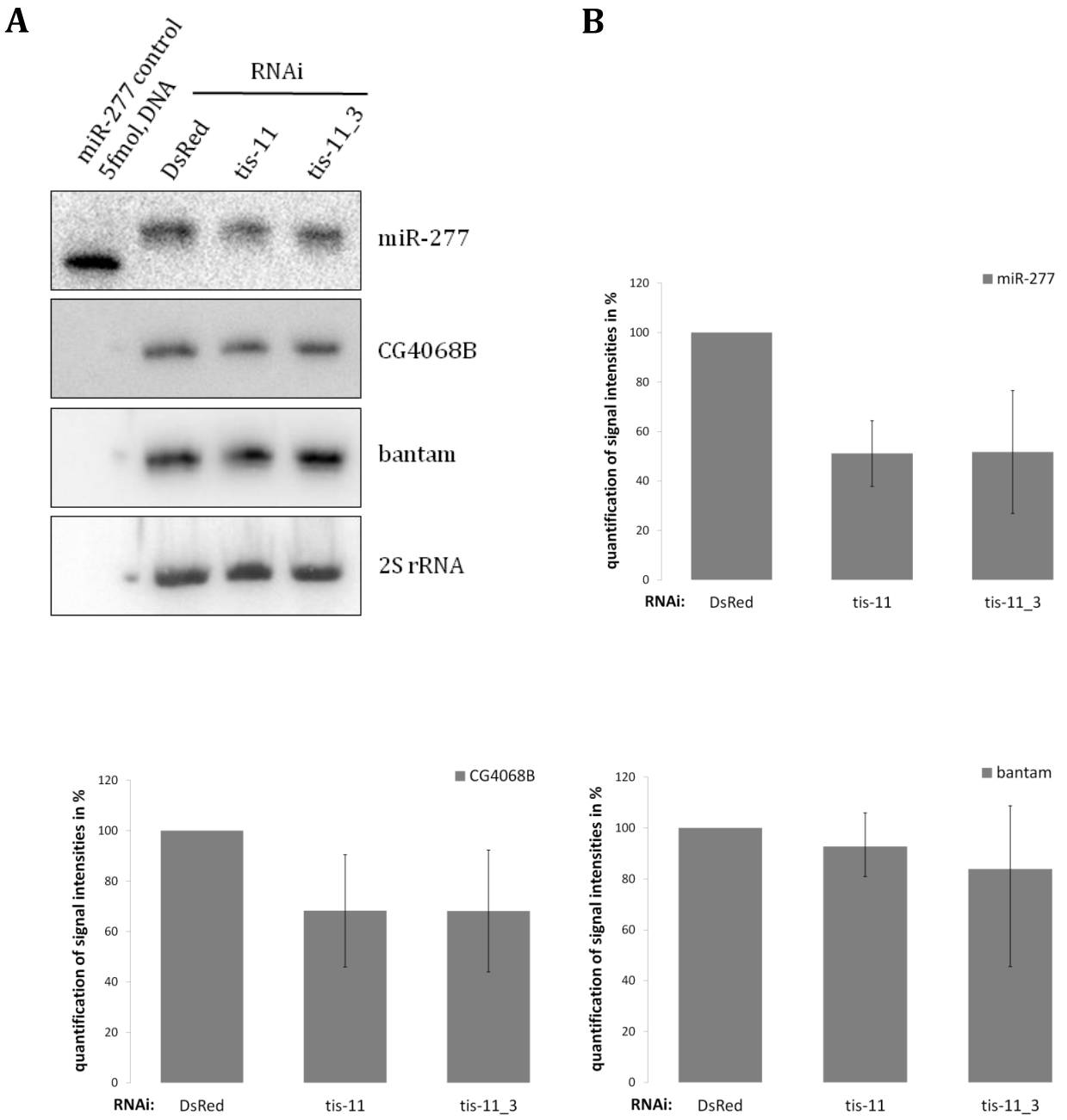

Figure 4-19: **Silencing of tis-11 impairs biogenesis of some Ago2-loaded small RNAs.**
A) *Drosophila* S2 cells were treated twice with dsRNA constructs *dstis-11*, *dstis-11_3* and DsRed as control. RNA was isolated and analyzed by Northern Blotting. 5 fmol of the miR-277 DNA oligo were also loaded. DNA probes against miR-277 (upper panel), hairpin-derived endo-siRNA CG4068B (second panel), and bantam miRNA (third panel) were used. 2S rRNA (bottom panel) served as a control for loading.
B) Changes of small RNA abundance were quantified and presented as a mean of four independent trials ± SD respectively.

4.8 Depletion of *tis-11* impairs the biogenesis of some Ago2-loaded small RNAs

At first S2 cells were treated with dsRNAs directed against *tis-11* and as control DsRed. After RNA isolation the small RNAs were analyzed by Northern blotting (Figure 4-19A) and quantified after normalization with the ribosomal 2S rRNA (Figure 4-19B). Depletion of *tis-11* leads to significantly lowered levels of mature miR-277 and the endo-siRNA CG4068 compared to control RNAi. Only about 50% of mature miR-277 ($p<0.005$ or $p<0.03$, Student's T-Test) and 70% of CG4068 ($p<0.02$ or $p<0.08$, Student's T-Test) remained. CG4068 is derived from a long hairpin and like all endo-siRNAs primarily loaded into RISC with Ago2 (Okamura, Chung et al. 2008). In contrast the levels of mature bantam, which is predominantly loaded into Ago1-RISC, were not decreased.

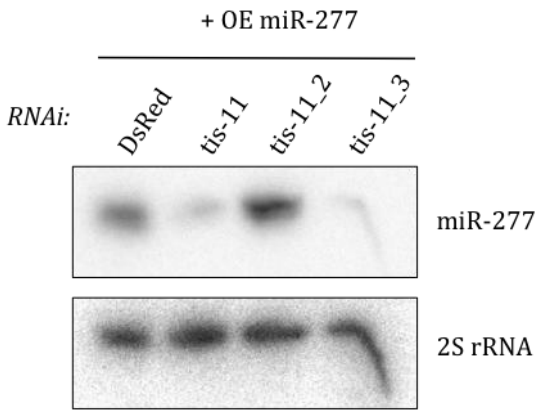

Figure 4-20: **Tis-11 does not regulate the transcription of miR-277.**
S2 cells were treated with dsRNA constructs *dstis-11*, *dstis-11_2*, *dstis-11_3* and DsRed as control and co-transfected with a plasmid overexpressing miR-277 (pKF84). RNA was analyzed on a Northern blot. The membrane was hybridized with DNA probes against miR-277 (upper panel), and 2S rRNA (bottom panel) as loading control.

This could be either due to inhibited transcription of the precursor or a difficulty later on in the biogenesis pathway of miR-277. We tested if the endogenous promotor of miR-277 is impaired after depletion of Tis-11 by transfecting S2 cells with a vector expressing miR-277 under the control of the ubiquitin-promotor (pKF84). Afterwards *tis-11* was silenced via RNAi with three different constructs and DsRed as control. The RNAs were analyzed with Northern Blotting probed for miR-277 and 2S rRNA (Figure 4-20). Using both constructs *dstis-11* and *dstis-11_3* the levels of mature miR-277 are clearly lowered compared to dsRNA directed against DsRed. Only *dstis-11_2*

showed no alteration in expression of the miRNA, which could be explained by the inefficient depletion of Tis-11 protein by this trigger (Figure 4-11). Since even when miR-277 was expressed from a heterologous promotor its levels were reduced upon *tis-11* depletion, transcriptional regulation cannot be the mechanism.

Another possible explanation for the lowered levels of mature miR-277 could be that the miR-277/277* duplex is not loaded into Ago2 due to the silencing of Tis-11. Consequently the miR-277*-strand is not degraded anymore and hence accumulates. An equivalent Northern Blot as used above was probed for miR-277*. However, there was no enrichment of the passenger strand detectable (data not shown). We therefore conclude that the step of loading is not impaired.

4.9 The distribution of small RNAs loaded into effector complexes with either Ago1 or Ago2 is changed upon inhibition of *tis-11*

DmHen1 (CG12367, Pimet) is the *Drosophila* homologue of HEN1 first discovered in plants. It has a conserved RNA methyltransferase domain and catalyzes 2'-*O*-methylation at the 3'-termini of Ago2-associated RNAs (Figure 4-21 and Figure 2-2B). This modification protects the RNA from uridylation and subsequent degradation by the exonucleolytic machinery (Ameres, Horwich et al. ; Ji and Chen). Unlike plant HEN1, DmHen1 acts on single-stranded RNA, which is maybe the final step in assembly of RISC after conversion of the duplex into ssRNA (Horwich, Li et al. 2007; Saito, Sakaguchi et al. 2007).

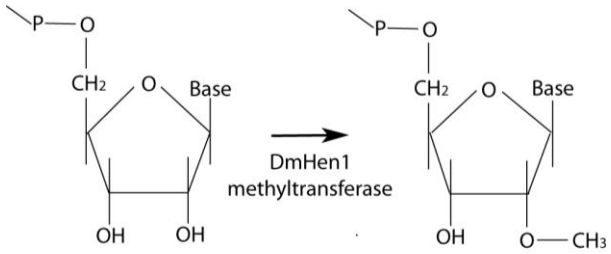

Figure 4-21: **DmHen1 catalyzes 2'-*O*-Methylation at the 3'-end of Ago2-loaded RNAs in *Drosophila*.**

The molecular structure of the RNA nucleotide at the 3'-end is represented. DmHen1 transfers a methylgroup from *S*-adenosyl-methionine (SAM) to the RNA in order to enhance its stability.

One other possibility is that Ago2-loaded small RNAs could not be stabilized anymore when Tis-11 is missing. Either the duplex is not even loaded into Ago2-RISC or DmHen1 does not methylate the guide strand. Tis-11 is possibly important for recruitment of the RNA methyltransferase to Ago2-RISC, its complete functionality or the loading of the duplex into Ago2. The methylation of the guide strand enables Ago2 to bind and cleave targets with extensive complementarity, because basepairing of the 3'-end of a small RNA displaces it from its usual binding site in the Ago2-PAZ domain and makes it susceptible for nucleases. DmHen1 does not modify Ago1-loaded RNAs, so they are restricted to regulate only partially complementary targets (Ameres, Horwich et al.).
In flies Ago1- and Ago2-loaded RNAs can be distinguished using the method of β-elimination. This includes first an oxidation step of the nucleic acid and then the switch of pH into high basic range. If the small RNA has two neighbouring free hydroxyl-groups at its 3'-end, i.e. it is not methylated at the 2'-OH-group, it can be oxidized. Through elevation of the pH value parts of the ribose backbone of the last nucleotide were split off. This can be visualized by Northern blotting in terms of a shift in mobility by about 1 nt. The RNA is resistant to the oxidation and the β-elimination procedure in presence of a modified 2'-OH-group.

A

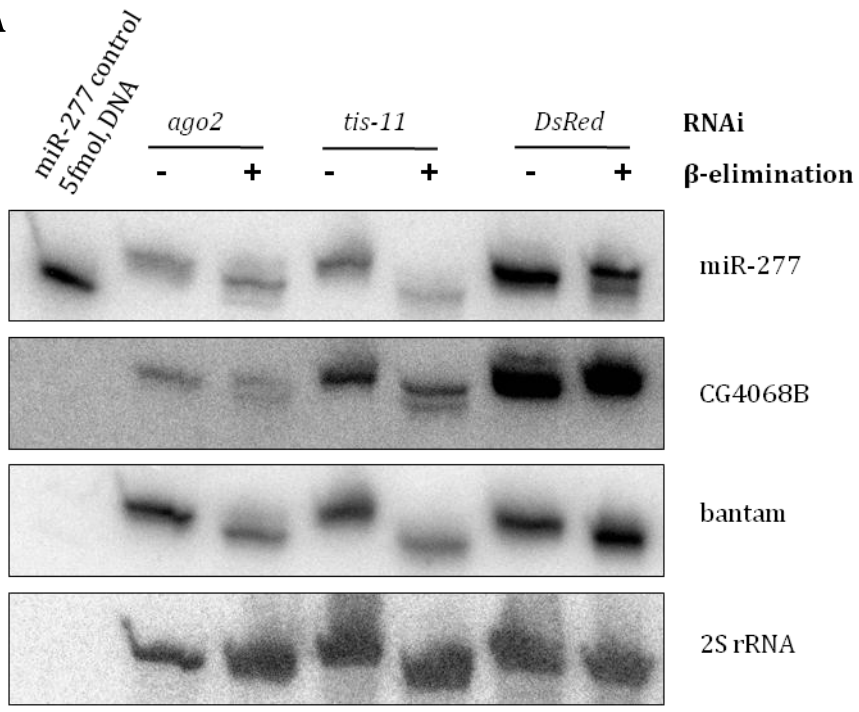

(figure continued on p.63)

B

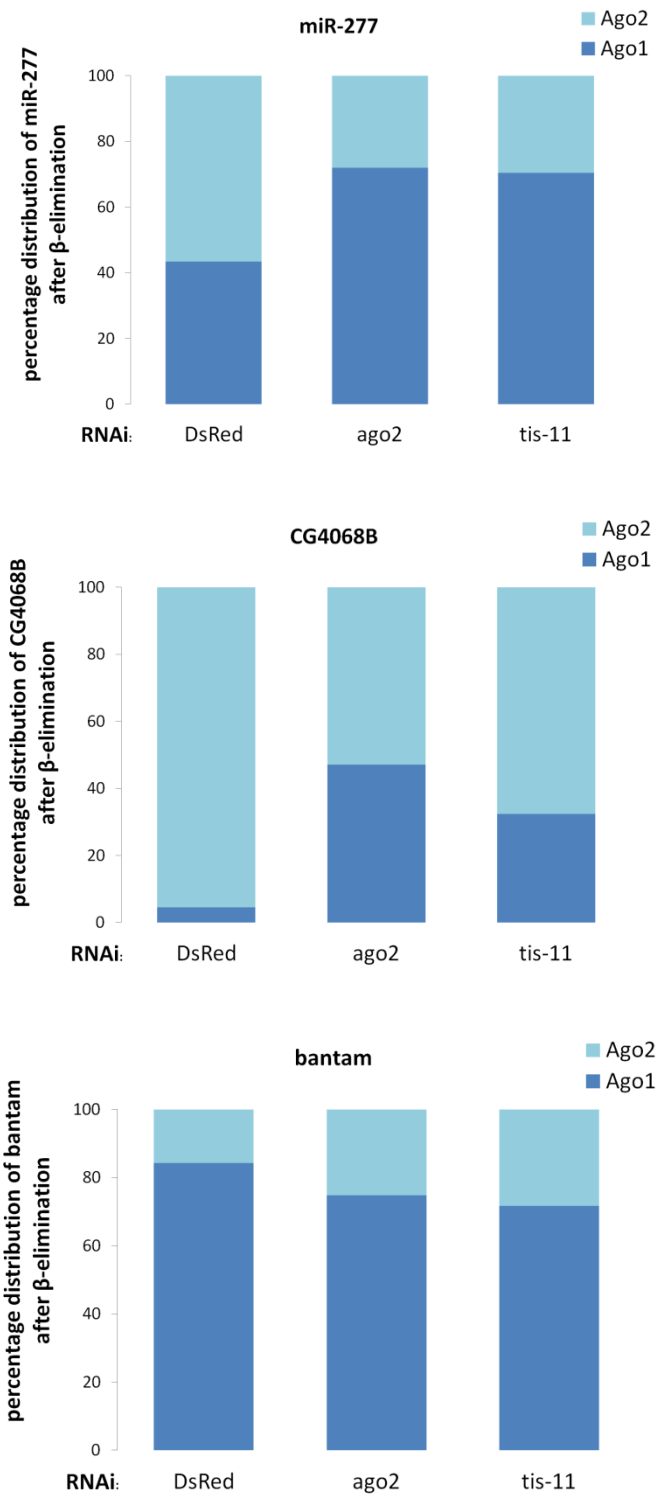

Figure 4-22: **The loading behaviour of small RNAs into effector complexes with Ago1 or Ago2 is altered after depletion of Tis-11** (figure legend continued on p.64).

(figure legend continued from p.63)
A) *tis-11*, *ago2* and DsRed were silenced in S2 cells and 40µg of the isolated RNAs were exposed to β-elimination. Untreated and treated RNA fractions were analyzed by Northern blotting. 5 fmol of the miR-277 DNA oligo were also loaded. The membrane was hybridized with DNA probes against miR-277 (upper panel), hairpin-derived endo-siRNA CG4068B (second panel), and bantam miRNA (third panel). 2S rRNA (bottom panel) served as a control for efficiency of β-elimination treatment.
B) Quantification of the distribution between methylated (light blue) and unmethylated (dark blue) fractions of the RNAs for miR-277, CG4068B and microRNA bantam. Values are the mean of two experiments.

The isolated RNA was exposed to β-elimination after depletion of *tis-11*, *ago2* and DsRed via RNAi in S2 cells. Figure 4-22A displays a Northern Blot with the β-eliminated RNA probed for miR-277, CG4068B, bantam and 2S rRNA. The distribution of unmethylated and methylated fractions of the RNA were quantified and displayed separately in Figure 4-22B. The miR277/277* duplex is more extensively basepaired than typical miRNA duplexes that are interrupted by mismatches and therefore predominantly loaded into Ago2 (Forstemann, Horwich et al. 2007). As expected almost 60% of miR-277 are loaded into RISC with Ago2 and methylated under control conditions (RNAi DsRed, Figure 4-22 upper panel). Cellular concentrations of miR-277 were decreased after depletion of *ago2*. Under these conditions also more Ago1-loaded miR-277 (+20%) could be observed (Figure 4-22 upper panel). Interestingly the same is true after silencing of *tis-11*. The level of miR-277 is lowered and also the stabilization of the RNA is clearly diminished. Hence more Ago1-loaded RISC complexes were programmed (Forstemann, Horwich et al. 2007).
A similar behaviour can be observed for the hairpin-derived endo-siRNA CG4068B that is primarily associated with the Ago2-effector complex (90%) and therefore methylated (Figure 4-22 second panel). Again *dstis-11* and *dsago2* result in higher fractions of unmethylated RNA species respectively. The miRNA bantam is described to be predominantly loaded into RISC with Ago1 (80%) and hence prone to β-elimination (Okamura, Ishizuka et al. 2004). Silencing of *tis-11* and *ago2* do not change this distribution (Figure 4-22 third panel). All together Tis-11 seems to be involved either in the loading of the RNA into RISC or the proper function of DmHen1.

4.10 Tis-11 is transiently associated with Ago2 and Dcr-2

In order to over-express Tis-11 in S2 cells the sequences of both isoforms with a N-terminal tandem-myc-tag were inserted into a *Drosophila* expression vector. A tubulin-promotor drives the expression of both isoforms Tis-11 PA (pSH13) and Tis-11 PB (pSH15, Figure 4-23).

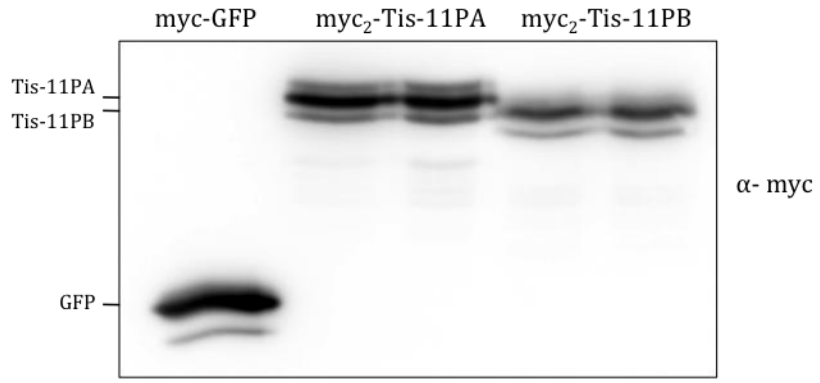

Figure 4-23: **Tis-11PA and Tis-11PB could be over-expressed in S2 cells.**
S2 cells were transfected with vectors driving the expression of myc_2-Tis-11PA (pSH13) and myc_2-Tis11-PB (pSH15, both tubulin-promotor) and myc-GFP (pKF63, ubiquitin-promotor) as control. Proteins were isolated and analyzed by Western blotting (each 30µg extract). α-myc detects the over-expressed proteins. Tis-11 migrates as a double band due to different phosphorylation status (Lauwers, Twyffels et al. 2009).

Previously it was shown that inhibition of *tis-11* results in de-repression of the reporter in miR-277-responsive cells (67-1D, Figure 4-10B). So the question rose if over-expression of Tis-11 leads to a hyper-repression of the GFP-signal in the same reporter cells. Therefore endo-siRNA reporter cells (63-N1) and 67-1D cells were transiently transfected with a construct over-expressing miR-277 (pKF84) and the Tis-11 encoding plasmids pSH13 and pSH15. The fluorescence was measured after four days and normalized to transfection control with pUC18 (Figure 4-24). As expected, an elevated miR-277 level (pKF84) resulted in hyper-repression of the GFP-reporter in 67-1D cells compared to the control (Figure 4-24B). However the over-expression of Tis-11 had no effect on both reporter cell lines.

The next aim was to identify factors of the small RNA silencing pathway as potential interaction partners of Tis-11. If Tis-11 is required for the loading of RNAs into Ago2-RISC it may interact with factors of the RLC. For that reason myc-tagged R2D2 and also different isoforms of Loquacious (Loqs) were precipitated and tested by Western Blotting if endogenous Tis-11 is bound to each of them. Neither R2D2 nor Loqs PB, Loqs PD (Figure 4-25), Loqs PA (data not shown) are associated with Tis-11.

Tis-11 PA (pSH13) and Tis-11 PB (pSH15) were immuno-purified with beads binding solely the myc-tagged constructs (Figure 4-26, bottom panel). Afterwards the recovered fractions could be analyzed regarding the identification of putative binding partners. Figure 4-30 demonstrates that not only Ago2 (upper panel) but also Dcr-2 (middle panel) are bound to both isoforms of Tis-11. Furthermore Ago2 is not bound to the negative control myc-GFP and only a minor fraction of Dcr-2

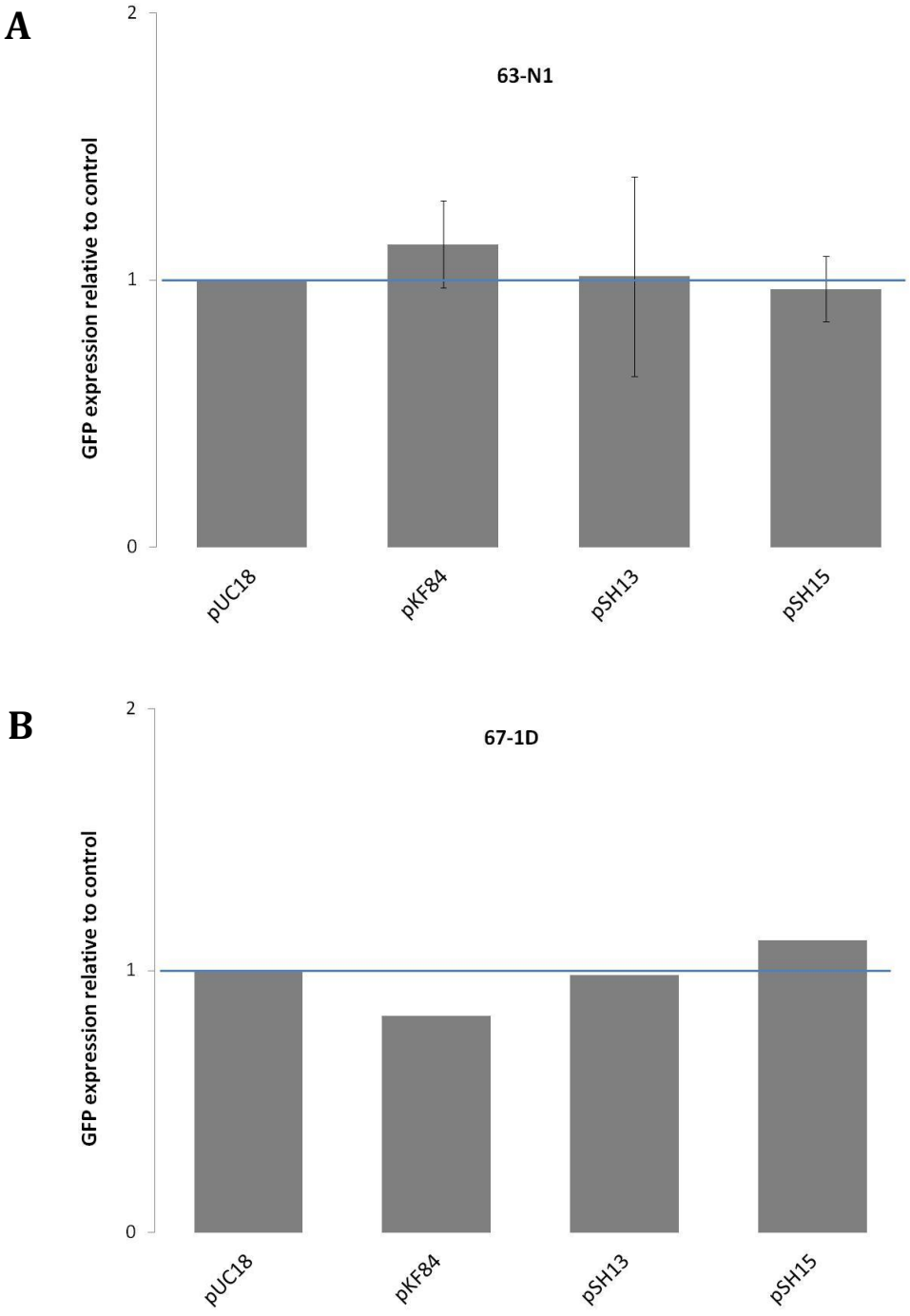

Figure 4-24: **Overexpression of Tis-11 does not lead to a hyper-repression of Ago2-reporter cells.**
A) Endo-siRNA reporter cells (63-N1) were transfected with plasmids overexpressing miR-277 (pKF84), Tis-11PA (pSH13), Tis-11PB (pSH15) and the unrelated control pUC18. GFP-fluorescence was measured by flow cytometry and normalized to the control pUC18. Values are mean ± SD (n=3). The horizontal blue line marks no change compared to the control.
B) analogous to **A)** using miR-277 reporter cells (67-1D), with two perfectly matching sites for miR-277 in the 3'UTR of GFP. Values are the mean of two experiments.

is associated with it in an unspecific manner, which can be neglected. In addition, the precipitation of flag-tagged Ago2 could demonstrate that at least a small fraction of Tis-11 PA and Tis-11 PB is bound to Ago2 (Figure 4-27).

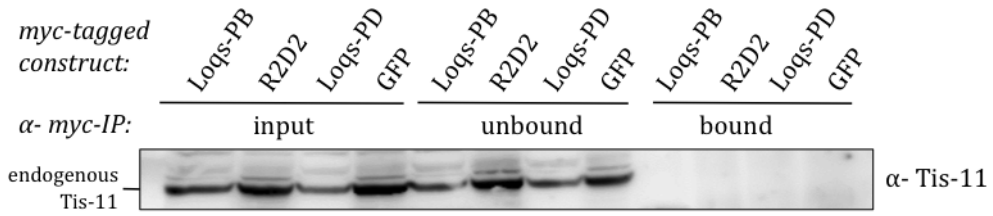

Figure 4-25: **Endogenous Tis-11 is not associated with R2D2 and Loquacious.**
Detection of endogenous Tis-11 using α-Tis-11-HHYA from S2 cell extracts after immunoprecipitation of myc-R2D2, myc-LoqsPB and myc-LoqsPD. Agarose-beads coated with α-myc antibody were used for IP; myc-GFP served as a control.

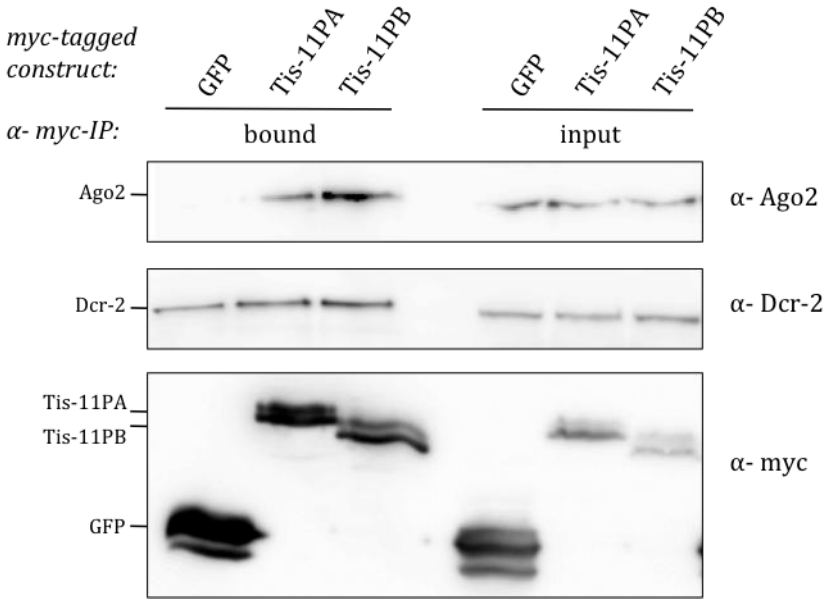

Figure 4-26: **Ago2 and Dcr-2 are bound to Tis-11.**
Both myc-tagged isoforms of Tis-11 were over-expressed in S2 cells and isolated from the whole cell extract using agarose-beads coated with α-myc antibody. Myc-GFP served as an unrelated control. The Western blot was probed with α-Ago2-QGQ (upper panel), α-Dcr-2 (middle panel) and α-myc (bottom panel) to verify successful immunoprecipitation of Tis-11.

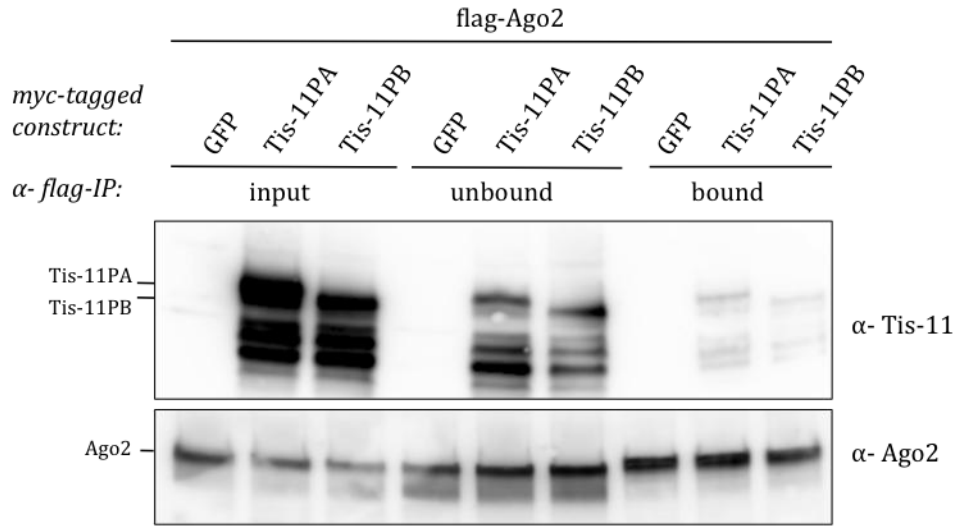

Figure 4-27: **Tis-11 is associated with flag-Ago2.**
Plasmids expressing flag-Ago2 and myc-Tis-11 (pSH13, pSH15) were co-transfected into S2 cells. Myc-GFP acts as an unrelated control. α-flag antibody was used for IP. The immunoprecipitates were analyzed with Western blotting using α-myc to detect Tis-11 (upper panel) and α-Ago2-QGQ to verify successful isolation of Ago2.

The protein extract of S2 cells transfected with pSH13 and pSH15 respectively was treated with RNaseA, an endoribonuclease that cleaves single-stranded RNA, to investigate if the association of Tis-11 and Ago2 is RNA dependent. Subsequently, the myc-tagged proteins were precipitated and analyzed by Western Blotting. The binding of Tis-11 and Ago2 is diminished after incubation with RNaseA (Figure 4-28B) in comparison with the untreated control (Figure 4-28A). We conclude that RNA mediates the interaction between Tis-11 and Ago2.

In a parallel experiment it was tested whether Tis-11 is also bound to some small RNAs. Therefore myc-Tis-11, flag-Ago2 and endogenous Ago1 were immunoprecipitated from S2 cells. The isolated RNAs were purified with TRIzol and visualised by Northern Blotting (Figure 4-29). MiR-277 is known to be associated with both Ago2 and Ago1, however preferentially loaded into RISC with Ago2 (Forstemann, Horwich et al. 2007). MiR-277 could be recovered more efficient in the Ago1 precipitate than in Ago2, because flag-Ago2 is present in addition to endogenous Ago2 in the cell. Therefore, the precipitated flag-Ago2 did not capture the entire pool of Ago2-loaded small RNAs. But both isoforms of Tis-11 were not associated with miR-277 (Figure 4-29, upper panel).

As expected the miRNA bantam is exclusively bound to Ago1 and the endo-siRNA CG4068B to Ago2. However neither bantam nor CG4068B were detectably bound to Tis-11PA and Tis-11PB (Figure 4-

29, middle panel). The ribosomal 2S rRNA was used as a control (Figure 4-29, bottom panel). Taken together none of the tested RNAs is stably associated with Tis-11.

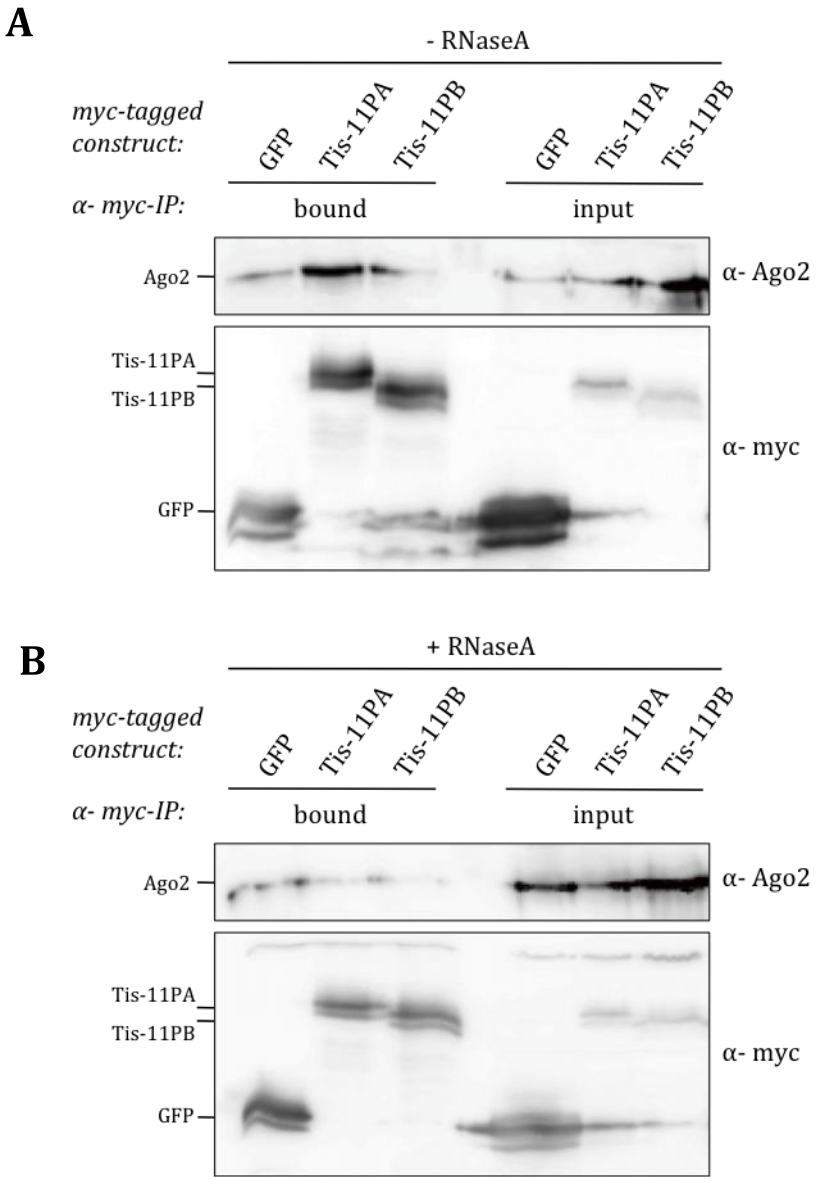

Figure 4-28: **RNA mediates the association of Tis-11 and Ago2.**
A) Co-immunoprecipitation of myc-Tis-11 (pSH13, pSH15) and tomato-Ago2 from S2 cells. Myc-GFP served as a control. Agarose-beads coated with α-myc antibody were used for IP. The Western blot was probed with α-Ago2-QGQ (upper panel) and α-myc (bottom panel) to verify successful immunoprecipitation of Tis-11.
B) analogous to **A)**. However the protein extract was incubated with RNaseA in order to deplete nucleic acids from the reaction and determine if RNA is required for binding of Ago2 and Tis-11.

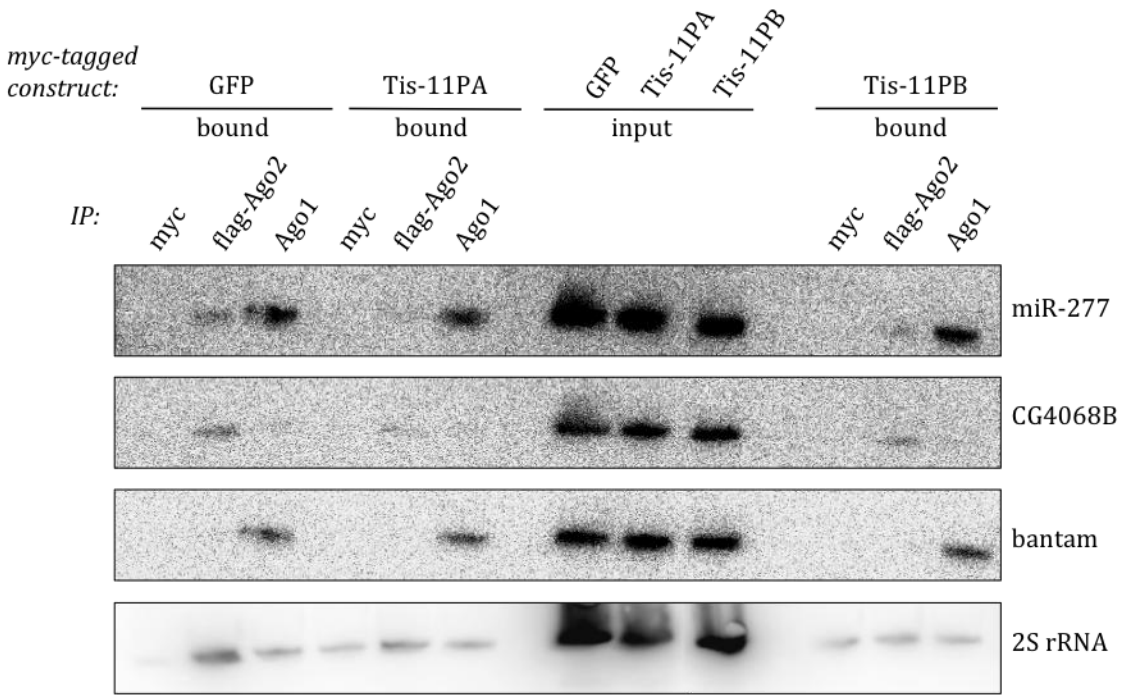

Figure 4-29: **Tis-11 is neither stably associated with miR-277, CG4068B nor bantam.**
Vectors encoding flag-Ago2 and myc-Tis-11 (pSH13, pSH15) were co-transfected into S2 cells. Myc-GFP served as a control. α-myc, α-flag and α-Ago1 antibody were used for IP. Bound RNA was isolated and analyzed with Northern blotting. The same membrane was hybridized with DNA probes against miR-277 (upper panel), hairpin-derived endo-siRNA CG4068B (second panel), microRNA bantam (third panel) and 2S rRNA (bottom panel).

4.11 Hen1-Methyltransferase is not in complex with Tis-11

In order to further localize the exact step of Tis-11 action in the small RNA silencing pathway a plasmid encoding the methyltransferase DmHen1 was generated. The reason for this was that it was previously shown that Tis-11 is possibly required for the stabilization of the RNA by DmHen1 (see chapter 4.9). Figure 4-30 illustrates the expression of flag-tagged DmHen1 in S2 cells under the control of a tubulin-promotor. To analyze if Tis-11 and DmHen1 are bound to each other both proteins were simultaneously over-expressed in *Drosophila* cells. Afterwards both isoforms of Tis-11 were immunoprecipitated via their myc-tag and analyzed if flag-DmHen1 is recovered in the bound fractions (Figure 4-31). Co-transfection and immunoprecipitation of myc-GFP and flag-DmHen1 served as a control. No association with flag-DmHen1 could be detected in the bound

fractions of myc-Tis-11PA and myc-Tis-11PB. Hence it is unlikely that Tis-11 is necessary for recruitment of DmHen1 to Ago2-RISC.

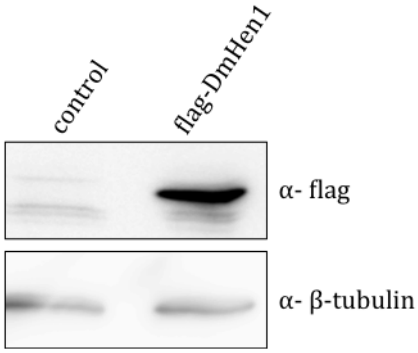

Figure 4-30: **Over-expression of flag-DmHen1 in *Drosophila* S2 cells.**
Plasmid encoding for flag-DmHen1 was transfected into S2 cells. The expression of flag-DmHen1 was detected by Western blotting using α-flag antibody and anti-β-tubulin as loading control.

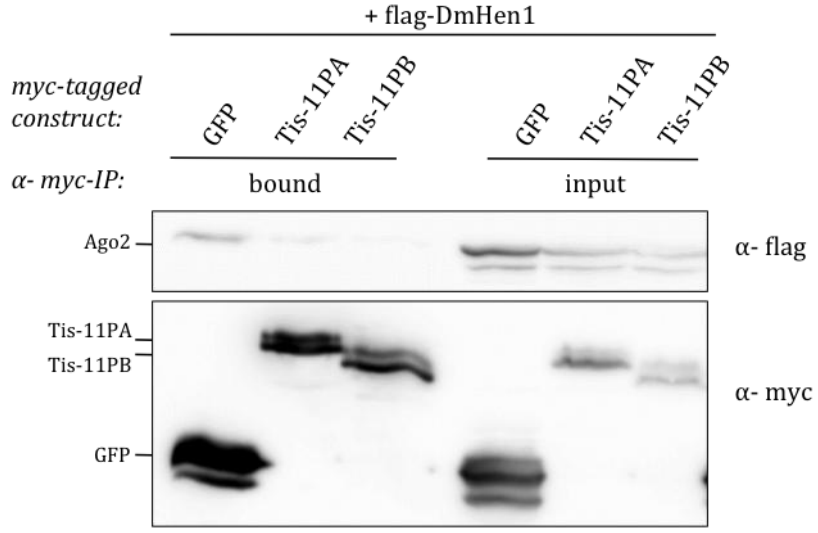

Figure 4-31: **DmHen1 is not bound to Tis-11.**
Flag-DmHen1 and myc-Tis-11 (pSH13, pSH15) were co-expressed in S2 cells. Myc-GFP was used as control. α-myc antibody was used for IP. The isolated fractions were analyzed by Western blotting using α-flag to detect DmHen1 (upper panel) and α-myc (bottom panel) to verify the successful immunoprecipitation of Tis-11.

4.12 Generation of transgenic flies over-expressing Tis-11 *in vivo*

The UAS/Gal4-system from yeast could be used for expression of almost any gene of interest in *Drosophila*. A big advantage of this system is the possibility to activate the expression of a gene only in special cell types or at a specific time point. There exist many different fly lines expressing the yeast transcription factor Gal4 under the control of a tissue-specific promotor. Mating these Gal4-driver-lines to strains carrying the sequence of gene X fused to an upstream activating sequence (UAS) element start the expression of gene X in the particular cell types. Gal4 binds with its DNA-binding domain to the UAS-element and induces transcription of gene X via its activation domain (Figure 4-32). The effects of gene X could then be studied in the progeny (St Johnston 2002).

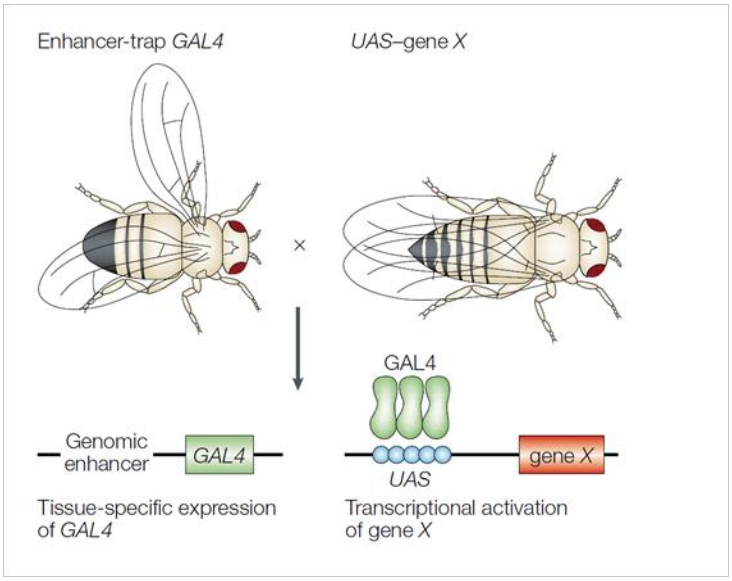

Figure 4-32: **Gal4-UAS system for directed gene expression.**
Flies carrying a transgene with a UAS-promotor element are mated with a driver line, encoding for the yeast transcription factor Gal4 in a tissue-specific manner. The gene of interest is activated in the offspring. Adapted from (St Johnston 2002).

The bacteriophage ΦC31-integrase system is an efficient tool to insert P-elements at a specific position in the *Drosophila* genome and hence generate transgenic flies. To obtain a non-random integration, a characterized attP-landing site (phage-attachment site) in the genome and the integration vector carrying the complementary attB-site (bacterial-attachment site) are required. The vector carrying the transgene and the attB-sites is injected into recipient embryos harbouring the attP-landing-sites. These two sites share a central region where the crossover can occur and is

flanked by imperfect repeats. The ΦC31-integrase is endogenously expressed in germ cells via the *vasa* promotor and after the recombination the attB and attP sites are no longer substrates for the integrase. The integration occurs at the provided landing site with a high degree of specificity, to enable site-specific integration of the transgene. Over one hundred fly lines with installed attP-landing sites throughout the genome are generated and molecularly characterized (Figure 4-33, (Bischof, Maeda et al. 2007; Bischof and Basler 2008).

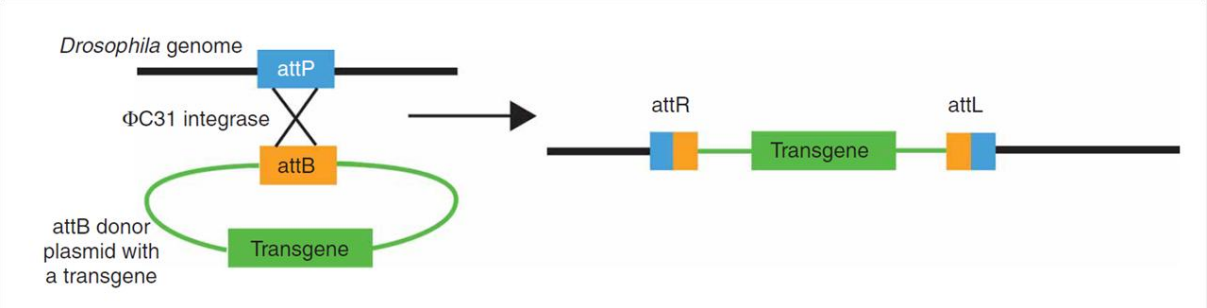

Figure 4-33: **Schematic overview of ΦC31-mediated integration.**
ΦC31 integrase mediates recombination between attP site in the *Drosophila* genome and the attB site present on a vector. This allows site-specific integration of any gene of interest in the *Drosophila* genome in order to generate transgenic flies. Adapted from (Fish, Groth et al. 2007).

Transgenic flies were generated to express both isoforms of Tis-11 with a N-terminal tandem-myc-tag under the control of the UAS/Gal4-system. The coding sequences of Tis-11 PA and Tis-11 PB were inserted in the pUAST-attB vector and transfected in S2 cells together with a plasmid expressing Gal4 under the control of a tubulin-promotor. After three days proteins were isolated and analyzed by Western blotting (Figure 4-34A). The signal intensity of the antibody directed against the myc-tag demonstrates that both isoforms are highly expressed. So the plasmids were sent for embryo injection and a couple of homozygous fly lines were recovered for each Tis-11 isoform.

These flies were crossed to different Gal4-driver-lines, which express Gal4 and consequently Tis-11 in a tissue-specific manner. An expression of both Tis-11 isoforms in the nervous-system (elav-Gal4) and ubiquitously (actin-Gal4) has deleterious effects in the fly and leads to an early larval lethality (data not shown). Furthermore, muscle-specific over-expression (mhc-Gal4) of Tis-11 leads to a drastic delay in the development and the offspring hatched not until about 16 days (compared to 10 days in wild type, data not shown). Additionally they showed a severe phenotype know as erect wing (ewg). Protein was extracted from parental flies, adult and larval offspring and

analyzed by Western blotting (Figure 4-34B). Tis-11 expression could only be detected in the fractions obtained from the muscle tissue of the adult progeny.

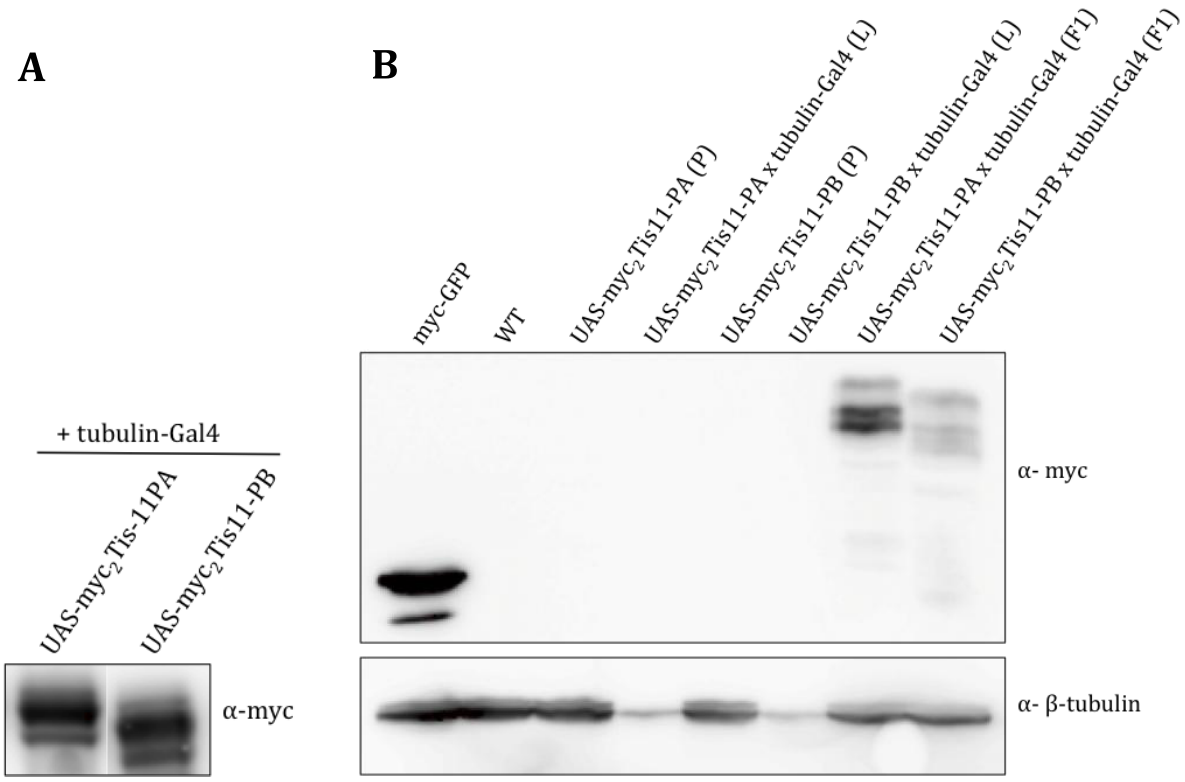

Figure 4-34: **Generation of transgenic flies expressing myc-Tis-11 *in vivo*.**
A) Expressiontest of UAS-myc$_2$-Tis-11PA and UAS-myc$_2$-Tis-11PB co-transfected with tubulin-Gal4 in S2 cells. Proteins were analyzed by Western blotting using α-Tis-11-HHY9 antibody.
B) Transgenic flies carrying UAS-myc$_2$-Tis-11PA and UAS-myc$_2$-Tis-11PB respectively were crossed with mhc-Gal4 flies, which express Gal4 specifically in muscle cells. Proteins were extracted from larval and adult progeny. Parental flies, WT and myc-GFP expressing flies were used as controls. Western Blot was probed with α-myc (upper panel) and anti-β-tubulin as loading control.

4.13 Heterologous expression of Tis-11 and characterization of the binding behaviour

Recombinant Tis-11 was expressed in *E.coli* to further characterize its role in the siRNA pathway. Using anisotropy measurements it would be possible to test if and how tight Tis-11 binds to factors of the small RNA system, more precisely recombinant Dcr-2, Dcr-2/Loqs-complex, R2D2 and Ago2.

Also binding assays with different small RNA constructs were thinkable to study the binding behaviour of Tis-11.

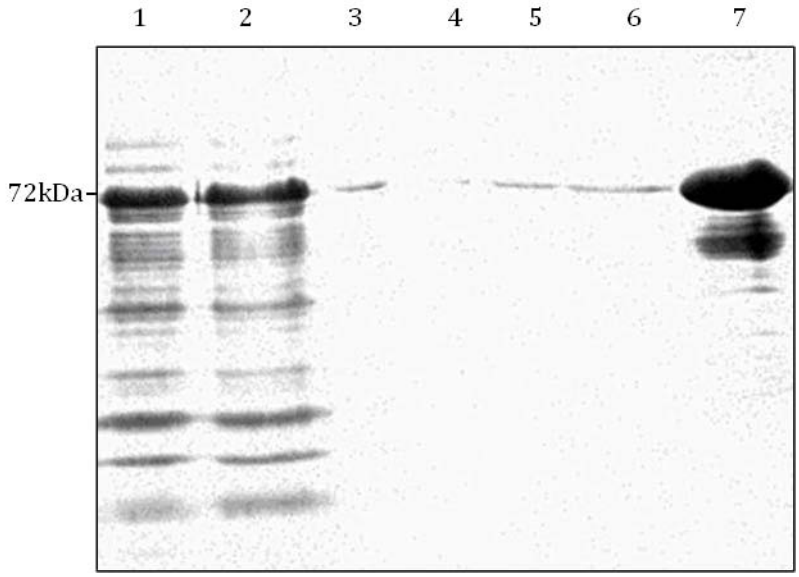

Figure 4-35: **Expression and purification of heterologous GST-Tis-11PA.**
Samples from different steps of expression and subsequent purification of GST-tagged Tis-11PA were analyzed on a 12% SDS-PAGE. Lane 1 visualized over-expressed GST-Tis-11PA after induction with 1 mM IPTG for 4h. In order to isolate GST-tagged Tis-11 the protein extract was incubated with GSH-beads. Lane 2 showed the unbound fraction and Lanes 3 to 6 different washing steps with low salt buffer to remove unspecifically bound proteins. The eluted GST-Tis-11PA is visible in Lane 7.

The conditions of Tis-11PA expression and the subsequent step of purification of the protein were optimized with the help of Saskia Gressel.

The coding sequence of Tis-11PA was inserted into the inducible vector pGEX6. After IPTG induction Tis-11PA is expressed with a N-terminal GST-tag, which enables the isolation of the desired protein from the whole cell extract.

After several steps of variation in conditions for expression and purification of Tis-11 the optimal requirements were achieved. Tis-11PA could be solubly expressed after induction with 1mM IPTG and incubation at 37°C for 4 hours (Figure 4-35). Afterwards GST-tagged Tis-11PA could be isolated from the cell suspension and purified by incubation with GSH-beads and its subsequent elution. The eluate was dialyzed with the PreScission protease, which removes the GST-tag from the protein. The removal of the tag was very efficient, because only a small fraction of uncut fusion protein remained in the samples (Figure 4-36A). To eliminate the sole GST-tag and the uncut proteins the

sample was again purified with a GST-column. The desired Tis-11PA protein that had no GST-tag anymore was recovered almost pure in the unbound fraction (Figure 4-36B). This sample was used to investigate the binding with dsRNA via fluorescence polarization. However only a few preliminary data sets for the binding behaviour of Tis-11PA were obtained, because the parameters for the measurement have to be optimized first. The sole reliable result we achieved until now was that Tis-11PA definitely binds to dsRNA and the calculated equilibrium constant K_D falls in the range of 300nM (data not shown).

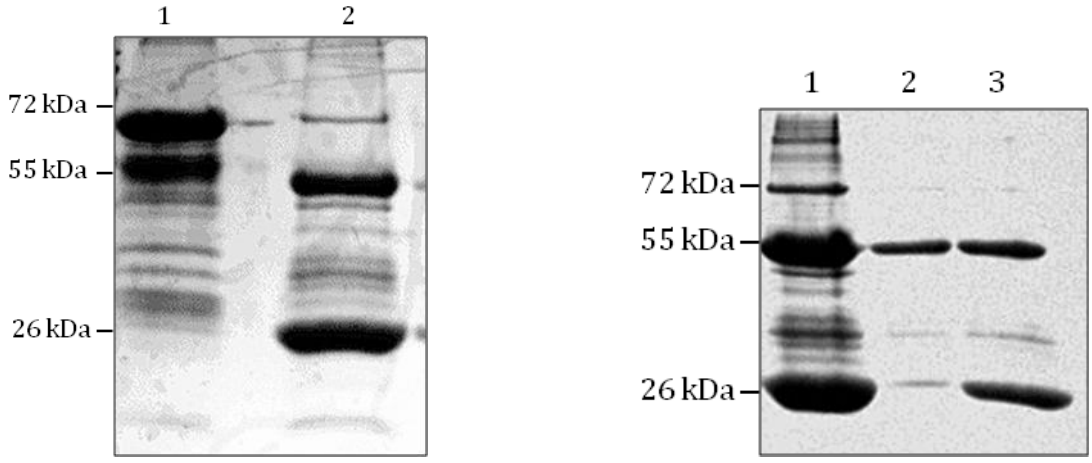

Figure 4-36: **Heterologous Tis-11PA after removal of the GST-tag.**
A) The eluted GST-tagged Tis-11PA from Figure 4-35 (lane 1) was incubated with the PreScission protease in order to remove the GST-tag (lane 2).
B) The digested samples of **A)** were incubated with GSH-beads to eliminate the sole GST-tag and also uncut protein. The almost pure Tis-11PA is located in the unbound fraction.

4.14 Silencing of *tis-11 in vivo*

In vivo silencing of *tis-11* showed also an obvious phenotype. RNAi in flies could be accomplished by mating a tissue-specific Gal4-driver line to flies expressing small hairpin RNAs (hpRNAs) under the control of UAS-elements. They are processed by Dicer into siRNAs and lead to silencing of a gene of interest in the specific cell types (Figure 4-37). Two different RNAi fly lines are available to deplete *tis-11 in vivo*, VDRC line 12259 and 101765. The cross of the VDRC line 12259 with actin-Gal4-

driver line showed early embryonic lethality. Further the offspring of Mef2-Gal4 (muscle-specific expression of Gal4) was unable to finally hatch out of the pupae. Using the second VDRC line 101765 the progeny was viable in both cases, but the knock-down of *tis-11* was not very efficient (data not shown). The hairpins expressed from the RNAi-lines differ clearly in the number of trinucleotide-repeats they contain. VDRC line 12259 includes 14 CAN-repeats and is predicted to have 621 off-targets. Interestingly *ago2* is not among them. In contrast to VDRC line 101765 has just 2 CAN-repeats and did not target other mRNAs besides *tis-11*. So it is likely that a trans-effect on other mRNAs led to this severe phenotype of VDRC line 12259.

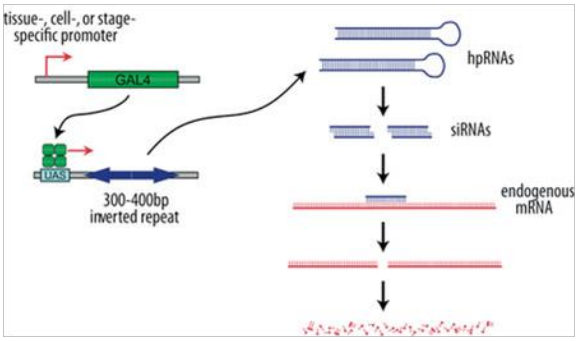

Figure 4-37: **RNAi in *Drosophila*.**
Gal4-UAS system can drive the expression of a double-stranded hairpin RNAs. These are processed by the RNaseIII enzyme Dicer into siRNAs that induce the decay of their cognate target mRNAs. Adapted from http://stockcenter.vdrc.at/control/rnailibrary.

4.15 Repetitive sequences in the transcripts of both, *tis-11* and *ago2*, imply an indirect effect after depletion of *tis-11* on the small RNA machinery due to reduced *ago2*-mRNA levels

So far, all observations place Tis-11 in an identical position as Ago2 with respect to siRNA biogenesis. We therefore assessed any potential off-target effects to exclude indirect modulation of Ago2 levels. $(CAN)_n$-repeats are present in many transcripts, and both *ago2* and *tis-11* are among them (Ma, Creanga et al. 2006). Before it was already shown that the protein level of Ago2 did not change after RNAi against *tis-11* (Figure 4-17A).

To this end, the mRNA level of *ago2* was measured after depletion of *tis-11*. Therefore, Ago2 and Tis-11 were silenced in S2 cells with the previously used RNAi triggers. Subsequently the mRNA

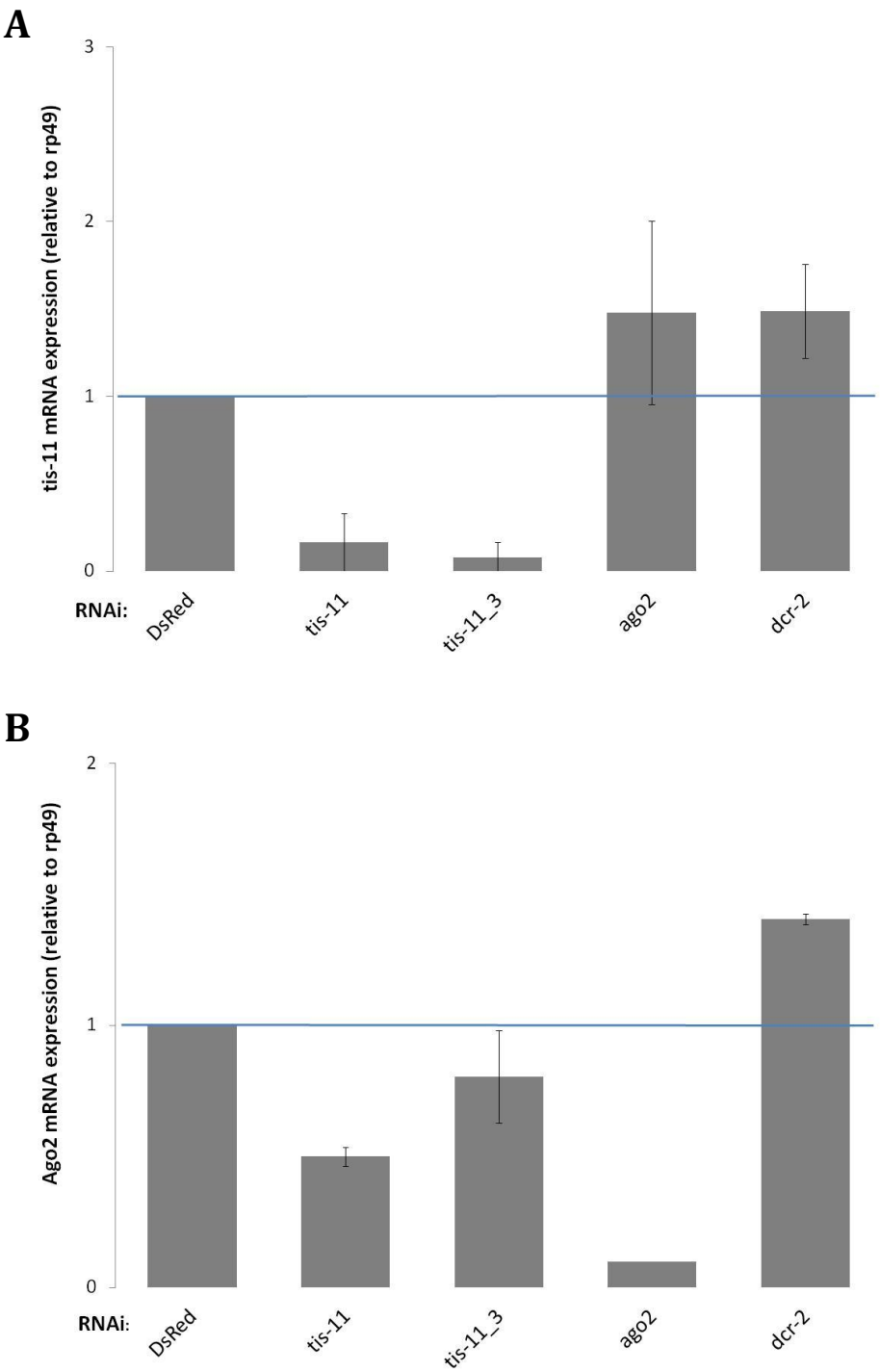

Figure 4-38: **Silencing of tis-11 reduces also *ago2*-mRNA levels.**
A) S2 cells were treated twice with RNAi triggers *dstis-11, dstis-11_3, dsago2* and dsDsRed as control. RNA was isolated, reverse transcribed and the *tis-11* mRNA level was measured by qRT-PCR to verify the silencing of *tis-11*. The values represent the fold change of each RNA (normalized to rp49) and control cells (DsRed). Values are mean ± SD (n=3). The horizontal blue line indicates a value of 1 (=no change relative to control).
B) analogous **A)** *ago2*-mRNA level was determined. The changes after depletion of tis-11 were significant when compared to the DsRed control ($p<0.002$, student's t-test, n=3).

levels were determined by qRT-PCR and normalized to the ribosomal *rp49*-mRNA. Figure 4-38A demonstrates the efficient knock-down of *tis-11*-mRNA with both dsRNAs ds*tis-11* and ds*tis-11_3*. The RNAi trigger *dstis-11_3* showed a slight reduction of *ago2* compared to the control, but with a high variability. However after depletion of *tis-11* with the construct *dstis-11* only 50% of the initial *ago2*-mRNA level was retained (Figure 4-38B).

Consequently a new pair of dsRNAs directed against *tis-11* was designed, which did not target the glycine- and glutamine-rich regions. Like in chapter 4.4 63-N1 and 67-1D cells were treated with these triggers (*dstis-11_4* and *dstis-11_5*) separately and a mixture of both dsRNAs (*dstis-11_4+5*). After 6 days GFP intensity was measured and normalized to the control DsRed (Figure 4-39). Neither of the constructs resulted in a de-repression of the fluorescence in the siRNA-reporter cell lines.

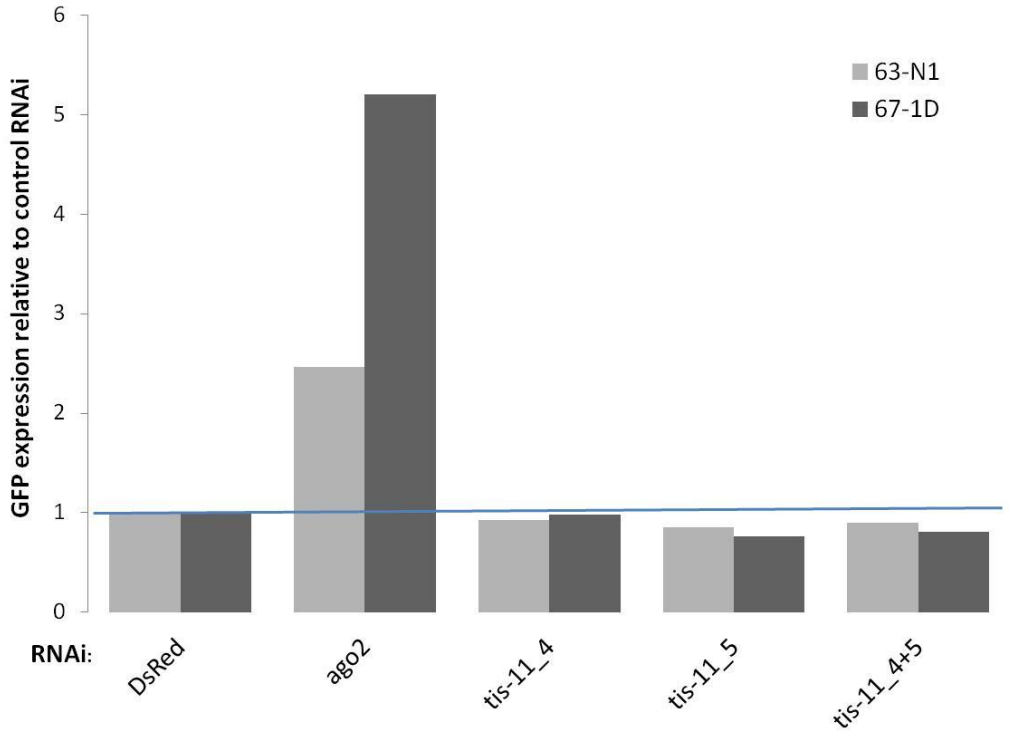

Figure 4-39: **RNAi triggers targeting $(CAN)_n$-repeats in the mRNAs of both *tis-11* and *ago2* leads to unwanted off-target effects.**

Endo-siRNA reporter cells (63-N1) and miR-277 reporter cells (67-1D) were treated twice with dsRNA constructs indicated below the bars targeting non-repetitive regions of *tis-11*. Ago2 served as positive control. GFP-fluorescence was measured by flow cytometry and normalized to control knock-down directed against DsRed. Values are the mean of two experiments. The horizontal blue line marks no change compared to the control.

Taken together this leads to the conclusion that at least part of the effects detected and analyzed after depletion of *tis-11* so far are a consequence of the lowered *ago2*-mRNA level by an indirect effect. Only two out of five dsRNA constructs directed against *tis-11* resulted in a de-repression of GFP in the exo-siRNA reporter cells (67-1D). Unfortunately both target the repetitive regions of the *tis-11*-mRNA and consequently may have many off-target effects.

5. Discussion

5.1 Factors of the small RNA silencing pathway are not required for AMD in *Drosophila* and mammals

Our findings that AMD can occur independently of the small RNA pathway in *Drosophila* cells contradict a former publication (Jing, Huang et al. 2005). In their manuscript S2 cells were screened in order to identify genes that are required for decay of β-globin reporter transcripts with mammalian 3'-UTRs harbouring AREs (identical to the 3'-UTRs we used). They found that Dicer-1, Ago1 and Ago2 were required for ARE-mRNA degradation in *Drosophila* and that miR-289 is responsible for recognition of ARE-sequences. Jing and colleagues conclude that cooperation of AUBPs and the miRNA system is substantial for recognition of AREs and triggering mRNA decay. In contrast we could show that AMD did not universally depend on components of the small RNA decay machinery (Figure 4-4, Figure 4-6). Moreover a recent publication demonstrated that depletion of Ago1 and Ago2 in S2 cells did not stabilize reporter constructs containing AREs of mouse IL-3 in its 3'-UTR, indicating that in general Ago proteins were not required for AMD in *Drosophila* (Spasic, Friedel et al.).

Additionally Jing *et al*. claimed that this mechanism is conserved, because in mammalian cell culture TNF-α transcripts were stabilized in a Dicer- and miR-16- dependent manner. miR-16 had to bind to ARE-sequences and recruit RISC and TTP, which leads to destabilization of the mRNA. Our co-authors Johanna Schott and Georg Stoecklin (Helfer, Schott et al.) addressed the question if miRNAs in general are required for the activity of TTP in mammalian AMD. Therefore they used dicer-deficient mouse embryonic fibroblasts (MEFs) to measure the decay rate of ier3-mRNA, a known target of TTP (Glasmacher, Hoefig et al. ; Lai, Parker et al. 2006). In contrast to WT-MEF cells, these mutant MEFs were not able to process mature miR-16. They could observe that degradation rates of ier3-transcript are indistinguishable in dicer-deficient and WT-cells. Summing up neither Dicer nor miR-16 were required for ier3-mRNA decay. These findings provide further support for our hypothesis that AMD did not generally depend on the miRNA pathway to induce decay in mammals and *Drosophila*.

5.2 Technical differences between our study and the publication of Jing *et al*. could not account for the deviating results

There are several technical differences between our study and the one of Jing and colleagues that had to be mentioned. First they determined mRNA half-lives by qRT-PCR whereas our analysis in S2 cells is based on reporter-protein expression and steady-state mRNA levels. Basically it is possible that components of the small RNA system destabilize ARE-mRNAs and increase their transcription or translation rate at the same time. Especially the interplay of miRNAs and ARE-sequences was previously shown in another context. In mammals miRNAs were able to switch from repression to activation and stimulate translation of ARE-transcripts upon cellular stress (Vasudevan and Steitz 2007; Vasudevan, Tong et al. 2007). On the other hand since almost five years no more data were published based on these revolutionary findings. This led to speculations that these reports were somehow questionable, too.

In our study such a compensating effect by stimulation of transcription or translation is unlikely, since the same extent of de-repression at protein and mRNA level was observed for GFP-3xARE reporter (Figure 4-3, Figure 4-5).

Second, the 3'-UTRs in the publication of Jing *et al*. were attached to β-globin mRNA, whereas a fusion with GFP was used in our experiments. The choice of a reporter is important and might account for small differences, but it is unlikely that ARE-function is completely diminished. We could show that insertion of authentic and artificial ARE-sequences into the 3'-UTR of GFP indeed lowered the stability of the transcripts. Furthermore, GFP-reporters have already successfully been used for analysis of AMD in mammalian cells (Benjamin, Colombi et al. 2006). Also insertion of miRNA target sites into the 3'-UTR of GFP led to robust repression indicating that RISC can access this region of the transcript (see Figure 4-7A and (Forstemann, Horwich et al. 2007; Shah and Forstemann 2008).

Finally different promotors were used to express the reporter genes, that resulted in different steady-state levels of reporter mRNA. Our system was previously used to detect miR-mediated repression (Forstemann, Horwich et al. 2007; Shah and Forstemann 2008) and the de-repression of the GFP-reporter after depletion of *tis-11* (see Figure 4-3) indicated that the system has not been saturated.

Taken together our data and that obtained from mammalian cell culture (Helfer, Schott et al. ; Spasic, Friedel et al.) strongly suggest that the small RNA silencing system is not generally required

for ARE-mediated mRNA decay. However it is not completely excluded that ARE and small RNA-binding sites may cooperate or interfere with each other in the context of a specific transcript.

5.3 Over-expression of Tis-11 leads to a dominant-negative effect in flies

Over-expression of Tis-11 in the whole fly or specifically the nervous system led to lethality in transgenic flies (see chapter 4.12). Compared to wildtype flies they showed an extreme delay in development when Tis-11 is over-expressed in muscle tissue. And they exhibit the so called erect wing (ewg) phenotype. These flies have severe abnormalities in the indirect flight muscles, which results in protruding wings (DeSimone, Coelho et al. 1996). According to gene ontology categories *Drosophila* ARE-mRNAs were not enriched in muscle developmental processes (Cairrao, Halees et al. 2009). So Tis-11 may act at an earlier time point during cell growth.

Mainly cellular and developmental processes were regulated by ARE-mRNAs. In addition several signaling pathways can be adjusted by the action of transcripts containing AREs. As already shown in human cells, genes encoding transcription factors were also enriched in ARE-mRNAs (Bakheet, Williams et al. 2006). It was demonstrated that Tis-11 regulates the level of the antimicrobial peptide CecA1 (Lauwers, Twyffels et al. 2009) and the question arose if it is perhaps even a general posttranscriptional regulator of immune genes in *Drosophila* and led to this severe phenotypes.

5.4 Identification of novel components in the *Drosophila* small RNA silencing system using genomewide screens

In the publication of Dorner *et al*. a genomewide screen was adopted in order to identify genes that affect the RNAi response in *Drosophila* cell culture (Dorner, Lum et al. 2006). They used the dual-luciferase reporter system to monitor RNAi-mediated response. S2 cells were treated with a library of different dsRNAs (approx. 20,000 dsRNAs), transiently transfected with luciferase-reporter plasmids and a dsRNA directed against Renilla-luciferase. In case the first dsRNA construct depletes an essential factor of the RNAi machinery, silencing of Renilla-luciferase is impaired and the reporter will be de-repressed (in principle similar to the approach we used in Figure 4-13A). As expected depletion of *ago2* led to increased luminescence, but this system failed to identify a number of known components of the RNAi system, like Dcr-2 and R2D2. Therefore, they argued

that their screen was not comprehensive in its identification of components that were essential in the RNAi silencing system, but nevertheless some new candidate genes might emerge. After re-screening with newly synthesized RNAi triggers 25 interesting candidate genes were identified, which potentially are important in small RNA silencing. In some of the candidate genes repetitive sequences were found. Hence it was indispensable to generate dsRNAs directed against distinct parts of the genes. Tis-11 was one of the candidates that also carries highly repetitive-regions. Two RNAi triggers against Tis-11 target the glycin-glutamine-rich regions and resulted in a clear de-repression of the reporter (19-fold and 15-fold de-repression compared to RNAi directed against an unrelated control). A third dsRNA, which was not directed against the repetitive regions of *tis-11*, showed only a modest effect on the luciferase-reporter system (2-fold de-repression compared to the control).

Besides that, Dorner and colleagues analyzed mRNA- and protein-levels of Ago2 after silencing of the candidate genes to exclude indirect effects on the overall Ago2 expression. Ago2 protein levels did not change compared to the control when *tis-11* is depleted. The same was concluded for ago2-mRNA levels, which were examined by Northern blotting. Nonetheless, a reduction in ago2-mRNA-levels of 40% ± 10% was determined. Furthermore it must be added that they did not mention which dsRNA construct out of the three was used for these evalutions.

Another report (Zhou, Hotta et al. 2008) applied S2 cells stably expressing Renilla-luciferase and a hairpin-construct with appropriate sequence that is cleaved by Dicer and thereby generates siRNAs directed against Renilla-luciferase. A collection of approx. 21,000 dsRNAs was screened to identify novel components that have an impact on the siRNA pathway. Like in the former publication additional independent dsRNAs were generated to avoid potential off-target effects due to highly repetitive regions. Only genes targeted by at least two independent dsRNAs that showed an effect on the reporter system were scored as final candidates. To validate their system they found *dcr-2* and *ago2* among the essential genes for the siRNA pathway. All together 116 candidates were identified which de-repressed the luciferase-reporter, however *tis-11* is not among them.

To sum up two genomewide screens were performed in *Drosophila* S2 cells in order to identify novel components of the small RNA silencing pathways. Tis-11 was only detected in the approach of Dorner *et al*. Though the screen of Zhou *et al*. was more sensitive (116 discovered candidate genes for the siRNA pathway vs. 25 candidates) it failed to identify Tis-11. In retrospect, parts of the data published of Dorner and colleagues need to be interpreted with caution. First candidate genes enriched in repetitive sequences were over-represented in their screen and they failed to identify the known RNAi component Dcr-2. Second, concerning Tis-11 two dsRNAs targeting the highly

repetitive regions of its gene showed clear effects on the reporter (15- 19-fold de-repression). In contrast, the de-repression after depletion of *tis-11* using the third RNAi trigger directed against non-repetitive sequences had barely an effect (2-fold de-repression), which might be negligible despite it being statistically significant. Finally they mentioned nowhere in their report which RNAi trigger directed against *tis-11* was used to verify that the levels of Ago2-protein and mRNA did not change after the treatment.

5.5 Not all effects after depletion of Tis-11 can be explained by indirect regulation of Ago2 expression

Basically most of our observations set Tis-11 in the same position as Ago2 with regard to the RNAi pathway. Though we had observed before that after silencing of *tis-11* with both RNAi triggers *tis-11* and *tis-11_3* the protein levels of Ago2 remained unchanged (Figure 4-17), we decided to measure also the ago2-mRNA levels. Only 10% ago2-mRNA was left after using dsRNA directed against *ago2*. While the amount of ago2-mRNA was only slightly lowered (ca. 15%) using *dstis-11_3*, treatment with *dstis-11* reduces the ago2-mRNA level clearly by 50% (Figure 4-38).

This could explain the effect on the ban-si-reporter constructs after silencing *tis-11* (Figure 4-12). Because depletion of *tis-11* using the RNAi triggers *tis-11* (50% ago2-mRNA indirectly targeted) and *tis-11_3* (15% ago2-mRNA targeted) led to a 3-fold and 1.5-fold de-repression of GFP respectively. This is in a comparable range with the 6-fold increase in fluorescence after the nearly complete knock-down of *ago2* (only 10% ago2-mRNA left). The same is true regarding the effect of Tis-11 on the luciferase reporter suitable to detect endo-siRNA mediated silencing (Figure 4-14). Silencing of *ago2* resulted in a 2.5-fold increase of luminescence compared to 1.5-fold de-repression after knock-down of *tis-11* (*dstis-11*). Also the inhibition of exo-siRNA silencing after depletion of *tis-11* (Figure 4-13) could be explained with the indirect modulation of ago2-mRNA expression levels (60% silencing activity inhibited after knock-down *ago2* vs. 15% after *dstis-11*). Finally only the biogenesis of Ago2-loaded RNAs, miR-277 and endo-siRNA CG4068B was blocked in *tis-11* depleted cells (Figure 4-19). And the distribution of miR-277 and CG4068B between effector complexes with Ago2 or Ago1 after knock-down of *tis-11* showed basically the same pattern as *ago2*-depleted cells (Figure 4-22). The Ago1-loaded miRNA bantam remained unaffected in both experiments.

Nevertheless several effects could not solely be explained with lowered levels of ago2-mRNA. For example the impact on 67-1D cells after knock-down of *tis-11* led to a 3- 4.5-fold de-repression using *dstis-11* construct and 2.5-fold using *dstis-11_3*. In contrast to this, depletion of 90% ago-mRNA resulted only in a 5- 6-fold increase of GFP fluorescence, which is not quantitative comparable (Figure 4-9B, Figure 4-10B, Figure 4-15). On the other hand the three dsRNA triggers which target the non-repetitive regions of *tis-11* showed no effect on 67-1D reporter cells (Figure 4-10B, Figure 4-39).

Taken together not all effects we had observed could be explained by indirect modulation of Ago2 expression. But it is not possible to separate them. Unfortunately most of the experiments were done using the dsRNAs which target the $(CAN)_n$-repeat-regions of *tis-11* and therefore it is likely that they cause many off-target effects.

5.6 Common strategies to minimize off-target effects and validation of knock-down specificity

In many organisms RNAi became a powerful tool to perform studies where gene function is specifically inhibited. Large dsRNAs are successfully used in *D. melanogaster* and *C. elegans* to induce RNAi. Many siRNAs are generated from the 300-800 bp dsRNAs by the endonuclease Dicer (Seinen, Burgerhof et al.). But long dsRNA have the potential to generate non-specific off-target effects like reported for short RNAs in mammalian cells (Lin, Ruan et al. 2005; Jackson, Burchard et al. 2006). Thus length and sequence of the designed dsRNAs are important for specificity. Highly repetitive or conserved regions should be avoided to minimize the likelihood of nonspecific off-target effects. Genes containing these regions are over-represented in candidate lists from screens, where they might be part of a huge class of false positives (Echeverri and Perrimon 2006; Ma, Creanga et al. 2006).

In mammals it is known that dsRNAs longer than 30 bp can induce innate immune response, such as interferon response (Yang, Buchholz et al. 2002). To avoid this different methods are used to perform RNAi in mammalian cells.

In most cases chemically synthesized siRNAs are transfected into the cells, but can vary dramatically concerning their silencing efficiency. Therefore, each mRNA must be screened for a potent siRNA, which is time consuming and expensive. RNAi can also be induced using short hairpin

RNAs (shRNAs) expressed from plasmids or viral vectors (Paddison, Caudy et al. 2002; Kittler, Surendranath et al. 2007).

Another method employed endonucleolytic cleavage of target specific long dsRNAs by *E.coli* RNaseIII *in vitro*. Thereby, a diverse pool of siRNAs is produced which is named endoribonuclease-prepared siRNAs (esiRNA) (Yang, Buchholz et al. 2002; Kittler, Surendranath et al. 2007). The same principle as before uses recombinant human Dicer to generate so called dicer-generated siRNAs (d-siRNAs; (Myers, Jones et al. 2003). They share the same end-structures, 5'-phosphate, 3'-hydroxylgroup and 2 nt-overhangs, as usual siRNAs, which are important for RNAi activity (Elbashir, Martinez et al. 2001). The diced siRNA pools contain hundreds of individual siRNAs, hence they are able to target multiple sites within one transcript (Myers, Chi et al. 2006).

Both synthetic siRNAs and diced siRNAs mediate efficient silencing of reporter constructs or endogenous targets (Yang, Buchholz et al. 2002). But there are differences comparing their specificity. Many synthesized siRNAs produce off-target effects, whereas the complex mixture of esiRNAs leads to more specific silencing. Due to the high complexity of diced siRNAs, the concentration of any individual problematic siRNA is in theory too low to result in a significant off-target effect (Myers, Chi et al. 2006).

There are different potential sources to generate nonspecific off-target effects. High numbers of siRNAs can saturate the endogenous RNAi machinery and thereby inhibit the function of endogenous miRNAs (Grimm, Streetz et al. 2006). Or one of the strands can hybridize with unintended transcripts. Already short stretches of 7 nt can act like a seed-region and cause translational repression (Jackson, Bartz et al. 2003; Birmingham, Anderson et al. 2006; Jackson, Burchard et al. 2006).

It is not only important to minimize the probability of off-target effects, but also to validate the specificity of a knock-down. First, it is essential to treat the cells also with a siRNA directed against an unrelated control, e.g. DsRed or luciferase, to guarantee that the observed phenotype is not an indirect effect. Second, two or three different siRNAs should be designed that target distinct regions of the transcript and if the knock-down is specific all constructs should show the same phenotype. Another possibility is to validate the knock-down by rescuing the mutant phenotype. Therefore a resistant form of the target mRNA could be artificially expressed in the cell (2003; Moffat, Reiling et al. 2007).

During our study we followed these guidelines to confirm specificity of the RNAi treatments. The cells were always incubated in parallel with a control dsRNA directed against an unrelated control, mainly DsRed. Regarding the silencing of *tis-11*, both mRNA- and protein-levels of *tis-11* were

determined to validate its depletion and consequently exclude indirect effects due to global translational repression (Figure 4-11). Finally the effects on the 67-1D reporter after depletion of the candidate genes *elav*, *rbp6* and *tis-11* were tested with at least two different dsRNAs. However, only the effect after knock-down of *tis-11* could be confirmed as specific using two independent RNAi triggers (Figure 4-10). Hence the specificity of knock-down *tis-11* could be validated. The indirect modulation of ago2-levels using these dsRNA constructs was detected at a later time point.

6. Appendix

6.1 Abbreviations

°C	degrees Celsius
Δ	deletion
63-N1	endo-siRNA cell culture reporter cell line
67-1D	siRNA cell culture reporter cell line
Ago	Argonaute protein
AMD	AU-rich mediated decay
Amp	ampicillin
AMPeps	antimicrobial peptides
APS	ammonium peroxodisulfate
ARE	AU-rich element
ATP	adenosine triphosphate
AUBP	AU-rich binding protein
Bnl	branchless
bp	base pair(s)
BSA	bovine serum albumine
C-term	protein C-terminus
cDNA	complementary DNA
CecA1	CecropinA1
CG4068	hairpin forming endo-siRNA precursor gene
co-IP	co-immunoprecipitation
CT-value	cycle of threshold value in qPCR
d	day(s)
D. melanogaster	*Drosophila melanogaster*
dcr	dicer gene
Dcr	Dicer protein
DMSO	dimethyl sulfoxide
DNA	desoxy-ribonucleic acid
dNTP	desoxy-nucleotide-tri-phosphate
ds	double-stranded
dsRBD	double-stranded RNA binding domain

dsRBP	double-stranded RNA binding domain protein
dsRNA	double-stranded RNA
DTT	dithiothreitol
E. coli	*Escherichia coli*
ECL	Enhanced Chemiluminescence
EGFP	Enhanced Green Fluorescent protein
Elav	embryonic lethal, abnormal vision
endo-	endogenous
endo-siRNA	endogenous small interfering RNA
esi-RNA	endoribonuclease-prepared siRNAs
exo-	exogenous
exo-siRNA	exogenous small-interfering RNA
FACS	Fluorescence Activated Cell Sorting
FBS	Fetal Bovine Serum
FMR1	Fragile Mental Retardation Protein 1
FXR-1	Fragile-X mental retardation-related protein 1
GFP	Green Fluorescent Protein
GM-SCF	granulocyte/macrophage colony-stimulating factor
GST	glutathione S-transferase
h	hour(s)
Hen1	HUA Enhancer 1
hpRNAs	hairpin RNAs
HRP	Horseradish Peroxidase
Ier3	immediate early response 3
IL	Interleukin
IP	immunoprecipitation
IPTG	Isopropyl-β-D-thiogalactopyranosid
Kana	kanamycin
Ko	knock-out
Luci	luciferase
MEF	mouse embryonic fibroblast
mg	milligram
miR	micro RNA
miRNA	micro RNA

ml	milliliter
mRNA	messenger RNA
N-term	protein N-terminus
Neo	neomycin
ng	nanogram
nt	nucleotide(s)
NTP	nucleotide-tri-phosphate
OD	optical density
ORF	open reading frame
p.a.	pro analysi
PA/PB/PC/PD	protein isoform A/B/C/D
PAGE	Polyacrylamide Gel Electrophoresis
PAZ	Piwi-Argonaute-Zwille domain of Dicer and Argonaute proteins
PCR	Polymerase Chain Reaction
piRNA	Piwi-interacting RNA
PNK	polynucleotide kinase
Pol II	DNA polymerase II
Poly-A	poly-adenylation
PVDF	Polyvinylidenfluoride
qPCR	quantitative Polymerase Chain Reaction
rb	rabbit
rel.	relative
RISC	RNA induced silencing complex
RLC	RISC loading complex
RNA	ribonucleic acid
RNAi	RNA interference
RNaseIII	endoribonuclease class III
rRNA	ribosomal RNA
RT	reverse transcription or real-time
S2 cell	Schneider-2 cell
SD	standard deviation
siRNA	small interfering RNA
SOB	Super Optimal Broth
SSC	sodium chloride/sodium citrate

SV40	Simian Virus 40
tech.	technical
Tis11	TPA-induced sequence 11
TTP	Tristetraprolin
UAS	yeast Upstream Activating Sequence
UTR	untranslated region
V	Volt
WT	wildtype
α	anti
µ	micro
µg	microgram

6.2 Acknowledgements

An erster Stelle möchte ich mich ganz herzlich bei meinem Doktorvater Klaus Förstemann bedanken, der es mir ermöglicht hat an einem interessanten und abwechslungsreichen Thema zu arbeiten. Besonders für die vielen neuen Ideen und Denkanstöße vor allem während herausfordernden Abschnitten des Projekts und seine unerschöpfliche Geduld möchte ich mich bedanken.

Dr. Dietmar Martin danke ich für die freundliche Übernahme des Zweigutachtens.

Meinem Thesis Advisory Committee Dr. Dierk Niessing und Dr. Thomas Becker danke ich für ihre hilfreichen Tipps und Ideen.

Den amtierenden und auch den bereits ausgeschiedenen Förstegirls möchte ich für die tolle Zusammenarbeit während der letzten Jahre und auch für die moralische, sowie tatkräftige Unterstützung während meiner Schreibphase danken. Vor allem die besonderen Feiertage und die einzigartige Atmosphäre haben das Laborleben immer sehr bereichert.

Romy Böttcher danke ich nicht nur für ihre Dienste als Kaffee-Fee und den turbulenten Fahrten zum Friedhof sondern besonders für ihre mütterliche Fürsorge in allen Lebenslagen.
Mili, danke für das Korrekturlesen der Arbeit, deinem meist unfehlbarem Gespür und der Erweiterung meiner Serbisch-Grundkenntnisse. Sribiče!
Für die nahezu traditionellen Fahrten mit „der letzten Ubahn“ und die legendären Firmenevents von S&S-Technologies möchte ich Stephanie danken!
Katha und dem Son of Hibatchi danke ich für die unzähligen Grillabende und den Shuttle-Service - mit oder ohne Sitz- zur Ubahn.

Henning Ruge möchte ich für die Unterstützung bei den Kreuzungen der transgenen Fliegen während seines Praktikums danken.
Ein großes Dankeschön geht an Saskia Gressel, die während ihrer Bachelorarbeit die Aufreiningung von rekombinantem Protein perfektioniert hat.
Sandra Kurz und Anselm Gruber danke ich für ihre Mithilfe an meinem Projekt im Rahmen ihrer Bachelorarbeiten.
Meinem Adoptiv-Praktikanten Paul Winkelmeier und Saskia Gressel danke ich zudem für die freundschaftliche Atmosphäre über den Laboralltag hinaus.

Mein größter Dank gilt meinen Eltern und meiner Familie, die mich stets ermutigt und an mich geglaubt haben. Ohne ihre Unterstützung wäre das alles nicht möglich gewesen. Danke!

7. References

(2003). "Whither RNAi?" Nat Cell Biol **5**(6): 489-90.
Ameres, S. L., M. D. Horwich, et al. "Target RNA-directed trimming and tailing of small silencing RNAs." Science **328**(5985): 1534-9.
Bakheet, T., B. R. Williams, et al. (2006). "ARED 3.0: the large and diverse AU-rich transcriptome." Nucleic Acids Res **34**(Database issue): D111-4.
Baou, M., A. Jewell, et al. (2009). "TIS11 family proteins and their roles in posttranscriptional gene regulation." J Biomed Biotechnol **2009**: 634520.
Barreau, C., L. Paillard, et al. (2005). "AU-rich elements and associated factors: are there unifying principles?" Nucleic Acids Res **33**(22): 7138-50.
Beisang, D. and P. R. Bohjanen "Perspectives on the ARE as it turns 25 years old." Wiley Interdiscip Rev RNA **3**(5): 719-31.
Benjamin, D., M. Colombi, et al. (2006). "A GFP-based assay for monitoring post-transcriptional regulation of ARE-mRNA turnover." Mol Biosyst **2**(11): 561-7.
Bhattacharyya, S. N., R. Habermacher, et al. (2006). "Relief of microRNA-mediated translational repression in human cells subjected to stress." Cell **125**(6): 1111-24.
Birmingham, A., E. M. Anderson, et al. (2006). "3' UTR seed matches, but not overall identity, are associated with RNAi off-targets." Nat Methods **3**(3): 199-204.
Bischof, J. and K. Basler (2008). "Recombinases and their use in gene activation, gene inactivation, and transgenesis." Methods Mol Biol **420**: 175-95.
Bischof, J., R. K. Maeda, et al. (2007). "An optimized transgenesis system for Drosophila using germ-line-specific phiC31 integrases." Proc Natl Acad Sci U S A **104**(9): 3312-7.
Brennan, C. M. and J. A. Steitz (2001). "HuR and mRNA stability." Cell Mol Life Sci **58**(2): 266-77.
Cairrao, F., A. S. Halees, et al. (2009). "AU-rich elements regulate Drosophila gene expression." Mol Cell Biol **29**(10): 2636-43.
Caput, D., B. Beutler, et al. (1986). "Identification of a common nucleotide sequence in the 3'-untranslated region of mRNA molecules specifying inflammatory mediators." Proc Natl Acad Sci U S A **83**(6): 1670-4.
Carballo, E., W. S. Lai, et al. (1998). "Feedback inhibition of macrophage tumor necrosis factor-alpha production by tristetraprolin." Science **281**(5379): 1001-5.
Chen, J., S. Larochelle, et al. (2003). "Xpd/Ercc2 regulates CAK activity and mitotic progression." Nature **424**(6945): 228-32.
Ciais, D., N. Cherradi, et al. "Multiple functions of tristetraprolin/TIS11 RNA-binding proteins in the regulation of mRNA biogenesis and degradation." Cell Mol Life Sci.
Clement, S. L., C. Scheckel, et al. "Phosphorylation of tristetraprolin by MK2 impairs AU-rich element mRNA decay by preventing deadenylase recruitment." Mol Cell Biol **31**(2): 256-66.
Czech, B., C. D. Malone, et al. (2008). "An endogenous small interfering RNA pathway in Drosophila." Nature **453**(7196): 798-802.
DeSimone, S., C. Coelho, et al. (1996). "ERECT WING, the Drosophila member of a family of DNA binding proteins is required in imaginal myoblasts for flight muscle development." Development **122**(1): 31-9.
Dorner, S., L. Lum, et al. (2006). "A genomewide screen for components of the RNAi pathway in Drosophila cultured cells." Proc Natl Acad Sci U S A **103**(32): 11880-5.
Echeverri, C. J. and N. Perrimon (2006). "High-throughput RNAi screening in cultured cells: a user's guide." Nat Rev Genet **7**(5): 373-84.

Elbashir, S. M., J. Martinez, et al. (2001). "Functional anatomy of siRNAs for mediating efficient RNAi in Drosophila melanogaster embryo lysate." EMBO J **20**(23): 6877-88.

Fish, M. P., A. C. Groth, et al. (2007). "Creating transgenic Drosophila by microinjecting the site-specific phiC31 integrase mRNA and a transgene-containing donor plasmid." Nat Protoc **2**(10): 2325-31.

Forstemann, K., M. D. Horwich, et al. (2007). "Drosophila microRNAs Are Sorted into Functionally Distinct Argonaute Complexes after Production by Dicer-1." Cell **130**(2): 287-97.

Forstemann, K., Y. Tomari, et al. (2005). "Normal microRNA maturation and germ-line stem cell maintenance requires Loquacious, a double-stranded RNA-binding domain protein." PLoS Biol **3**(7): e236.

Ghildiyal, M. and P. D. Zamore (2009). "Small silencing RNAs: an expanding universe." Nat Rev Genet **10**(2): 94-108.

Glasmacher, E., K. P. Hoefig, et al. "Roquin binds inducible costimulator mRNA and effectors of mRNA decay to induce microRNA-independent post-transcriptional repression." Nat Immunol **11**(8): 725-33.

Grimm, D., K. L. Streetz, et al. (2006). "Fatality in mice due to oversaturation of cellular microRNA/short hairpin RNA pathways." Nature **441**(7092): 537-41.

Grishok, A., A. E. Pasquinelli, et al. (2001). "Genes and mechanisms related to RNA interference regulate expression of the small temporal RNAs that control C. elegans developmental timing." Cell **106**(1): 23-34.

Hartig, J. V., S. Esslinger, et al. (2009). "Endo-siRNAs depend on a new isoform of loquacious and target artificially introduced, high-copy sequences." EMBO J **28**(19): 2932-44.

Helfer, S., J. Schott, et al. "AU-rich element-mediated mRNA decay can occur independently of the miRNA machinery in mouse embryonic fibroblasts and Drosophila S2-cells." PLoS ONE **7**(1): e28907.

Hong, X., M. Hammell, et al. (2009). "Immunopurification of Ago1 miRNPs selects for a distinct class of microRNA targets." Proc Natl Acad Sci U S A **106**(35): 15085-90.

Horwich, M. D., C. Li, et al. (2007). "The Drosophila RNA methyltransferase, DmHen1, modifies germline piRNAs and single-stranded siRNAs in RISC." Curr Biol **17**(14): 1265-72.

Hutvagner, G., J. McLachlan, et al. (2001). "A cellular function for the RNA-interference enzyme Dicer in the maturation of the let-7 small temporal RNA." Science **293**(5531): 834-8.

Jackson, A. L., S. R. Bartz, et al. (2003). "Expression profiling reveals off-target gene regulation by RNAi." Nat Biotechnol **21**(6): 635-7.

Jackson, A. L., J. Burchard, et al. (2006). "Widespread siRNA "off-target" transcript silencing mediated by seed region sequence complementarity." Rna **12**(7): 1179-87.

Ji, L. and X. Chen "Regulation of small RNA stability: methylation and beyond." Cell Res **22**(4): 624-36.

Jing, Q., S. Huang, et al. (2005). "Involvement of microRNA in AU-rich element-mediated mRNA instability." Cell **120**(5): 623-34.

Kapsimali, M., W. P. Kloosterman, et al. (2007). "MicroRNAs show a wide diversity of expression profiles in the developing and mature central nervous system." Genome Biol **8**(8): R173.

Ketting, R. F., S. E. Fischer, et al. (2001). "Dicer functions in RNA interference and in synthesis of small RNA involved in developmental timing in C. elegans." Genes Dev **15**(20): 2654-9.

Kim, V. N., J. Han, et al. (2009). "Biogenesis of small RNAs in animals." Nat Rev Mol Cell Biol **10**(2): 126-39.

Kittler, R., V. Surendranath, et al. (2007). "Genome-wide resources of endoribonuclease-prepared short interfering RNAs for specific loss-of-function studies." Nat Methods **4**(4): 337-44.

Lai, W. S., J. S. Parker, et al. (2006). "Novel mRNA targets for tristetraprolin (TTP) identified by global analysis of stabilized transcripts in TTP-deficient fibroblasts." Mol Cell Biol **26**(24): 9196-208.

Lauwers, A., L. Twyffels, et al. (2009). "Post-transcriptional Regulation of Genes Encoding Anti-microbial Peptides in Drosophila." J Biol Chem **284**(13): 8973-83.

Lee, Y., K. Jeon, et al. (2002). "MicroRNA maturation: stepwise processing and subcellular localization." EMBO J **21**(17): 4663-70.

Lee, Y. S., K. Nakahara, et al. (2004). "Distinct roles for Drosophila Dicer-1 and Dicer-2 in the siRNA/miRNA silencing pathways." Cell **117**(1): 69-81.

Lin, X., X. Ruan, et al. (2005). "siRNA-mediated off-target gene silencing triggered by a 7 nt complementation." Nucleic Acids Res **33**(14): 4527-35.

Liu, Q., T. A. Rand, et al. (2003). "R2D2, a bridge between the initiation and effector steps of the Drosophila RNAi pathway." Science **301**(5641): 1921-5.

Liu, Y., H. Tan, et al. "Autoantigen La promotes efficient RNAi, antiviral response, and transposon silencing by facilitating multiple-turnover RISC catalysis." Mol Cell **44**(3): 502-8.

Livak, K. J. and T. D. Schmittgen (2001). "Analysis of relative gene expression data using real-time quantitative PCR and the 2(-Delta Delta C(T)) Method." Methods **25**(4): 402-8.

Ma, F., X. Liu, et al. "MicroRNA-466l upregulates IL-10 expression in TLR-triggered macrophages by antagonizing RNA-binding protein tristetraprolin-mediated IL-10 mRNA degradation." J Immunol **184**(11): 6053-9.

Ma, Y., A. Creanga, et al. (2006). "Prevalence of off-target effects in Drosophila RNA interference screens." Nature **443**(7109): 359-63.

Martinez, J., A. Patkaniowska, et al. (2002). "Single-stranded antisense siRNAs guide target RNA cleavage in RNAi." Cell **110**(5): 563-74.

mod, E. C., S. Roy, et al. "Identification of functional elements and regulatory circuits by Drosophila modENCODE." Science **330**(6012): 1787-97.

Moffat, J., J. H. Reiling, et al. (2007). "Off-target effects associated with long dsRNAs in Drosophila RNAi screens." Trends Pharmacol Sci **28**(4): 149-51.

Myers, J. W., J. T. Chi, et al. (2006). "Minimizing off-target effects by using diced siRNAs for RNA interference." J RNAi Gene Silencing **2**(2): 181-94.

Myers, J. W., J. T. Jones, et al. (2003). "Recombinant Dicer efficiently converts large dsRNAs into siRNAs suitable for gene silencing." Nat Biotechnol **21**(3): 324-8.

Okamura, K., W. J. Chung, et al. (2008). "The Drosophila hairpin RNA pathway generates endogenous short interfering RNAs." Nature **453**(7196): 803-6.

Okamura, K., A. Ishizuka, et al. (2004). "Distinct roles for Argonaute proteins in small RNA-directed RNA cleavage pathways." Genes Dev **18**(14): 1655-66.

Okamura, K. and E. C. Lai (2008). "Endogenous small interfering RNAs in animals." Nat Rev Mol Cell Biol **9**(9): 673-8.

Paddison, P. J., A. A. Caudy, et al. (2002). "Short hairpin RNAs (shRNAs) induce sequence-specific silencing in mammalian cells." Genes Dev **16**(8): 948-58.

Pham, J. W. and E. J. Sontheimer (2004). "The Making of an siRNA." Mol Cell **15**(2): 163-4.

Saito, K., Y. Sakaguchi, et al. (2007). "Pimet, the Drosophila homolog of HEN1, mediates 2'-O-methylation of Piwi- interacting RNAs at their 3' ends." Genes Dev **21**(13): 1603-8.

Sandler, H. and G. Stoecklin (2008). "Control of mRNA decay by phosphorylation of tristetraprolin." Biochem Soc Trans **36**(Pt 3): 491-6.

Seinen, E., J. G. Burgerhof, et al. "RNAi experiments in D. melanogaster: solutions to the overlooked problem of off-targets shared by independent dsRNAs." PLoS ONE **5**(10).

Shah, C. and K. Forstemann (2008). "Monitoring miRNA-mediated silencing in Drosophila melanogaster S2-cells." Biochim Biophys Acta **1779**(11): 766-72.

Sharova, L. V., A. A. Sharov, et al. (2009). "Database for mRNA half-life of 19 977 genes obtained by DNA microarray analysis of pluripotent and differentiating mouse embryonic stem cells." DNA Res **16**(1): 45-58.

Shaw, G. and R. Kamen (1986). "A conserved AU sequence from the 3' untranslated region of GM-CSF mRNA mediates selective mRNA degradation." Cell **46**(5): 659-67.

Spasic, M., C. C. Friedel, et al. "Genome-wide assessment of AU-rich elements by the AREScore algorithm." PLoS Genet **8**(1): e1002433.

St Johnston, D. (2002). "The art and design of genetic screens: Drosophila melanogaster." Nat Rev Genet **3**(3): 176-88.

Stark, A., M. F. Lin, et al. (2007). "Discovery of functional elements in 12 Drosophila genomes using evolutionary signatures." Nature **450**(7167): 219-232.

Temme, C., S. Zaessinger, et al. (2004). "A complex containing the CCR4 and CAF1 proteins is involved in mRNA deadenylation in Drosophila." EMBO J **23**(14): 2862-71.

Temme, C., L. Zhang, et al. "Subunits of the Drosophila CCR4-NOT complex and their roles in mRNA deadenylation." RNA **16**(7): 1356-70.

Tomari, Y., C. Matranga, et al. (2004). "A protein sensor for siRNA asymmetry." Science **306**(5700): 1377-80.

Vasudevan, S. and J. A. Steitz (2007). "AU-rich-element-mediated upregulation of translation by FXR1 and Argonaute 2." Cell **128**(6): 1105-18.

Vasudevan, S., Y. Tong, et al. (2007). "Switching from Repression to Activation: MicroRNAs Can Up-Regulate Translation." Science.

Vindry, C., A. Lauwers, et al. "dTIS11 Protein-dependent Polysomal Deadenylation Is the Key Step in AU-rich Element-mediated mRNA Decay in Drosophila Cells." J Biol Chem **287**(42): 35527-38.

von Roretz, C. and I. E. Gallouzi (2008). "Decoding ARE-mediated decay: is microRNA part of the equation?" J Cell Biol **181**(2): 189-94.

Wei, Y., Q. Xiao, et al. (2009). "Differential regulation of mRNA stability controls the transient expression of genes encoding Drosophila antimicrobial peptide with distinct immune response characteristics." Nucleic Acids Res **37**(19): 6550-61.

Worthington, M. T., J. W. Pelo, et al. (2002). "RNA binding properties of the AU-rich element-binding recombinant Nup475/TIS11/tristetraprolin protein." J Biol Chem **277**(50): 48558-64.

Yang, D., F. Buchholz, et al. (2002). "Short RNA duplexes produced by hydrolysis with Escherichia coli RNase III mediate effective RNA interference in mammalian cells." Proc Natl Acad Sci U S A **99**(15): 9942-7.

Yanisch-Perron, C., J. Vieira, et al. (1985). "Improved M13 phage cloning vectors and host strains: nucleotide sequences of the M13mp18 and pUC19 vectors." Gene **33**(1): 103-19.

Yeh, P. A., W. H. Yang, et al. "Drosophila eyes absent is a novel mRNA target of the tristetraprolin (TTP) protein DTIS11." Int J Biol Sci **8**(5): 606-19.

Zhou, R., I. Hotta, et al. (2008). "Comparative analysis of argonaute-dependent small RNA pathways in Drosophila." Mol Cell **32**(4): 592-9.